

High Power and High Frequency Class-DE Inverters

By

Ian Douglas de Vries



Thesis Presented for the Degree of
DOCTOR OF PHILOSOPHY
In the Department of Electrical Engineering
UNIVERSITY OF CAPE TOWN

August 1999

DECLARATION

This thesis is being submitted for the degree of Doctor of Philosophy in the department of Electrical Engineering at the University of Cape Town. It has not been submitted before for any degree or examination at this or any other university. The author wishes to declare that the work done in this dissertation is his own and includes nothing that is the outcome of work done in collaboration. The author confirms that in accordance with university rule GP7 (3) that he was the primary researcher where work described in this thesis was published under joint authorship.

Ian Douglas de Vries

16 August 1999

Email: ian.devries@ieee.org

ABSTRACT

Title: **High Power and High Frequency Class-DE Inverters**

This thesis investigates the various aspects of the theory, design and construction of a Class-DE type inverter and how these affect the power and frequency limits over which a Class-DE inverter can feasibly be used to produce AC (or RF) power. To this extent, an analysis of Class-DE operation in a half-bridge inverter is performed. A similar approach to Hamill [6] is adopted but a different time reference was used. This allows the concept of a conduction angle to be introduced and hence enables a more intuitive understanding of the equations thereafter. Equations to calculate circuit element values LCR network are developed. The amount above the resonant frequency of the LCR network that the switching frequency must be in order to obtain the correct phase lag of the load current is shown. The effect of a non-linear output capacitance is studied and equations are modified to take this effect into account. It was found that a Class-DE topology offers a theoretical power advantage over a Class-E topology. However this power advantage decreases with increasing frequency and is dependent on the output capacitance of the active switching devices. Using currently available MOSFETs, a Class-DE topology has a theoretical power advantage over a Class-E topology up to approximately 10MHz.

However, the practical problems of implementing a Class-DE inverter to work into the HF band are formidable. These practical problems and the extent to which they limit the operating frequency and power of a Class-DE type inverter are investigated. Guidelines to solving these practical problems are discussed and some novel solutions are developed that considerably extend the feasible operating frequency and power of a Class-DE inverter. These solutions enabled a broadband design of the control circuitry, communication-link and gate-drive to be developed. Using these designs, a prototype broadband half-bridge inverter was developed which was capable of switching from 50kHz through to 6MHz. When operated in the Class-DE mode, the inverter was found to be capable of delivering a power output of over 1kW from 50kHz to 5MHz with an efficiency of over 91%. The waveforms obtained from the inverter clearly show Class-DE operation. The results of this thesis prove that a Class-DE series resonant inverter can produce RF power up to a frequency of 5MHz with a higher combination of power and efficiency than any other present topology. The practical problems of even higher operating frequencies are discussed and some possible solutions suggested. The mismatched load tolerance of a Class-DE type inverter is briefly investigated.

A Class-DE type inverter could be used for any applications requiring RF power in the HF band, such as AM or SW transmitters, induction heating and plasma generators. The information presented in this thesis will be useful to designers wishing to implement such an inverter. In addition a Class-DE inverter could form the first stage of a highly efficient and high frequency DC-DC converter and the information presented here is directly applicable to such an application.

ACKNOWLEDGEMENTS

The author would like to thank the following:

- My supervisors, Mr. J.H. van Nierop for his conscientious help and for help with obtaining financial assistance, and to Prof. J.R. Greene for his advice.
- Mr. Stephen Schrire for his advice and discussions on technical matters.
- Dr. N. Morrison for his help with confirming the Fourier analysis results.
- The University of Cape Town Research Council and ESKOM for providing part of the financial support towards this project.
- Mr. N.O. Sokal for making the HB-Plus simulation program freely available.
- Dr. Clare Knapp, Dr. Jon Tapson, Mr. Jevon Davies and Mr. Irshad Khan for their encouragement and everyday company and cheer.
- Professor M.K. Kazimierczuk, Dr. F.H. Raab and Dr. D.C. Hamill for their critique of this thesis.

CONTENTS

TERMS AND SYMBOLS.....	vii
1. INTRODUCTION.....	1
1.1 BACKGROUND	1
1.2 THESIS OBJECTIVES.....	2
1.3 THESIS CONTENTS	3
2. ANALYSIS AND DESIGN EQUATIONS.....	4
2.1 THE CLASS-D VOLTAGE-FED SERIES RESONANT INVERTER.....	4
2.2 THE CLASS-DE VOLTAGE-FED SERIES RESONANT INVERTER	9
2.2.1 Operation	9
2.2.2 Fundamental Component of the Midpoint Voltage	12
2.2.3 LCR Series Resonant Network	14
2.2.4 The Effect of a Non-Linear Output Capacitance	18
2.2.5 Design Example.....	21
2.2.6 Other Class-DE Topologies.....	23
3. TOPOLOGY, SWITCHING DEVICES AND SIMULATION	24
3.1 CHOICE OF THE TOPOLOGY	24
3.2 CHOICE OF THE SWITCHING DEVICE	25
3.2.1 N-Channel Enhancement-Type MOSFET	25
3.2.2 Selection of the MOSFETs.....	27
3.3 SIMULATION OF THE INVERTER	29
3.3.1 Simulation of a Class-D Voltage-Fed Series Resonant Inverter	29
3.3.2 Simulation of a Class-DE Voltage-Fed Series Resonant Inverter	31
4. DRIVING THE INVERTER.....	34
4.1 DRIVING THE MOSFET GATE.....	35
4.1.1 Requirements of the Gate-driver	35
4.1.2 Choice of the Method Used to Drive the MOSFET Gates	36
4.1.3 The Gate-Driver.....	37
4.1.4 High and Low-side Gate-Driver Power Supplies	37
4.1.5 Final Gate-Drive System	38
4.1.6 Current into MOSFET Gate when Operating in Class-DE Mode.....	40

4.2 CONTROL SIGNAL GENERATION.....	42
4.2.1 Requirements of the Control-Signal-Generator	42
4.2.2 Conceptual Circuit used for the Control-Signal-Generator	42
4.2.3 Final Control-Signal-Generator Circuit	43
4.2.4 Possible Future Circuit	44
5. COMMUNICATION-LINK TO THE HIGH-SIDE SWITCH	45
5.1 REQUIREMENTS OF THE COMMUNICATION-LINK.....	46
5.2 METHODS OF CONTROLLING THE HIGH-SIDE SWITCH.....	47
5.2.1 Pulse Transformer.....	47
5.2.2 Electronic Level-Shifters.....	48
5.2.3 Opto-Couplers	49
5.2.4 Fiber Optic Link	49
5.2.5 RF Modulated Carrier Signal.....	50
5.2.6 Summary.....	50
5.3 IMPLEMENTATION OF A FIBER OPTIC COMMUNICATION-LINK.....	51
5.3.1 LED Transmitter Drive Circuit.....	51
5.3.2 Comparator	54
5.4 CONCLUSIONS.....	56
5.5 DISCUSSION	56
6. PHYSICAL CONSTRUCTION OF THE INVERTER	57
6.1 DESIGN CONSIDERATIONS OF THE INVERTER CONSTRUCTION	57
6.2 ACTUAL CONSTRUCTION OF THE INVERTER	59
6.3 RESONANT LOAD NETWORK	62
6.4 MEASUREMENTS.....	63
6.5 OVERVIEW OF THE WHOLE INVERTER.....	64
7. EXPERIMENTAL RESULTS	65
7.1 TUNING PROCEDURE FOR CLASS-DE OPERATION	66
7.2 OPERATING WAVEFORMS, POWER OUTPUT AND EFFICIENCY OF THE INVERTER.....	72

8. MISMATCHED LOAD TOLERANCE.....	81
8.1 IDEAL CLASS-D INVERTER	82
8.2 PRACTICAL CLASS-D INVERTER	83
8.3 THE CLASS-DE INVERTER	84
9. CONCLUSIONS.....	87
9.1 CLASS-DE VERSUS CLASS-E	89
9.2 ORIGINAL WORK	90
APPENDIX A. Fundamental Component of the Midpoint Voltage.....	91
APPENDIX B. HB-Plus Simulation Results of the Design Example.....	93
APPENDIX C. Circuit Diagrams.....	95
C.1 DRIVE-SIGNAL-GENERATOR CIRCUIT	95
C.2 GATE-DRIVER CIRCUIT	96
APPENDIX D. Design Equations of a Half-Bridge Class-DE Inverter	97
REFERENCES.....	99

TERMS AND SYMBOLS

Various means of producing RF power are often referred to as RF Amplifiers in the literature. The use of *Inverter* rather than *Amplifier* has been adopted here when applied to Class-D, Class-DE and Class-E topologies as these actually convert electrical power from DC to RF and do not amplify a signal as such.

TERMS

- Midpoint - The common point connecting the high and low-side switches of a half-bridge inverter.
- Midpoint voltage - The voltage of the midpoint referenced to ground.
- Load Current - Current out of the midpoint and into the load (i.e. into the LCR network).
- Switching Frequency - The frequency the inverter is being driven at (also referred to as the *driving frequency* or *operating frequency*).
- Switching Period - The inverse of the switching frequency.
- Conduction Angle - The angular portion of a full switching period over which the switch is fully on.
- On-time - The time the switch is on for in one switching period (related to the conduction angle)
- Dead-time - The time difference between one half of a switching period and the on-time.
- Drive-signal - The signal that controls the switch state (i.e On or Off)

SYMBOLS

- f_s Switching frequency
- T_s Switching period
- ω_s Angular switching frequency
- $v_m(t)$ Time varying midpoint voltage
- $i_L(t)$ Time varying load current
- I_p Peak value of the load current
- V_s The supply voltage (rail to rail potential difference)
- ϕ Conduction Angle of Switches
- t_{on} On-time
- t_d Dead-time
- C_o The output capacitance of the switching device
- Q_o The total charge removed from the midpoint during the dead-time by the load current
- S1 High-side switch of the half-bridge inverter
- S2 Low-side switch of the half-bridge inverter
- $v_{S1}(t)$ The time varying voltage across the high-side switch, S1
- $i_{S1}(t)$ The time varying current through the high-side switch, S1
- $i_{C1}(t)$ The time varying current through the high-side switch's output capacitance

$v_o(t)$	The time varying voltage across the load resistance
\bar{V}_1	The Fourier series coefficient of the fundamental component of the midpoint voltage
$v_{m1}(t)$	The fundamental component of the midpoint voltage
α	The phase angle between the fundamental component of the midpoint voltage and the load current
P_{out}	RF Power output of the inverter
I_{S-avg}	The average current through each switch
I_{S-rms}	The RMS current through each switch
Q	The loaded quality factor of a series LCR network
U	Switch Utilization factor
n	Number of switches used in the topology
ω_r	Natural resonant frequency of a resonant circuit
\bar{Z}	The Effective Load Impedance
X	The reactance of the effective load impedance
R	Resistance
L	Inductance
C	Capacitance
Q_T	Total charge needed to charge the output capacitance of a MOSFET to a specified voltage V_{DS}
C_{o-eff}	The effective output capacitance of a MOSFET at a particular supply voltage
V_{dri}	Supply voltage to the gate-driver output stage
η	Efficiency

CHAPTER 1. INTRODUCTION

1.1 BACKGROUND

Radio frequency (RF) power is widely used in industry for a variety of applications such as induction heating, dielectric heating and plasma generation. The majority of these applications generally require RF power at a single frequency, ranging from the tens of kHz through to 27 MHz. The power levels needed range from watts to MW, with the majority of applications requiring a few kW. The RF power sources providing the RF power needed for these applications use a variety of different types of topologies and active devices. The basic function required of a RF power source for these applications is to produce AC power at a single frequency from a DC input source, as shown in Figure 1.1. Various methods of producing this RF power are briefly described below.

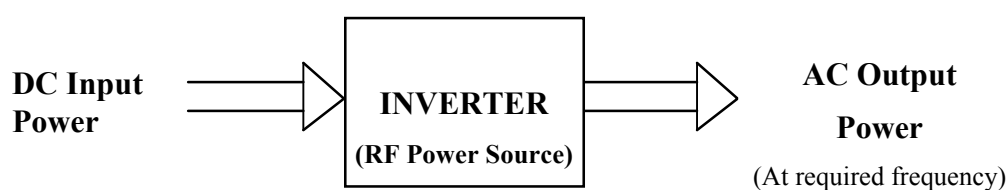


Figure 1.1 *Basic function of an RF power Source*

Pre-1980, triode valve oscillators were traditionally used to produce the RF power, and had a typical efficiency of approximately 60-65% [16]. As valves have a very large power dissipation capability, they are still the only means of producing power levels of more than 10 kW above a few MHz. However, valve oscillators have a number of disadvantages, which lead to the development of a number of different types of solid-state power sources, over the last two decades, for the various frequency ranges. Solid-state power sources offer numerous advantages over valve sources, such as the stability and control of the output power, repeatability, smaller size and weight, lower operating voltages, higher efficiency and a longer lifetime. For these reasons, solid-state power sources are required for many applications and have become widely used.

These solid-state sources employ a variety of different topologies depending on the application, frequency and power [2,16,17,55]. Traditionally, many of the HF solid-state power sources operated in a linear Class-B or Class-C mode. The problem with linear topologies is that the active device is used as a linear current source. This limits the theoretical efficiency of linear topologies, e.g. a Class-B amplifier delivering a full-output sinusoidal waveform into a pure resistive load will have a theoretical efficiency of 78.5%. In practice they have typical efficiencies of only 55-65%. This limits for the power output of a solid-state linear topology as transistors have poor power dissipation capabilities compared to valves. Thus for high power single frequency applications, efficiency is a priority concern in a solid state source.

To improve efficiency and increase the power output of a solid-state RF power source, one could switch the active devices on and off in a switch mode topology. An essential requirement of switching the active devices at

very high frequency is low switching losses. Various resonant mode type topologies exist that achieve low switching losses by employing zero current and/or zero voltage switching transitions. Of these, the most suitable resonant converter topologies for operation at very high frequency are the Class-D voltage-fed series resonant inverter, Class-E and more recently the Class-DE voltage-fed series resonant inverter [5,6,7,27].

Class-D switching type power sources are available for power levels of up to hundreds of kW and at frequencies approaching 1 MHz. At frequencies above 1 MHz, a Class-D type inverter suffers from practical implementation difficulties and its efficiency decreases as it starts to suffer from capacitive switching loss due to the parasitic output capacitances of the switching devices. These effects worsen with increasing voltage and frequency. These facts have limited the applications of relatively high power Class-D type topologies at frequencies higher than 1 MHz [3,5,6,7,47,48].

Class-E is a tuned single ended switching inverter that can operate at these frequencies with good efficiency [4]. It has *zero voltage, zero dv/dt* (zero load current) switching conditions and hence does not suffer from the switching loss of Class-D. It is also a single ended topology and hence the gate drive is much simpler to achieve than a two-switch Class-D. High frequency operation of a Class-E inverter has been shown to be feasible and commercial solid-state Class-E power sources are available up to power levels of 10 kW in the HF band. However, a Class-E topology has one main disadvantage over a Class-D circuit, in that its switch utilization factor is 0.098 and that of a Class-D is 0.159. This theoretically enables a Class-D circuit to produce 62% more power than a Class-E with the same current and voltage stresses on their switches.

Class-DE offers some of the better features of Class-D and Class-E. It is based on a Class-D voltage-fed series resonant inverter, but it employs the *zero-voltage and zero-load-current* turn-on transitions associated with a Class-E topology, and it has a switch utilization factor approaching that of a Class-D (0.159). Operating a voltage-fed series resonant circuit in the Class-DE mode effectively eliminates the capacitive switching losses and hence enables operation at higher frequencies [5,6,7].

1.2 THESIS OBJECTIVES

The aim of this thesis was to investigate the various aspects of the theory, design and construction of a Class-DE type inverter and how these affect the power and frequency limits over which a Class-DE inverter can feasibly be used to produce RF power. To this extent an analysis and a description of Class-DE operation was undertaken with the intent of developing simple and intuitive design equations. The effect of the non-linear output capacitance was investigated and found to be considerable and hence the equations were adapted to take this effect into account. It was found that a Class-DE topology, using current power MOSFETs, offers a theoretical power advantage over a Class-E topology up to approximately 10 MHz, depending on the output capacitance of the switching MOSFET. However, an investigation into the technical aspects of implementing a Class-DE inverter to work up to this frequency were found to be formidable and to a large extent these technical problems have limited the practical applications of half-bridge inverters to less than 1 MHz. Aspects of these technical problems and guidelines to solving them are discussed. Areas that could be improved were

investigated and some novel solutions were developed that considerably extended the feasible operating frequency of a high power half-bridge inverter. Using these solutions, the development of prototype voltage-fed half-bridge series resonant inverter that could operate in Class-DE mode was undertaken. An initial target of 1 kW at 5 MHz was thought to be feasible. Some of the practical problems of even higher operating frequencies are discussed and some possible solutions suggested.

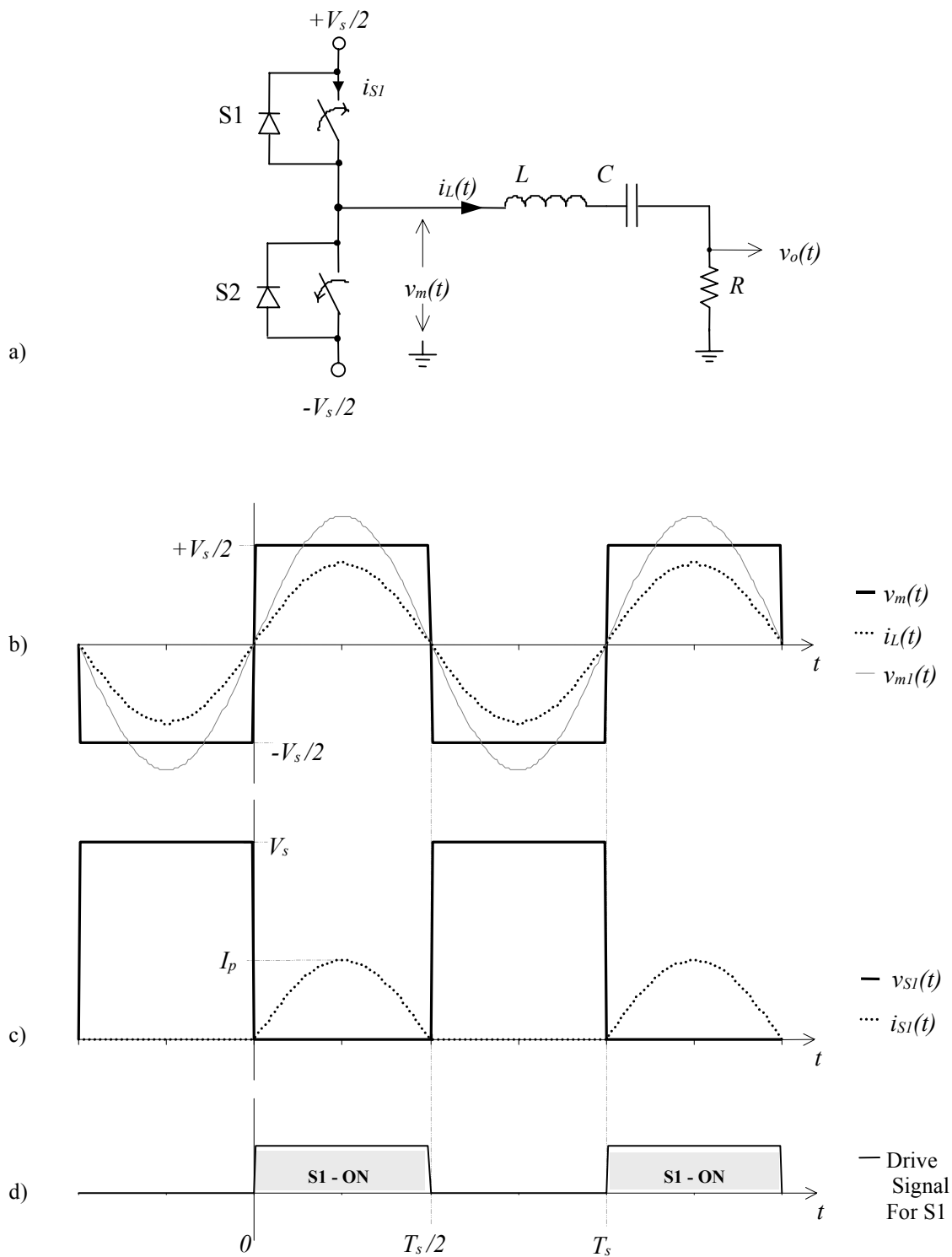
An isolated DC-DC converter basically consists of an inverter producing AC power from a DC power input, the AC power is then fed into a transformer, followed by a rectifier. A method of regulating the power flow through the inverter is used to maintain the correct DC output voltage. The desirable characteristics of an inverter used in a DC-DC converter are; high efficiency, high frequency, low EMI and a good switch utilization factor. A Class-DE inverter can potentially achieve very high efficiency at high frequencies (>1 MHz) with low switching losses, a good switch utilization factor, no turn-on current spikes and hence very low radiated EMI. This makes it a very attractive inverter for use in DC-DC converters. The design and construction of a Class-DE inverter is essentially the same whether the RF output is rectified into a DC voltage, or fed into a load, as shown in Figure 1.1. The issues investigated in this thesis will therefore be of directly applicable to designers when implementing a Class-DE type inverter in a DC-DC converter.

1.3 THESIS CONTENTS

Chapter 2 provides a description and an analysis of Class-DE operation. Design equations for calculating circuit element values are developed. The effect of a non-linear output capacitance is studied and the design equations are modified to take this effect into account. Chapter 3 deals with some of the aspects of implementing a real inverter, such as the choice of topology and the choice of the switching devices. Simulations of the inverter with the selected MOSFETs and topology are then performed. Chapter 4 investigates the various aspects of controlling the inverter in order to achieve Class-DE operation. These include driving the gate capacitance to achieve the required switching times and generation of the control signals for the high and low-side MOSFETs. Chapter 5 provides a summary of the various methods of controlling the high-side switch. A fiber optic communication-link is demonstrated to be the optimal choice, and a fiber optic link to control the high-side switch is developed. Chapter 6 investigates the aspects that affect the high frequency performance of a half-bridge inverter and deals with the design of the physical construction of the inverter. Chapter 7 presents the operating waveforms and results of the prototype inverter at various frequencies and powers. Chapter 8 investigates the effect of a mismatched load on the operation of the inverter and the factors affecting the tolerance of the inverter to mismatched loads. Conclusions drawn from the work and results presented in this thesis are given in chapter 9. Appendix A gives the derivation of the fundamental component of the midpoint voltage. Appendix B shows the HB-Plus simulation results of the theoretical design example given in chapter 2. Appendix C provides the circuit schematics of the various circuits used throughout the thesis. Appendix D gives a summary of the design equations for a Class-DE inverter developed in this thesis.

CHAPTER 2. ANALYSIS AND DESIGN EQUATIONS

2.1 THE CLASS-D VOLTAGE-FED SERIES RESONANT INVERTER



The classic Class-D voltage-fed half-bridge series resonant inverter was first introduced by Baxandall [1] and is given in Figure 2.1. It consists of a voltage-fed half-bridge inverter with a series LCR circuit added to the midpoint. The transfer function of this LCR network between the input at the inductor and the output across the resistor is given by

$$H(j\omega) = \frac{R}{R + j\omega L + \frac{1}{j\omega C}} \quad (2.1.1)$$

The natural resonant frequency, ω_r , and loaded quality factor, Q , of the LCR circuit are given by

$$\text{a) } \omega_r = \frac{1}{\sqrt{LC}} \quad \text{b) } Q = \frac{\omega_r L}{R} \quad (2.1.2)$$

An analysis of the Class-D operation begins by assuming the switches are ideal with zero switching times, no on-resistance and no parasitic capacitance [1,2,3]. As MOSFETs are the primary switching devices that are used in high frequency converters, an ideal diode is put in parallel with each switch to model the internal diode of the MOSFET. It is also assumed that all the components of the tuned LCR resonant network are lossless, time invariant and linear. For Class-D operation, the high and low-side switches of the half-bridge are alternately switched on and off with a 50% duty cycle. The mid-point voltage, $v_m(t)$, will therefore be a symmetrical square wave of amplitude $V_s/2$ as shown in Figure 2.1 (b). The Fourier series representation of $v_m(t)$ is then

$$v_m(t) = V_s \frac{2}{\pi} \sin(\omega_s t) + V_s \frac{2}{3\pi} \sin(3\omega_s t) + V_s \frac{2}{5\pi} \sin(5\omega_s t) \dots \quad (2.1.3)$$

where ω_s is the switching frequency (also referred to as the *operating frequency* or *driving frequency*) of the half-bridge inverter.

The switching frequency, ω_s , of the inverter is set *equal* to the resonant frequency, ω_r , of the LCR network, to obtain tuned series resonant operation. When this is the case, to find the output voltage across the load resistor, we must examine the Fourier series of the midpoint voltage and transfer function of the LCR network. The normalized moduli of the midpoint voltage's frequency spectrum, $|V_m(\omega)|$, and the transfer function, $|H(j\omega)|$, are plotted in Figure 2.2. The frequency spectrum of the output voltage is the product of $V_m(\omega)$ and $H(j\omega)$. The Dirac deltas of $V_m(\omega)$ thus sample the frequency response of $H(j\omega)$ at their respective frequencies. At the resonant frequency of the LCR circuit, the transfer function $H(j\omega)$ simply equals one. Thus the fundamental component of midpoint voltage, referred to as $v_{m1}(t)$, will be transmitted with no amplitude or phase change. To find the amplitude of the next most significant harmonic, namely the third, we must evaluate the transfer function at $\omega = 3\omega_r$. This can be done by using the following substitution,

$$QR = \omega_r L = \frac{1}{\omega_r C} \quad (2.1.4)$$

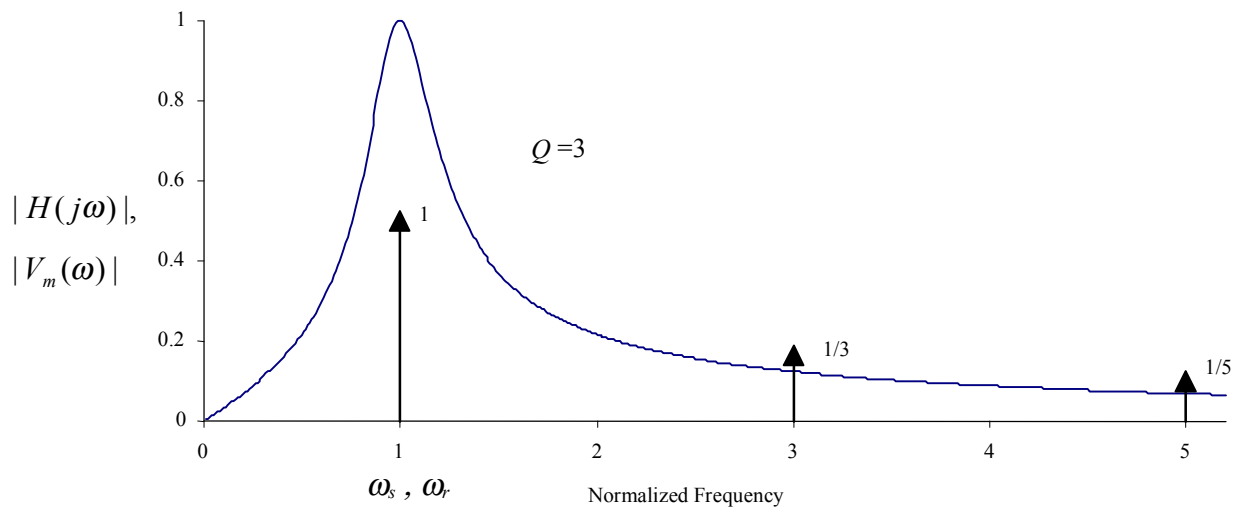


Figure 2.2 Frequency Spectrum of the Midpoint Voltage and Transfer Function of LCR tuned Circuit

Thus evaluating the transfer function at $\omega = 3\omega_r$ and using the substitutions of equation (2.1.4) we have

$$H(j3\omega_r) = \frac{3}{3 + j8Q} \quad (2.1.5)$$

and

$$|H(j3\omega_r)| = \frac{3}{\sqrt{9 + 64Q^2}} \quad (2.1.6)$$

From the Fourier series of the midpoint voltage we know that the amplitude of the third harmonic will be one third that of the fundamental. Hence the ratio of the of the third harmonic to the fundamental in the output voltage can now be found using equation (2.1.6), giving

$$\frac{|V_{m3}|}{|V_{m1}|} = \frac{1}{\sqrt{9 + 64Q^2}} \quad (2.1.7)$$

For a Q of 3, the ratio of the third harmonic to the fundamental is 4%. All higher harmonics will be reduced to an amplitude considerably less than this. The amount of harmonic content that can be tolerated depends on the application and is at the discretion of the designer. For the subsequent analysis, the Q will be assumed to be high enough to reduce all the harmonics to a negligible amount. The output voltage, $v_o(t)$, will then simply be the fundamental component of midpoint voltage, referred to as $v_{m1}(t)$, given by

$$v_o(t) = v_{m1}(t) = \frac{2V_s}{\pi} \sin(\omega_s t). \quad (2.1.8)$$

The fundamental component of the midpoint voltage, $v_{m1}(t)$, which is also the output voltage, $v_o(t)$, can be seen in Figure 2.1 (b).

The current out of the midpoint and into the LCR network (referred to as the *load current*) will be the same as the current through the load resistor. The current through the load resistor is determined by the output voltage across it and will therefore be a sinusoid in phase with the driving voltage, as shown in Figure 2.1 (b), given by

$$i_L(t) = \frac{v_o(t)}{R} = \frac{2V_s}{\pi R} \sin(\omega_s t) = I_p \sin(\omega_s t) \quad (2.1.9)$$

where

$$I_p = \frac{2 V_s}{\pi R} \quad (2.1.10)$$

The load current is alternately conducted by each switch for half a period. The current through each switch when it is on is thus a half sinusoid with a peak value of I_p . When the switch is off the voltage across it will be the rail to rail potential difference, V_s . This can be seen in Figure 2.1 (c), which shows the voltage across the high side switch S1, $v_{S1}(t)$, and the current through it, $i_{S1}(t)$. The average current, I_{S-avg} , and the RMS current, I_{S-rms} , through each switch are then

$$\text{a) } I_{S-avg} = \frac{I_p}{\pi} \quad \text{b) } I_{S-rms} = \frac{I_p}{2} \quad (2.1.11)$$

The power output, P_{out} , delivered to the load resistance is

$$P_{out} = \frac{I_p^2 R}{2} = \frac{2 V_s^2}{\pi^2 R} \quad (2.1.12)$$

An alternative way to calculate the power output is to multiply the average current delivered through each switch from the supply to the midpoint, by the supply voltage. Thus the output power can also be expressed as

$$P_{out} = \frac{V_s I_p}{\pi} \quad (2.1.13)$$

This method will be used in later power output calculations. The switch utilization factor, U , for switches used in a Class-D topology is defined by the following equation,

$$U = \frac{P_{out}}{n V_p I_p} = \frac{1}{2\pi} \quad (2.1.14)$$

where P_{out} is the power output of the inverter, n is the number of switches used and V_p and I_p are the peak voltage and current imposed stresses on each switch.. For the classic Class-D inverter $U = 1/2\pi = 0.159$, when the maximum peak current is used in the calculation. A perfect converter topology with the highest possible switch utilization factor would have a square voltage and current imposed on its switches [3]. It has a switch utilization factor of $U = 0.25$, to which Class-D compares favorably.

If the switching devices are MOSFETS however, it is more meaningful to use the maximum permissible RMS current to calculate the switch utilization factor, which then gives the ideal converter a switch utilization factor of $U = 0.354$. Using the maximum permissible RMS current to calculate the switch utilization factor for a Class-D topology, gives it a switch utilization factor of $U = 0.318$. The Class-D series resonant inverter would then compare very favorably to the ideal topology.

In Figure 2.1 (c) it can be seen that each switch never simultaneously has voltage across it and current through it. Ideally this would mean that no power is dissipated in the switches and the efficiency is theoretically 100%. However, each switch turns on at zero-load-current but must swing the midpoint voltage from one rail to the other instantaneously. In practice this is impossible, as each switching device has an output capacitance. The switch turning on will have to discharge its own capacitance and charge the other device's capacitance from one supply rail to the other. This will cause a capacitive energy loss during each switching transition and hence the total power loss, P_D , will be proportional to the switching frequency and is given by the expression,

$$P_D = 2 C_o V_s^2 f_s \quad (2.1.15)$$

where C_o is the output capacitance of each switch, and f_s is the switching frequency of the inverter. To calculate a more realistic power loss when using MOSFETs with a non-linear output capacitance, it will be more practical to use the effective output capacitance in equation (2.1.15) defined later in the text in section 2.2.4. However, from equation (2.1.15) we can see the power dissipation increases with increasing switching frequency and hence the efficiency of a Class-D series resonant inverter will therefore decrease with increasing operating frequencies.

2.2 THE CLASS-DE VOLTAGE-FED SERIES RESONANT INVERTER

2.2.1 Operation

Figure 2.3 (a) shows a voltage-fed half-bridge series resonant inverter with each switch having an output capacitance, C_o . All components are assumed to be ideal and time invariant. The inverter is operated in a similar manner to a Class-D inverter but with some key differences in order to achieve Class-DE type operation, which are now elaborated upon. The capacitive switching losses present in classic Class-D operation can be reduced by simply operating the inverter *above* the resonant frequency of the tuned circuit and reducing the conduction angle of the switches i.e. reducing the duty cycle below 50%, [3]. If the switching frequency of the inverter is above the resonant frequency of the LCR network, the load will look inductive and hence the load current will be lagging the (driving) midpoint voltage. The Q of the series resonant is assumed to be high enough to force the load current to be sinusoidal and the harmonic content negligible. The phase lag of the load current and the conduction angle of the switches can be actually be adjusted until each switch turns on when the load current is zero and there is zero voltage across it. The mechanism of operation may be described by the following sequence of events:

The conducting switch will turn off before the current through it has completed a half sinusoid. This current will then be diverted into the two output capacitances and start to charge them, and thus the midpoint voltage will swing towards the opposite rail. One output capacitance will be charging and the other will be discharging. The curve traced out by the midpoint voltage as it swings from one rail to the other during the dead-time will be the last part of a sinusoidal waveform. If the phase lag and dead-time are correct, then the midpoint voltage should reach the opposite rail as the load current reaches zero. The opposing switch now turns on with zero voltage across it and as the load current is zero, there will be *zero* dv/dt across the switch and zero current through it. The switch therefore will not have to conduct any load current as it turns on. Hence *zero-voltage and zero-load-current* turn-on is achieved [27,5,6,7]. This will give Class-E switching conditions in a traditional Class-D topology and thus this method of operation has been termed Class-DE [7]. The energy stored in the output capacitances is simply oscillated from one to the other with no power dissipation occurring. These effects can be seen in the waveforms of Figure 2.3. Class-DE effectively utilizes the intrinsic output capacitances of the switching devices as loss-less snubbers and hence this method of operation is theoretically 100% efficient.

If the load current is defined as,

$$i_L(t) = I_p \sin(\omega_s t) \quad (2.2.1)$$

and the inverter is operated in Class-DE mode, then the waveforms shown in Figure 2.3 are obtained. Shown in Figure 2.3 (b) is the midpoint voltage, $v_m(t)$, the current out of the midpoint, $i_L(t)$, and the fundamental component of the midpoint voltage, $v_{m1}(t)$. Figure 2.3 (c) shows the voltage across, $v_{S1}(t)$, and the current through, $i_{S1}(t)$, the high side switch, S1. Figure 2.3 (d) shows the current through the high side switch's output capacitance, $i_{C1}(t)$. The voltage and current waveforms for S2 are identical to those of S1 but are phase shifted by exactly 180°.

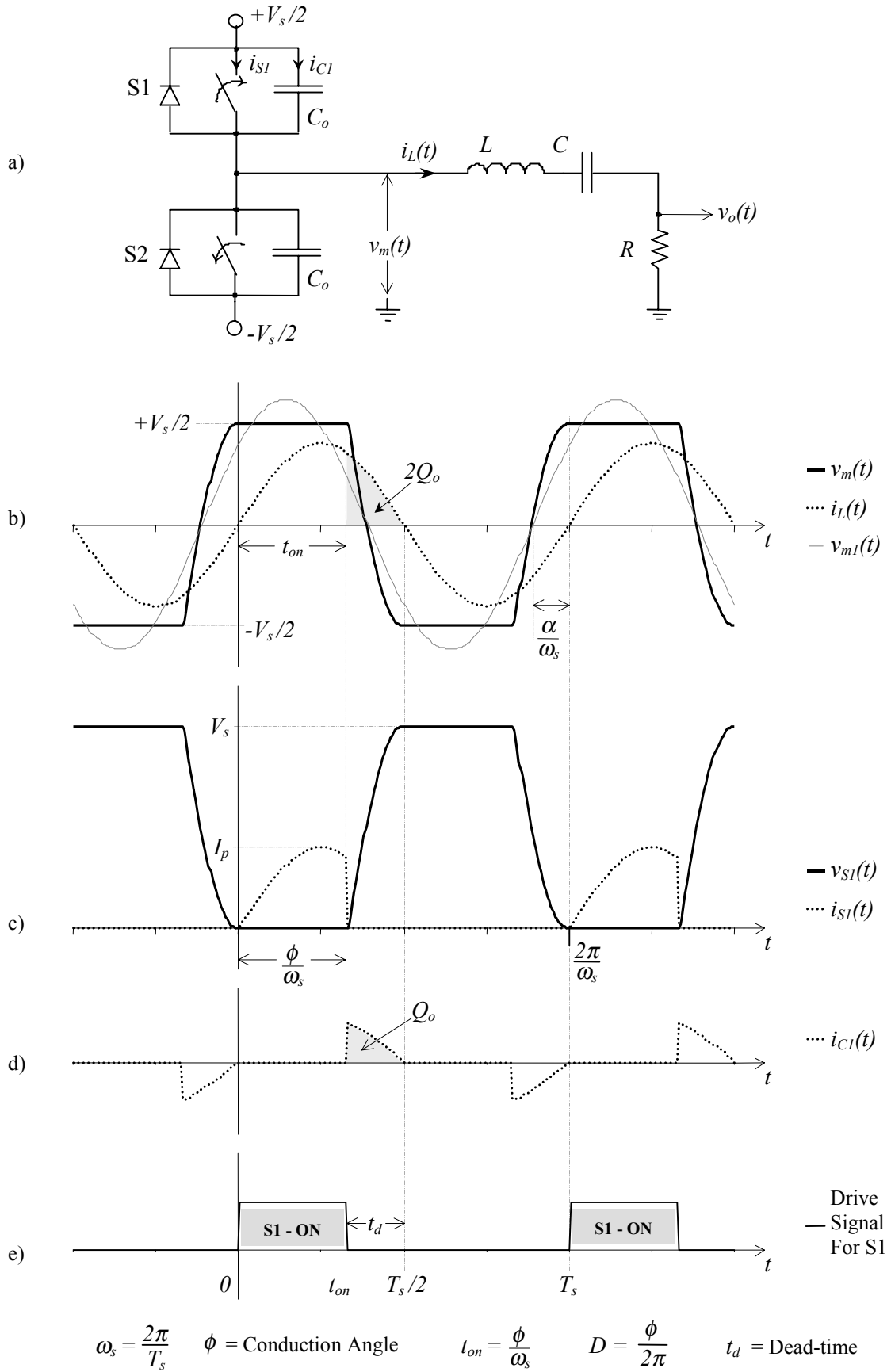


Figure 2.3 Schematic and Operational Waveforms of a Class-DE Inverter

The analysis of Class-DE operation begins by examining the conditions under which zero-voltage and zero-load-current turn-on is achieved. In order to achieve zero-voltage and zero-load-current turn-on, the total charge, $2Q_o$, removed from midpoint by the load current during the dead-time must equal the total charge required to charge both output capacitances through a voltage of V_s . To calculate the conduction angle (or duty-cycle, D) required to obtain this, these two are equated, giving

$$2Q_o = 2C_o V_s$$

$$\text{Expanding for } 2Q_o \quad \int_{\phi/\omega_s}^{\pi/\omega_s} I_p \sin(\omega_s t) dt = 2C_o V_s \quad (2.2.2)$$

This can be solved for $\cos \phi$ giving

$$\cos \phi = \frac{2\omega_s C_o V_s}{I_p} - 1 \quad \phi \in [0, \pi] \quad (2.2.3)$$

The conduction angle of the switches can vary from zero to a maximum value of 180° . A conduction angle of 180° represents the classic Class-D operation. The maximum frequency of operation for a given I_p and C_o is obtained when the conduction angle approaches its minimum value (i.e. zero). Setting the conduction angle to zero gives a *maximum operating frequency* of

$$\omega_{\max} = \frac{I_p}{C_o V_s} \quad (2.2.4)$$

Thus for high-frequency operation, a high ratio of I_p/V_s and a low output capacitance, C_o , are preferable. A more realistic minimum conduction angle of 90° gives a maximum operating frequency of half of the above. The above expression is only valid for Class-DE operation. Higher frequencies can be achieved if capacitive switching losses are allowed.

The average current through each switch for a conduction angle of ϕ may be expressed as

$$\begin{aligned} I_{S-avg} &= \frac{1}{T_s} \int_0^{t_{on}} I_p \sin(\omega_s t) dt \\ &= \frac{I_p}{2\pi} (1 - \cos \phi) \end{aligned} \quad (2.2.5)$$

The RMS current through each switch for a conduction angle of ϕ is

$$\begin{aligned} I_{S-rms} &= \sqrt{\frac{1}{T_s} \int_0^{t_{on}} I_p^2 \sin^2(\omega_s t) dt} \\ &= \frac{I_p}{2} \sqrt{\frac{(2\phi - \sin 2\phi)}{2\pi}} \end{aligned} \quad (2.2.6)$$

Apart from the usual ratings of a switch, another specification is of importance at high frequencies and pertains to the maximum allowed rate of change of voltage across the switch. The *maximum voltage slew rate* (dv/dt) imposed on a switch occurs at the instant of its turn off. At this point the load current has a value of $I_p \sin\phi$ and it is all being diverted into the two output capacitances, thus using $dv/dt = I/C$, we have

$$\frac{dv}{dt}_{MAX} = \frac{I_p}{2C_o} \sin\phi \quad (2.2.7)$$

At operating frequencies considerably lower than the upper limit of the MOSFET, discrete capacitance may be added to the midpoint to increase C_o , hence lowering the dv/dt and reducing the amount of EMI produced.

The power output of the inverter can be calculated by multiplying the average current delivered through each switch by the supply voltage, giving

$$P_{out} = \frac{V_s I_p}{2\pi} (1 - \cos\phi) \quad (2.2.8)$$

From this equation, it can be seen that power flow through the inverter may be controlled by varying the conduction angle. As the conduction angle is varied from 180° to zero, the power output will be reduced from its maximum value down to zero. This should be useful in such applications as DC-DC converters.

The switch utilization factor, U , of Class-DE operation depends on the conduction angle and is given below

$$U = \frac{P_{out}}{n V_p I_p} = \frac{1}{4\pi} (1 - \cos\phi) \quad (2.2.9)$$

The switch utilization factor approaches that of a Class-D topology (0.159), as the conduction angle approaches 180° . For a conduction angle of 90° , the switch utilization factor is 0.08.

2.2.2 Fundamental Component of the Midpoint Voltage

The path the midpoint voltage traces out during the first dead-time will be a part of a sinusoid and is given by

$$v_m(t) = -\frac{1}{2C_o} \int I_p \sin(\omega_s t) dt + K \quad t \in [t_{on}, T_s/2] \quad (2.2.10)$$

Integrating and using the boundary condition that $v_m(t_{on}) = V_s/2$, gives

$$v_m(t) = \frac{V_s}{(1 + \cos\phi)} \cos(\omega_s t) + \frac{V_s}{2} \left[\frac{1 - \cos\phi}{1 + \cos\phi} \right] \quad t \in [t_{on}, T_s/2] \quad (2.2.11)$$

A similar result can be obtained for the path the midpoint voltage traces out during the second dead-time. The midpoint voltage is thus defined for a full period and its fundamental component can be found using Fourier analysis. If a complex exponential Fourier series representation of the midpoint voltage is used, the positive coefficient of the fundamental component is shown in Appendix A to be

$$\bar{V}_1 = \frac{V_s}{2\pi(1+\cos\phi)} \left[(\pi - \phi + \sin\phi \cos\phi) - j \sin^2\phi \right] \quad (2.2.12)$$

The fundamental component, $v_{m1}(t)$, of the midpoint voltage, $v_m(t)$, is then shown in Appendix A to be given by

$$v_{m1}(t) = 2 |\bar{V}_1| \cos(\omega_s t + \beta) \quad (2.2.13)$$

where
$$|\bar{V}_1| = \frac{V_s}{2\pi(1+\cos\phi)} \sqrt{(\pi - \phi + \sin\phi \cos\phi)^2 + \sin^4\phi} \quad (2.2.14)$$

and
$$\beta = \tan^{-1} \left(\frac{-\sin^2\phi}{\pi - \phi + \sin\phi \cos\phi} \right) \quad (2.2.15)$$

The amplitude of the fundamental varies from $2V_s/\pi$ for a conduction angle of 180° , down to $V_s/2$ for a conduction angle of zero. The phase angle, α , between the fundamental and the load current will then be given by, $\alpha = \beta + \pi/2$. This is equivalent to shifting the fundamental by 90° which can be done by multiplying its phasor representation by j . Hence the phase angle α may be expressed as

$$\alpha = \tan^{-1} \left(\frac{\pi - \phi + \sin\phi \cos\phi}{\sin^2\phi} \right) \quad (2.2.16)$$

A graph of the phase angle, α , versus the conduction angle, ϕ , is shown in Figure 2.4. From Figure 2.4 it can be seen that for a conduction angle of 180° (i.e. classic Class-D operation), the phase angle is zero and so the load current will be in phase with the fundamental as expected. As the conduction angle is reduced the phase lag of the load current is increased, reaching 90° for a conduction angle of zero. At this point the load appears as a pure inductance and hence there will be zero power output.

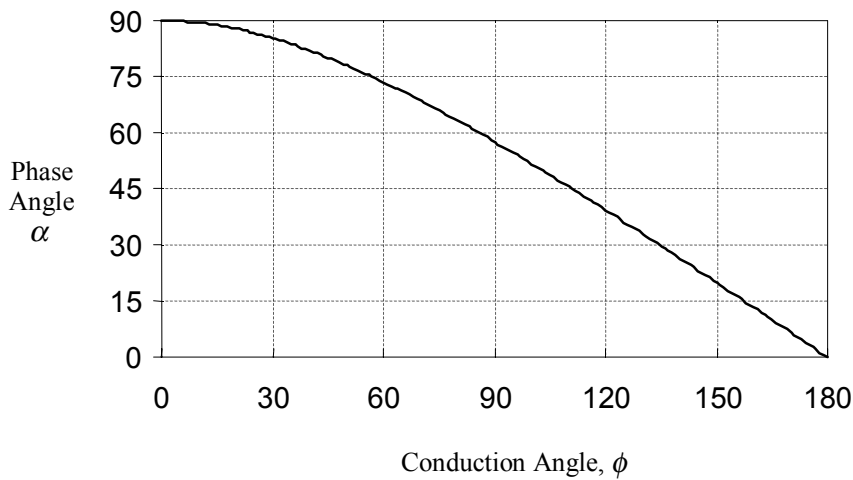


Figure 2.4 The Phase Angle, α , between the Load current and the Fundamental Component of the Midpoint Voltage versus the Conduction Angle, ϕ .

2.2.3 LCR Series Resonant Network

The characteristic parameters of a series LCR network are defined below

$$\text{The natural resonant frequency} \quad \omega_r = \frac{1}{\sqrt{LC}} \quad (2.2.16)$$

$$\text{The loaded quality factor} \quad Q = \frac{\omega_r L}{R} = \frac{1}{\omega_r CR} \quad (2.2.17)$$

The input impedance of the LCR network at a frequency of ω is given by

$$\bar{Z} = R + j \left(\omega L - \frac{1}{\omega C} \right) = R \left[1 + jQ \left(\frac{\omega}{\omega_r} - \frac{\omega_r}{\omega} \right) \right] \quad (2.2.18)$$

$$= |\bar{Z}| e^{j\theta} = R + jX \quad (2.2.19)$$

where

$$|\bar{Z}| = R \sqrt{1 + jQ^2 \left(\frac{\omega}{\omega_r} - \frac{\omega_r}{\omega} \right)^2} \quad (2.2.20)$$

$$\theta = \tan^{-1} \left[Q \left(\frac{\omega}{\omega_r} - \frac{\omega_r}{\omega} \right) \right] \quad (2.2.21)$$

$$R = |\bar{Z}| \cos \theta \quad (2.2.22)$$

$$X = |\bar{Z}| \sin \theta \quad (2.2.23)$$

Dividing equation (2.2.23) by (2.2.22) and equating the result to equation (2.2.21) we have

$$\tan \theta = \frac{X}{R} = Q \left(\frac{\omega}{\omega_r} - \frac{\omega_r}{\omega} \right) \quad (2.2.24)$$

For Class-DE operation the load current must be lagging the fundamental component of the midpoint voltage. The inductive reactance required to obtain a lagging load current can simply be achieved by driving the LCR network above its resonant frequency. The fundamental component of the midpoint voltage will then see an *Effective Load Impedance*, \bar{Z} , comprised of jX and R . The LCR network may then be separated into a hypothetical equivalent circuit, shown in Figure 2.5, consisting of a series resonant tank (L_s and C) and the effective load impedance, \bar{Z} . The series resonant tank can be considered to eliminate all of the harmonics of the midpoint voltage except for the fundamental component, which will appear across the effective load impedance \bar{Z} . To find out what the effective load impedance must be for Class-DE operation, the fundamental component of the midpoint voltage must be related to the load current.

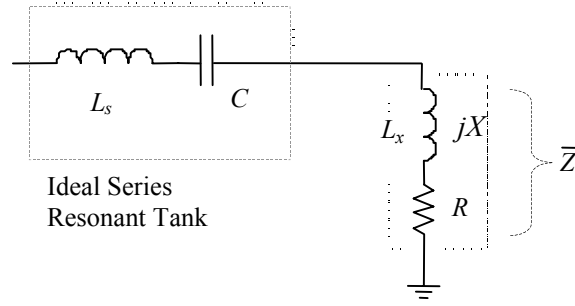


Figure 2.5 Effective Load Impedance Representation of the LCR Series Resonant Network

The fundamental component, $v_{m1}(t)$, can be represented by the real part of the phasor $2\bar{V}_1 e^{j\omega_s t}$, as shown in Appendix A. The load current can be represented by the real part of the phasor $-jI_p e^{j\omega_s t}$. Hence the effective load impedance required to achieve the correct magnitude and phase lag of the load current can be found by using the phasor relationship $\bar{V} = \bar{I} \cdot \bar{Z}$, giving

$$2\bar{V}_1 e^{j\omega_s t} = -jI_p e^{j\omega_s t} \cdot \bar{Z} \quad (2.2.25)$$

Rearranging for \bar{Z} gives

$$\begin{aligned} \bar{Z} &= \frac{2\bar{V}_1}{-jI_p} \\ &= \frac{V_s}{\pi I_p} (1 - \cos \phi) + j \frac{V_s}{\pi I_p} \left[\frac{\pi - \phi + \sin \phi \cos \phi}{1 + \cos \phi} \right] \end{aligned} \quad (2.2.26)$$

Putting $\bar{Z} = R + jX$ where R is the real part of the load impedance and X is the reactive part (inductive), then

$$R = \frac{V_s}{\pi I_p} (1 - \cos \phi) \quad (2.2.27)$$

$$X = \frac{V_s}{\pi I_p} \left[\frac{\pi - \phi + \sin \phi \cos \phi}{1 + \cos \phi} \right] \quad (2.2.28)$$

For Class-DE operation, the equations above show what the effective load impedance must be with various conduction angles and operating impedance levels ($\sim V_s/I_p$). It can be seen how R and X vary over the full range of the conduction angle by normalizing R and X to R' and X' by setting $V_s/I_p = 1$. Figure 2.6 shows plots of R' and X' versus the conduction angle.

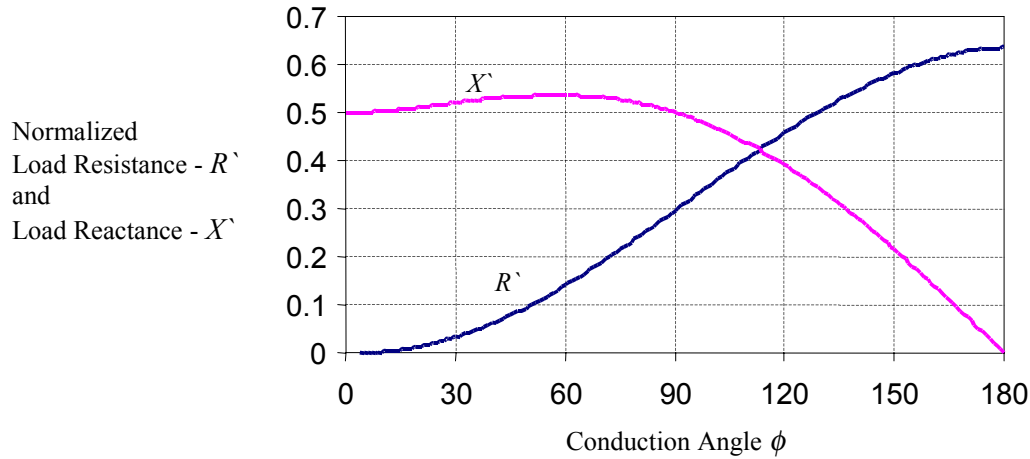


Figure 2.6 Normalized Effective Load Resistance and Reactance versus the Conduction Angle

The required circuit element values of the LCR network to obtain Class-DE operation must now be found. The resistance will simply be the value given by equation (2.2.27). The values of the inductance and capacitance in the LCR network can now be found by using the values of R and X calculated in equations (2.2.27) and (2.2.28) in equation (2.2.24). Thus we have

$$\tan \theta = \tan \alpha = \frac{X}{R} = \frac{\pi - \phi + \sin \phi \cos \phi}{\sin^2 \phi} = Q \left(\frac{\omega_s}{\omega_r} - \frac{\omega_r}{\omega_s} \right) \quad (2.2.29)$$

Rearranging the above equation will result in a quadratic equation in ω_r . Taking the positive root of the quadratic gives the following expression for ω_r

$$\omega_r = \frac{\omega_s}{2} \left[\sqrt{\left(\frac{\tan \alpha}{Q} \right)^2 + 4} - \frac{\tan \alpha}{Q} \right] \quad (2.2.30)$$

The switching frequency ω_s and $\tan \alpha$ are known and the designer must now select the desired value for the Q of the LCR network (usually in the region of 3 to 5). The natural resonant frequency ω_r of the LCR network can then be calculated. Using this value of ω_r , the value of the inductance and capacitance in the LCR network can be found using the following two expressions

$$\text{a) } L = \frac{QR}{\omega_r} \quad \text{b) } C = \frac{1}{\omega_r^2 L} \quad (2.2.31)$$

An alternative method to calculate the circuit element values of the LCR network is for the designer to specify the series resonant capacitance, C, as opposed to the Q of the network. The inductance of the LCR circuit can then be found using the equivalent circuit representation of the LCR network giving

$$L_x = \frac{X}{\omega_s} \quad L_s = \frac{1}{\omega_s^2 C} \quad L = L_s + L_x \quad (2.2.31)$$

The inductive reactance of the load impedance is achieved by driving the LCR circuit above its resonant frequency. The amount above the resonant frequency, ω_r , by which the LCR circuit must be driven depends on the Q of the LCR network and the conduction angle required. An expression showing the ratio of the switching frequency, ω_s , to the resonant frequency, ω_r , can be found using equation (2.2.30) and is given below

$$\frac{\omega_r}{\omega_s} = \frac{1}{2} \left[\sqrt{\left(\frac{\tan \alpha}{Q}\right)^2 + 4} - \frac{\tan \alpha}{Q} \right] \quad (2.2.32)$$

Plots of ω_s/ω_r versus the conduction angle and for various values of Q are given in Figure 2.7. For a given Q , conduction angle and desired operating frequency, ω_s , the required resonant frequency of LCR network can be found from Figure 2.7.

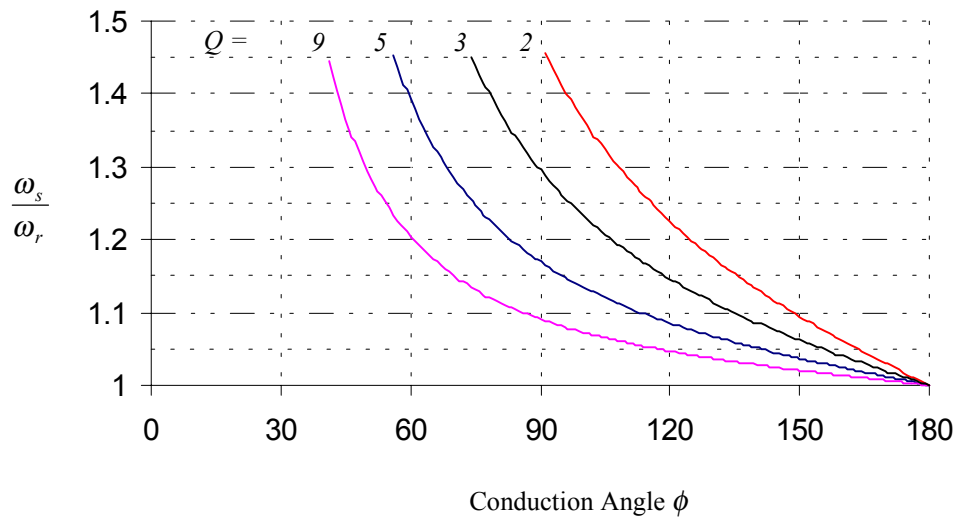


Figure 2.7 Switching frequency required referenced to the resonant frequency of the LCR network versus the conduction Angle

2.2.4 The Effect of a Non-Linear Output Capacitance

For high frequency (>1 MHz) and high power (>100 W), the most suitable switching devices are currently MOSFETs. If the operating frequency is approaching the upper limits of the MOSFET, any added capacitance to the midpoint should be kept to a minimum and the output capacitance will be predominated by the intrinsic output capacitance of the device [13,55]. The output capacitance of a MOSFET is highly non-linear and varies with the applied drain-source voltage. A plot of the output capacitance of an IRF450 versus drain source voltage is given in Figure 2.8. This variation of output capacitance with applied drain-source voltage is typical of most MOSFETs.

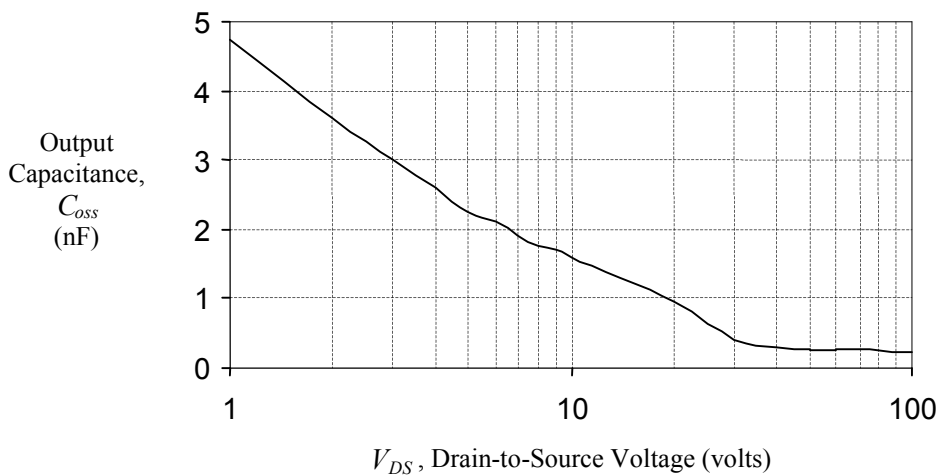


Figure 2.8 Output Capacitance of an IRF450 MOSFET (Reproduced from Manufacturer's Data Sheet)

This large variation of the output capacitance leads to a difficulty in selecting an actual value for the output capacitance when calculating the conduction angle. The output capacitance given in the data sheet of a MOSFET is specified at $V_{DS} = 25$ V. This value of capacitance will not give an accurate result if used in Equation (2.2.3) to calculate the conduction angle. An alternative method of calculating the conduction angle is now developed to take in account the effect of the non-linear capacitance.

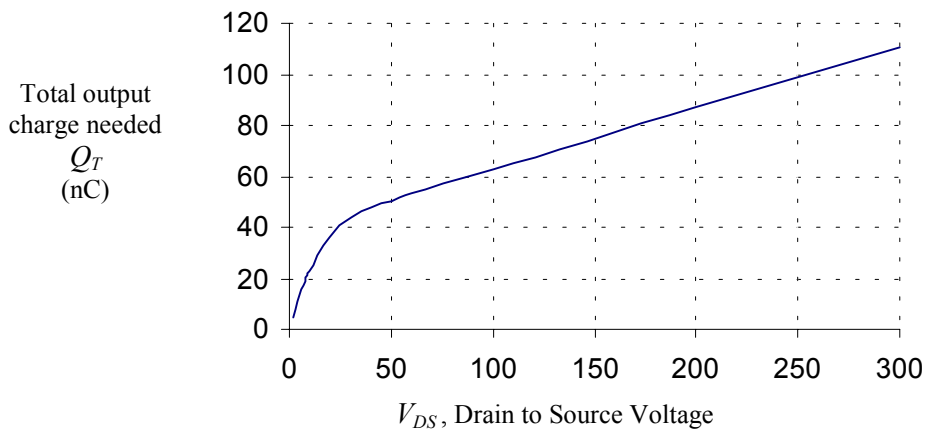


Figure 2.9 Total charge needed, Q_T , to charge the output capacitance of an IRF450 to V_{DS}

Figure 2.9 shows the total amount of charge needed, Q_T , to charge the output capacitance of an IRF450 to a drain source voltage of V_{DS} . The charge needed can either be measured experimentally (with the gate-source shorted) or calculated using numerical integration of the output capacitance given in the data sheets [9]. Figure 2.9 is the result of such a numerical integration. The energy stored in the output capacitance is the area between the y-axis and the charging curve of Figure 2.9.

This non-linear capacitance will affect the shape of the midpoint voltage as it swings from one rail to the other during the dead-time, which will no longer be sinusoidal. To study the affect that this non-linear capacitance has on the midpoint voltage, it will be assumed that the output capacitance is a *loss-less* non-linear capacitor with no hysteresis i.e. the energy required to charge it equals the energy returned during discharging and the charge/discharge curves are identical. It is also assumed that the load current is still sinusoidal and that the inverter is operating in Class-DE mode. With these assumptions, the effect that this loss-less non-linear capacitor has on the shape of the midpoint voltage can be calculated using numerical integration. The result of such a numerical integration can be seen in Figure 2.10, which shows the voltage across the high side switch, $v_{SI}(t)$, for both a linear and a non-linear output capacitance, and the current into the high side switch, $i_{SI}(t)$, which is the same in both cases. The waveforms observed experimentally showed a similar effect on the midpoint voltage.

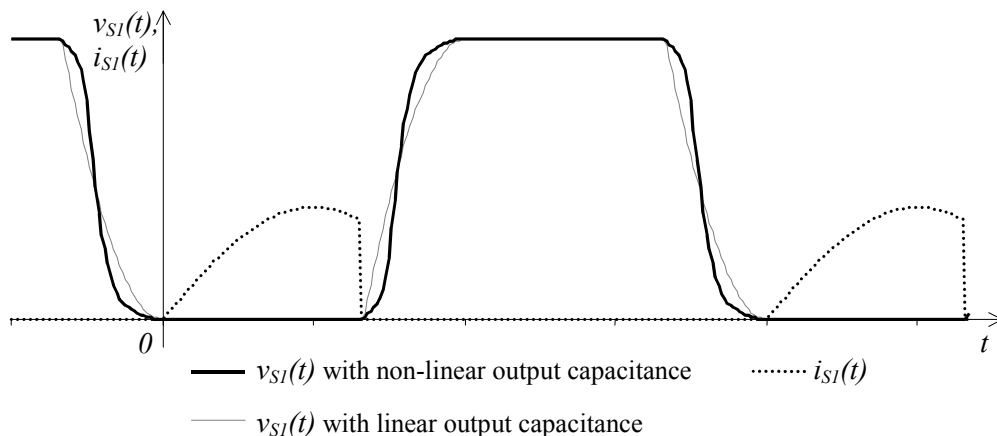


Figure 2.10 The affect of a Non-Linear Output Capacitance on the Midpoint Voltage

This non-linear capacitance has a number of advantageous effects for high frequency operation. The first is that it will lower the initial dv/dt imposed on the switch immediately after turn-off. For the interval just after turn-off, the drain-source voltage is kept at a lower value for a longer time, and as a real switch will take a finite time to turn off, this will lessen the turn-off switching losses. For the interval just before turn-on, the drain-source voltage stays close to zero for a longer time allowing more latitude of the turn-on instant. As the switch turning off will have a larger output capacitance, a larger portion of the load current will be shunted into its capacitance and so less current has to be commutated into the opposite switches output capacitance. Hence both switches will experience a lower di/dt at the switch off instant.

From Figure 2.9 we can see that a MOSFET will require a specific amount of charge, Q_T , to raise its drain-source voltage to a given supply voltage, V_s . If the inverter is operating in Class-DE mode, then we can say the charge removed from the midpoint by the load current must equal the total charge needed to raise one and lower the other output capacitance of each MOSFET through a voltage of V_s . Thus, to calculate the conduction angle needed for this supply voltage, we can equate the charge removed from the midpoint during the dead-time to Q_T , giving

$$2Q_o = 2Q_T$$

$$\int_{\phi/\omega_s}^{\pi/\omega_s} I_p \sin(\omega_s t) dt = 2Q_T \quad (2.2.33)$$

Solving the integral, we have

$$\cos \phi = \frac{2\omega_s Q_T}{I_p} - 1 \quad (2.2.34)$$

This equation has effectively replaced $C_o V_s$ with the total charge needed to charge the output capacitance, Q_T , and as Q_T is a measurable fixed quantity, it will give a more definitive result for the conduction angle required. As Q_T is a non-linear function of V_s , the conduction angle required (given a constant load) will now vary as V_s changes and the conduction angle calculated above will only be true for one value of the supply voltage.

A useful quantity to the designer, namely the *effective output capacitance*, C_{o-eff} , of the MOSFET is now defined as

$$C_{o-eff} = \frac{Q_T}{V_s} \quad (2.2.35)$$

This is the effective output capacitance of the MOSFET at only one particular supply voltage. However, if it is calculated for its normal operating voltage level e.g. 80% of its maximum V_{DS} , it will give the designer a good measure of the MOSFET high-frequency characteristics. This value of output capacitance can be used in simulations of the inverter, in power dissipation calculations and in equation (2.2.4) to calculate the maximum operating frequency. It will also give the same result as equation (2.2.34) for the conduction angle if used in equation (2.2.3).

If turn-on occurs at zero-load-current, then the power delivered can be calculated as before in equation (2.2.8) by multiplying average current through each switch by the supply voltage, giving

$$P_{out} = \frac{V_s I_p}{2\pi} (1 - \cos \phi) \quad (2.2.36)$$

Since this result is not dependent on the wave-shape of the midpoint voltage during the dead-time, this equation will hold for non ZVS provided turn on occurs at zero-load-current. If the output capacitance is loss-less, the real part of the load impedance may be calculated by equating power delivered to power dissipated, giving

$$\frac{V_s I_p}{2\pi} (1 - \cos \phi) = \frac{I_p^2 R}{2} \quad (2.2.37)$$

Rearranging the above for R we have

$$R = \frac{V_s}{\pi I_p} (1 - \cos \phi) \quad (2.2.38)$$

This is the result obtained previously in equation (2.2.27) using the effective load impedance approach, however this result shows that the value of R required is not dependent on the shape of the midpoint voltage during the dead-time. The phase of the fundamental of the midpoint voltage with a non-linear capacitance will be similar to that of the one with a linear capacitance. Thus, the inductance and capacitance required in the LCR network may be found to a good degree of accuracy by using the conduction angle calculated in (2.2.34) in the equations developed previously (2.2.27-2.2.31) using the effective load impedance approach.

2.2.5 Design Example

A summary of the design equations and procedure followed when designing a half-bridge Class-DE inverter is given in Appendix D. A typical design procedure for a Class-DE inverter would start by selecting the desired operating Voltage V_s and peak current I_p for a particular switching device. In this case, the switching devices being used are two IRFP450 MOSFETS. These are 500 V, 14 A devices with an output capacitance of, $C_{oss} = 720$ pF, specified at $V_{DS} = 25$ V. The supply voltage of the inverter is selected to be $V_s = 300$ V, the peak current through the device to be $I_p = 16$ A, and the desired operating frequency to be 5 MHz. The conduction angle required at this supply voltage, operating current and frequency must now be calculated. If the specified output capacitance, C_{oss} , given in the data sheet as 720 pF, is used in equation (2.2.3), then

$$\phi = \cos^{-1} \left(\frac{2\omega_s C_o V_s}{I_p} - 1 \right) = 99^\circ$$

The above method produces an inaccurate value of ϕ because of the large variation of the output capacitance, but is included here for comparison with the total charge method. The total charge needed to charge the output capacitance to 300 V can be seen from Figure 2.9 to be 110 nC. Using $Q_T = 110$ nC in equation (2.2.34), we have

$$\phi = \cos^{-1} \left(\frac{2\omega_s Q_T}{I_p} - 1 \right) = 125^\circ$$

This is a more accurate result and thus this conduction angle will be used in the following calculations. The power output of the inverter will be given by equation (2.2.8), thus

$$P_{out} = \frac{V_s I_p}{2\pi} (1 - \cos \phi) = 1.202 \text{ kW}$$

The phase lag, α , between the fundamental component of the midpoint voltage and the load current can be found using equation (2.2.16), hence

$$\alpha = \tan^{-1} \left(\frac{\pi - \phi + \sin \phi \cos \phi}{\sin^2 \phi} \right) = 36^\circ$$

The designer must now select the desired value of the Q of the resonant LCR network (usually about 3 to 5). Selecting $Q = 3.74$ (this value is selected with prior knowledge of the actual practical value of the series resonant capacitance used later in the text), the natural resonant frequency of the LCR network can then be found using equation (2.2.30), giving

$$f_r = \frac{f_s}{2} \left[\sqrt{\left(\frac{\tan \alpha}{Q} \right)^2 + 4} - \frac{\tan \alpha}{Q} \right] = 4.54 \text{ MHz}$$

Using this value of f_r , the value of the resistance, inductance and capacitance in the LCR network can be found using equation (2.2.27) and the following expressions (where $\omega_r = 2\pi f_r$)

$$R = \frac{V_s}{\pi I_p} (1 - \cos \phi) = 9.4 \Omega$$

$$L = \frac{QR}{\omega_r} = 1.23 \mu\text{H} \quad C = \frac{1}{\omega_r^2 L} = \frac{1}{\omega_r QR} = 1 \text{ nF}$$

The Average current and RMS current through each switch can be using equation (2.2.22) and (2.2.23)

$$I_{S-avg} = \frac{I_p}{2\pi} (1 - \cos \phi) = 4 \text{ A} \quad I_{S-rms} = \frac{I_p}{2} \sqrt{\frac{(2\phi - \sin 2\phi)}{2\pi}} = 7.3 \text{ A}$$

To summarize:

The total inductance of the LCR network must be 1.23 μH , the capacitance is 1 nF and the load resistance is 9.4 Ω . The resonant frequency of the LCR network will be 4.54 MHz. The peak current through the MOSFETs is 16 A, the RMS current is 7.3A and the maximum voltage across them will be 300 V. The power output of the inverter will be 1.2 kW at 5 MHz, and the switches will have to be operated at a conduction angle of 125 $^\circ$ (i.e. a duty cycle of 35 %).

The theoretical analysis and design equations were confirmed by simulation on HB-Plus. The above design example was simulated on HB-Plus [57] using ideal switches with an effective output capacitance of 367 pF (calculated using equation (2.2.35)). The results can be seen in Appendix B and are in excellent agreement with theoretical predictions.

2.6 Other Class-DE Topologies

The two other topology types capable of operating in Class-DE mode are the voltage-fed series resonant full-bridge inverter and the voltage-fed series resonant push-pull inverter. The principle of the operation is identical to that of a half-bridge. The design equations for these will require impedance transformations of the equations developed for a half-bridge inverter. The various realizations of these two topologies are not investigated here. One fact of concern in a push-pull inverter however, is that when a switch turns off, half the current will be commutated into its output capacitance, but the other half must be instantaneously commutated into the other leg of the transformer, to charge the other switch's output capacitance. Rapidly changing currents in transformers will cause practical problems. In addition to Class-DE inverters, a family of Class-DE rectifiers has also been introduced by Hamill [8,25]. This gives rise to the possibility of Class-DE² DC/DC converters but neither of these is discussed here.

CHAPTER 3. TOPOLOGY, SWITCHING DEVICES AND SIMULATION

3.1 CHOICE OF THE TOPOLOGY

The three main realizations of a Class-DE inverter are in the form of a half-bridge inverter, full-bridge inverter and a push-pull inverter. Push-Pull offers some advantages over the full-bridge or half-bridge form. The main advantage of the push-pull form is that the drive signals (i.e. Gate drive signal) for both switches are referenced to ground. Hence there is no level shifting required and an absence of all its associated practical problems. For this reason the first attempt of implementing a Class-DE inverter was in the form of a 1 MHz, 500 W push-pull inverter using a conventional transformer. However, there are some inherent limitations of a push-pull inverter associated with its coupling transformer. Conventional transformers have a maximum frequency and power limit. They also have inherent parasitic leakage inductances, coupling capacitances and winding capacitances. These parasitics made the operational waveforms of the push-pull inverter extremely oscillatory and thus very difficult to adjust the inverter to Class-DE operation. A better solution when implementing a push-pull topology would be to use a hybrid-balun type transformer with the DC supply connected to the common center terminal. This has a better high frequency response than a conventional transformer but will still have the limitations mentioned above. High efficiency operation may possibly be attained with some tuning at a specific frequency but some ringing will always be present. Thus using a push-pull topology it is difficult to obtain discernible Class-DE operation in the HF band at power levels above a few hundred watts.

A half-bridge inverter has a major advantage over a push-pull topology in that it does not require a transformer and hence does not have the inherent practical limitations associated with it. If the parasitic impedances due to the inter-connections and the physical construction of the inverter can be reduced to an acceptably low magnitude at the operating frequency, then a half-bridge inverter is almost certain to be perform as expected. The actual operation of a half-bridge inverter can be deduced from the midpoint voltage and load current for almost all load conditions. The inverter can be adjusted to Class-DE mode of operation by simply observing the midpoint voltage. A half-bridge inverter is fundamentally a very broadband topology and its bandwidth can potentially extend from DC to its highest designed operating frequency. However, the major disadvantage of a half bridge inverter is that it has two independent switches, one of which is floating. Hence, in the MHz region, there are considerable practical problems associated with physical construction of the half-bridge inverter and layout difficulties caused by having two independent switches. Likewise, the control, timing and gate-drive of two independent MOSFETs, one of which is floating, present some challenging technical problems in the MHz region. However, the practical problems associated with a half-bridge inverter at high powers and high frequencies (MHz region) are found in this thesis to be solvable to a satisfactory degree.

A full-bridge inverter has the same switch utilization factor as a half-bridge inverter. However it requires four switches instead of two, which multiply the technical problems associated with the physical construction of the inverter and time skew between the various drive signals. At MHz frequencies, a full-bridge inverter thus offers

no advantages over a half-bridge inverter. It is therefore the author's opinion that the most suitable topology for a Class-DE inverter operating, in the HF band at power levels greater than a few hundred watts, is a voltage-fed half-bridge series resonant inverter.

3.2 CHOICE OF THE SWITCHING DEVICE

An ideal switch should have no on-resistance, an infinite blocking voltage capability, no parasitic inductance or capacitance and infinitesimal switching times. The switch should require minimal energy to change its state from on to off or vice-versa. Solid-state transistors approximate an ideal switch to a good degree up to many kHz. They have enabled power switch-mode type circuits to be widely implemented for many applications.

The principal requirement of a switching device used in a switch-mode type circuit is that it has fast enough switching times for operation at the desired frequency. As a rough guide it should be capable of switching completely on or off in less than 5% of the period. Presently, the solid-state power devices most suited for switching operation in the MHz region, are switch-mode and RF MOSFETs [16]. MOSFETs have fast switching times as they are majority carrier devices and hence their turn off time is not dependent on the recombination of minority carriers. The most common and fastest power MOSFET is an n-channel enhancement type.

3.2.1 N-Channel Enhancement-Type MOSFET

Figure 3.1 shows a cross section of a cell of planar vertical MOSFET typically used in power MOSFETs. The power MOSFET is comprised of many of these parallel-connected enhancement-mode MOSFET cells which cover the surface of the silicon die.

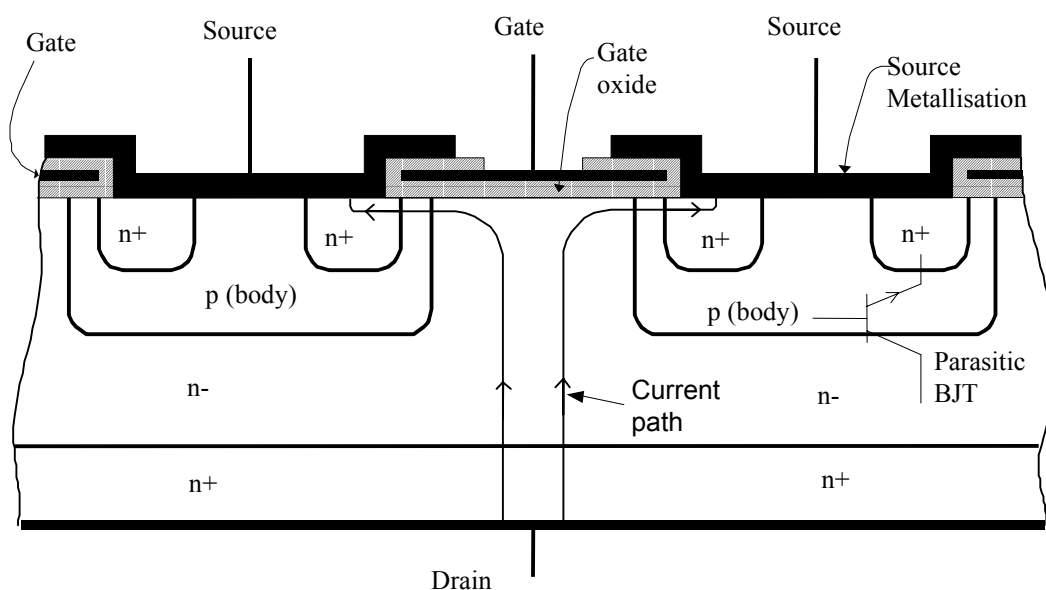
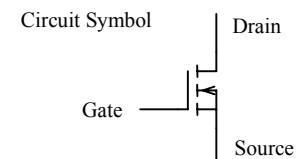


Figure 3.1 Structure of a vertical n-channel enhancement-type MOSFET

A n-channel MOSFET consists of a lightly doped p-type substrate between two n-type regions which form the drain and source. The region between the drain and source is termed the channel. Surface metallisation forms the source and drain contacts together with the gate electrode. The gate electrode is separated from the p-type substrate by an insulating layer of silicon dioxide. The source is usually shorted to the p-type substrate body as shown in Figure 3.1. When a positive field is applied between the gate electrode and the p-type substrate by increasing the gate-source voltage, n-type charge carriers are attracted into the channel region. If the gate-source voltage is increased sufficiently, the net negative charge density at the surface of the substrate becomes greater than the positive charge density causing the surface layer to invert, becoming n-type. This surface inversion layer provides a conducting channel between the n^+ source and drain regions.

The theoretical bandwidth of a MOSFET is dependent on the time it takes for the charge carriers to transverse the channel region. The theoretical switching time of the device will therefore be determined by the channel length and the drift velocity of the charge carriers. For a channel length of one micron and a drift velocity for electrons of 90km/s, the theoretical switching time is 12ps [9]. This is never approached in practice because of the various parasitic capacitances associated with the die structure and stray impedances due to packaging etc. limit the rate of change of voltages and currents in the device.

The limiting factor on the switching time of a MOSFET is thus determined by how fast the gate voltage can be changed and is not an inherent limitation due to the physics of operation. Figure 3.2 shows the approximate equivalent circuit model of a power MOSFET including the parasitic BJT. In the equivalent circuit, the various parasitic elements of the MOSFET are modeled as lumped components and these are added externally to an ideal MOSFET.

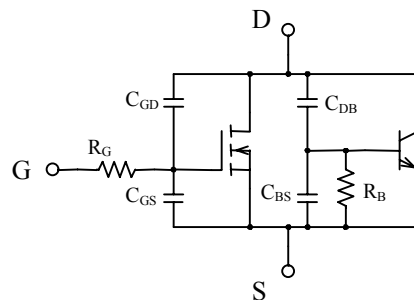


Figure 3. 2 Approximate equivalent circuit of a n-channel power MOSFET.

In practice R_G will be a distributed internal resistance due to the sheet resistance of the polysilicon gate electrode and various contact resistances. The gate capacitance will form a distributed RC network with the gate resistance. For high-frequency operation both gate resistance and gate capacitance should be as low as possible. MOSFETs have an integral reverse diode due to the short circuit between the source and the substrate. In the MHz region, the inverter can be assumed to never operate in the capacitive mode (i.e. a leading load current). Thus the integral diode of the MOSFET can be assumed to never conduct at the end of the conduction period and hence the reverse recovery ratings of the diode are of no concern. However, if the charge removed from the midpoint during the dead-time is too large, then the midpoint voltage will swing below or above the respective

rail voltage, causing a negative voltage across the MOSFET. This could cause the internal diodes to conduct for a short while at the beginning of the conduction period before the current reverses direction. At MHz frequencies, the amount of charge that flows through the diode will be relatively small and considerably less than the reverse recovery charge. The current through the MOSFET will then reverse direction and the MOSFET will conduct forward current as normal. Thus the forward current will return the charge removed out of the diode. The MOSFET will then turn off at the end of the conduction period as normal and experience the turn-off dv/dt . Whether the small amount of charge removed from the diode at the beginning of the conduction period will affect the turn-off dv/dt capability of the MOSFET at the end of the conduction period is not clear and remains to be investigated. A similar problem can occur in a Class-E inverter. However, the non-linear output capacitance of the MOSFET increases rapidly as the drain-source voltage approaches zero and as it swings negative. This will act to prevent the reverse diode from conducting under most normal load conditions.

3.2.2 Selection of the MOSFETs

The main objective of this thesis was to investigate the feasibility of producing RF power in the HF-band with a Class-DE topology. To this extent it was desired to produce the maximum RF power possible with only two MOSFETs at the highest practical frequency. To obtain the highest power output, the DC power handling capability of the MOSFET, (given by $V_{DS} \times I_D$), should be a maximum. MOSFETs with the highest power ratings lie in the 500-600 V region. For maximum operating frequency, the various capacitances of the MOSFET should all be a minimum. A MOSFET's parasitic capacitances increase with increasing current rating (i.e. increasing die size). The output capacitance can be accommodated by operating in Class-DE mode but it is still desirable to keep this to a minimum as a larger capacitance will decrease the upper operating frequency, reduce the power output and increase capacitive switching losses in the case of non-zero voltage switching. External discrete capacitance can always be added if it is found to be necessary. Driving the gate capacitance becomes the main limiting factor when switching a MOSFET at higher frequencies. As the switching frequency is increased, the gate drive currents become excessive and the power dissipation in the internal gate resistance and gate-driver becomes problematic. Hence for high-frequency operation the gate-source capacitance, reverse transfer capacitance and the internal distributed gate resistance should all be minimal. The power dissipation capability of the MOSFET should be a maximum as this will decrease its operating temperature and increase its reliability in the case of a mismatched load. Another specification of importance is the ability of the switch to withstand large voltage slew rates at turn off. The higher the operating frequency, current and supply voltage, the higher the voltage slew rate will be. This voltage slew rate requirement pertains to the normal turn-off dv/dt of the MOSFET (sometimes known as the off-state dv/dt [34]) and must not be confused with the reverse diode recovery dv/dt . The maximum dv/dt can be calculated using equation (2.2.7), and for 5 MHz 1 kW inverter can be expected to be in the region of 20-30 V/ns. The off-state dv/dt is not specified by the manufacturers, but is thought to be in the region of 100 V/ns for a 500 V MOSFET [34], which should be adequate for operation into the MHz region. The off-state dv/dt rating will be increased with smaller values of R_B and thus a low value of R_B is desirable. Any stray impedances that are added externally to the MOSFET due to packaging and layout will also greatly affect the switching performance. The gate, drain and source lead inductance due to packaging should be as small as possible. Layout and packaging requirements are discussed further in chapter 6.

An optimum ratio of the above requirements must be selected. An IRFP450 MOSFET was found to have a good balance between power rating, output capacitance and gate drive requirements. This is a 500 V, 14 A device with a total gate charge of 150 nC, an output capacitance, $C_{oss} = 720$ pF, and reverse transfer capacitance, $C_{rss} = 340$ pF, with both capacitances specified for $V_{DS} = 25$ V, $V_{GS} = 0$ V and measured at 1 MHz. Hinchliffe et al [19], showed that this MOSFET with an adequate gate driver and low inductance connections, is capable of turning completely on or off in less than 10ns. This switching time was thought to be fast enough for operation up to 5 MHz. This MOSFET was successfully used in a Class-E inverter operating up to 3.3 MHz, 450 W [18,21]. It was decided to first operate the MOSFETs with a maximum DC supply voltage of 300 V and at a peak current of 16 A. This would provide an adequate safety margin and allow the MOSFETs to run relatively cool. An ideal Class-DE inverter operating at 5 MHz with a 300 V DC supply and 16A-peak current should provide a theoretical output power of 1.2 kW as shown in section 2.2.5. A Spice simulation was then performed of a half bridge inverter using two IRFP450 MOSFETs, operating at 5 MHz. The results of the simulation are discussed in the following section.

The actual device used later to practically implement the inverter was the IRFP450LC. This has equivalent power ratings of an IRFP450 but has lower device capacitances. This makes it considerably more suitable for high frequency operation. The lower output capacitance means the gate drive requirements are reduced and a smaller conduction angle will be required. Hence the power output will be higher. These facts enable the device to operate at higher frequencies with a better efficiency.

3.3 SIMULATION OF THE INVERTER

The objective of the simulating the inverter was to gain insight into its operation and determine the feasibility of the inverter working up to 5 MHz using the IRFP450 MOSFETs selected in the previous section. The simulation will give a more realistic picture of the actual operation of the inverter when using non-ideal switches. It also enables the designer to learn what the effect of changing various parameters has on the operation of the inverter and thus gain insight into the mechanics of its operation and observe the voltages and currents that will be experienced in the circuit. The simulations were performed using PSpice.

3.3.1 Simulation of a Class-D Voltage-Fed Series Resonant Inverter

The first simulation attempted was of a classic Class-D half bridge inverter operating at 5 MHz with a 300V DC supply, using two IRFP450 MOSFETs, and is included here to show the effect of capacitive switching losses. The PSpice schematic circuit diagram used for the simulation of the Class-D inverter is given in Figure 3.3 and the results of the simulation are given in Figure 3.4. The MOSFET model used in the simulation was simply the IRF450 MOSFET model provided in the standard part libraries of the commercial version of PSpice.

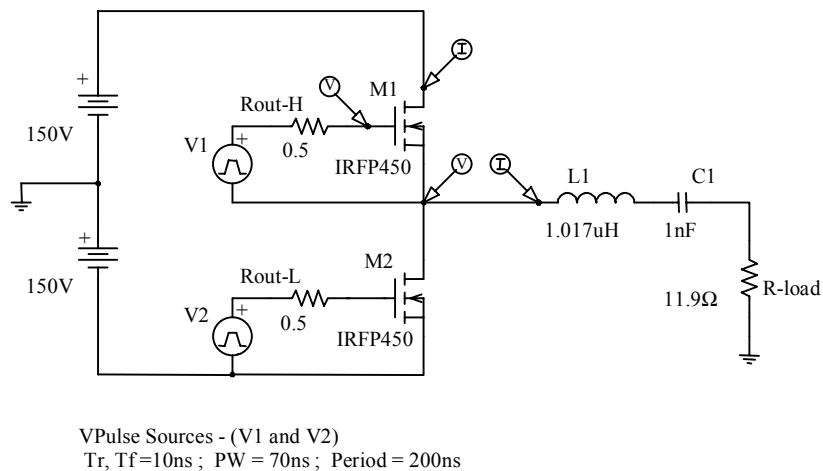


Figure 3.3 PSpice Schematic of the Class-D inverter

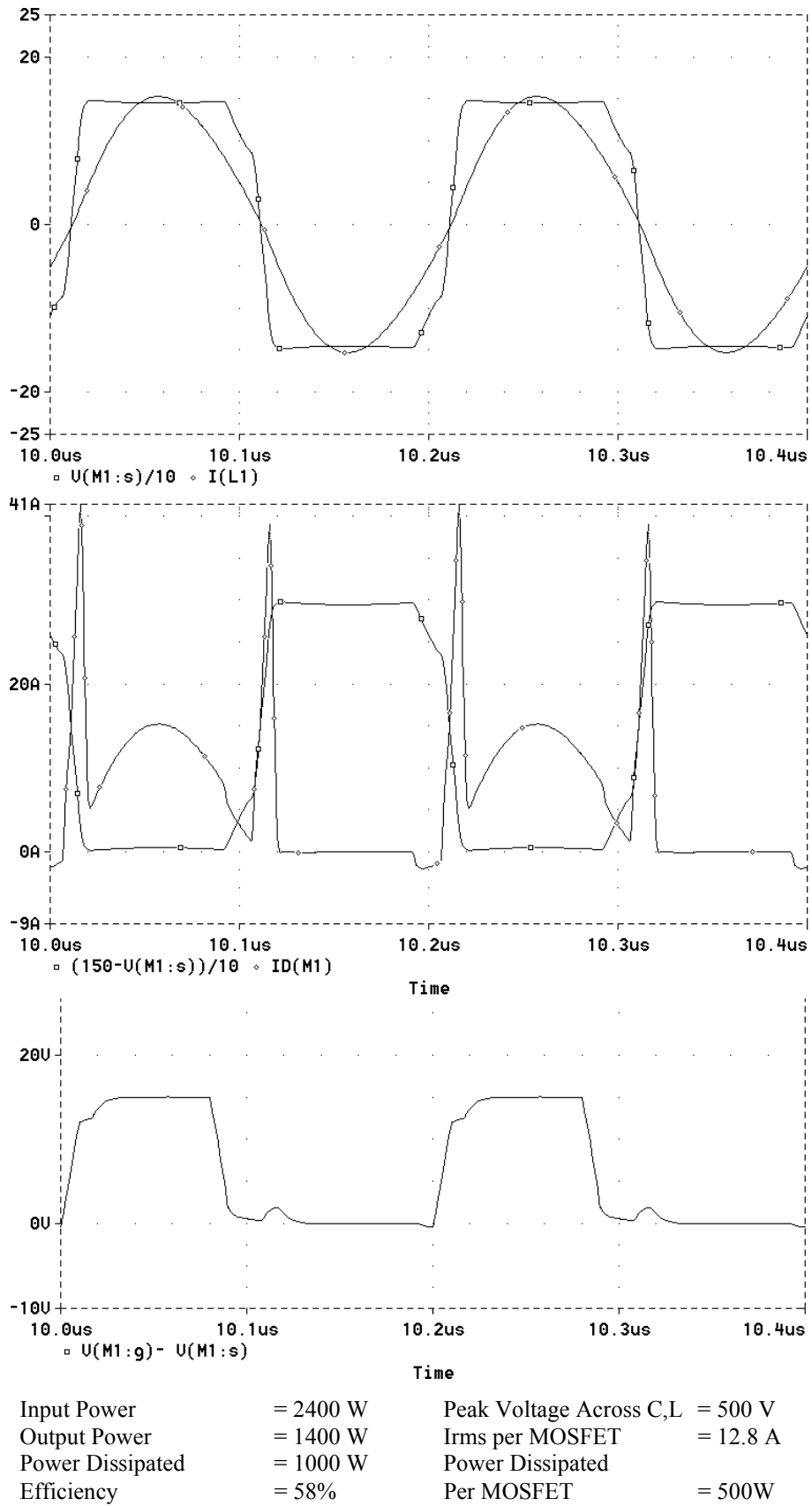


Figure 3.4 Simulation Waveforms and Results of the Class-D inverter

The series resonant capacitance of LCR load network was selected to be $1nF$ and the inductance found accordingly. The value of the load resistance required to achieve a peak current of 16A in a Class-D inverter can be calculated using equation (2.1.7) and was found to be 11.9 ohms. The dead-time between switching transitions must be selected by the designer and for this simulation it was chosen to be 10% of the period (20ns).

The simulation results of the Class-D inverter are given in Figure 3.4. The first plot of Figure 3.4 shows the midpoint voltage, $V(M1:s)$, and the load current, $I(L1)$, as indicated by the voltage and current markers on the circuit diagram. The second plot shows the voltage across, $(150-V(M1:s))$, and the current through, $ID(M1)$, the high side MOSFET. It should be noted that the current, $ID(M1)$, is the total switch current as it includes the current into the output capacitance which is an integral part of the MOSFET. The third plot shows the gate-to-source voltage, $(V(M1:g)-V(M1:s))$ of the high side MOSFET.

The various simulation calculations of power input, power output etc. are given below the simulation waveforms. The most prominent feature of the simulation waveforms in Figure 3.6 is the current spike needed to charge/discharge the output capacitances which must be provided by the MOSFET turning on. This causes excessive power loss and hence the inverter has an efficiency of only 58%. The high power dissipation in the MOSFETs (>500 W) makes such an inverter impractical.

3.3.2 Simulation of a Class-DE Voltage-Fed Series Resonant Inverter

The inverter given in design example of section 2.2.5 was then used as a basis for the next simulation. As the MOSFETs are not ideal switches, minor adjustments to the circuit parameters have to be made in order to achieve optimum Class-DE operation. The optimum values of the LCR circuit and duty-cycle are given in the PSpice schematic of Figure 3.5. The simulation results of the Class-DE inverter are given in Figure 3.6.

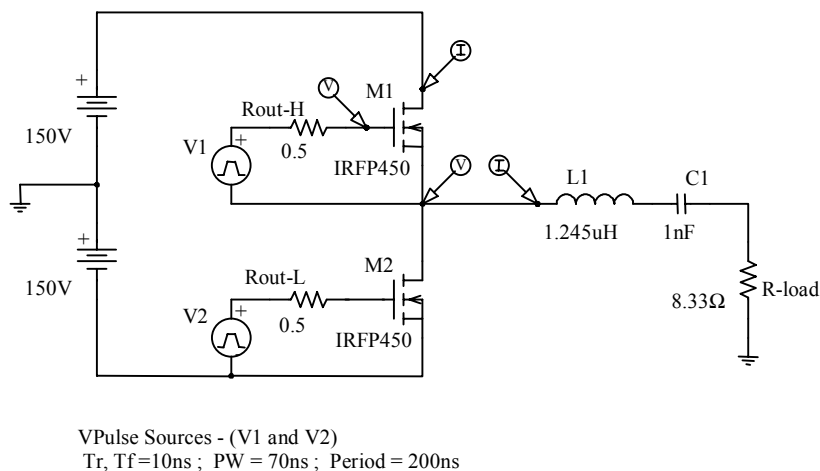
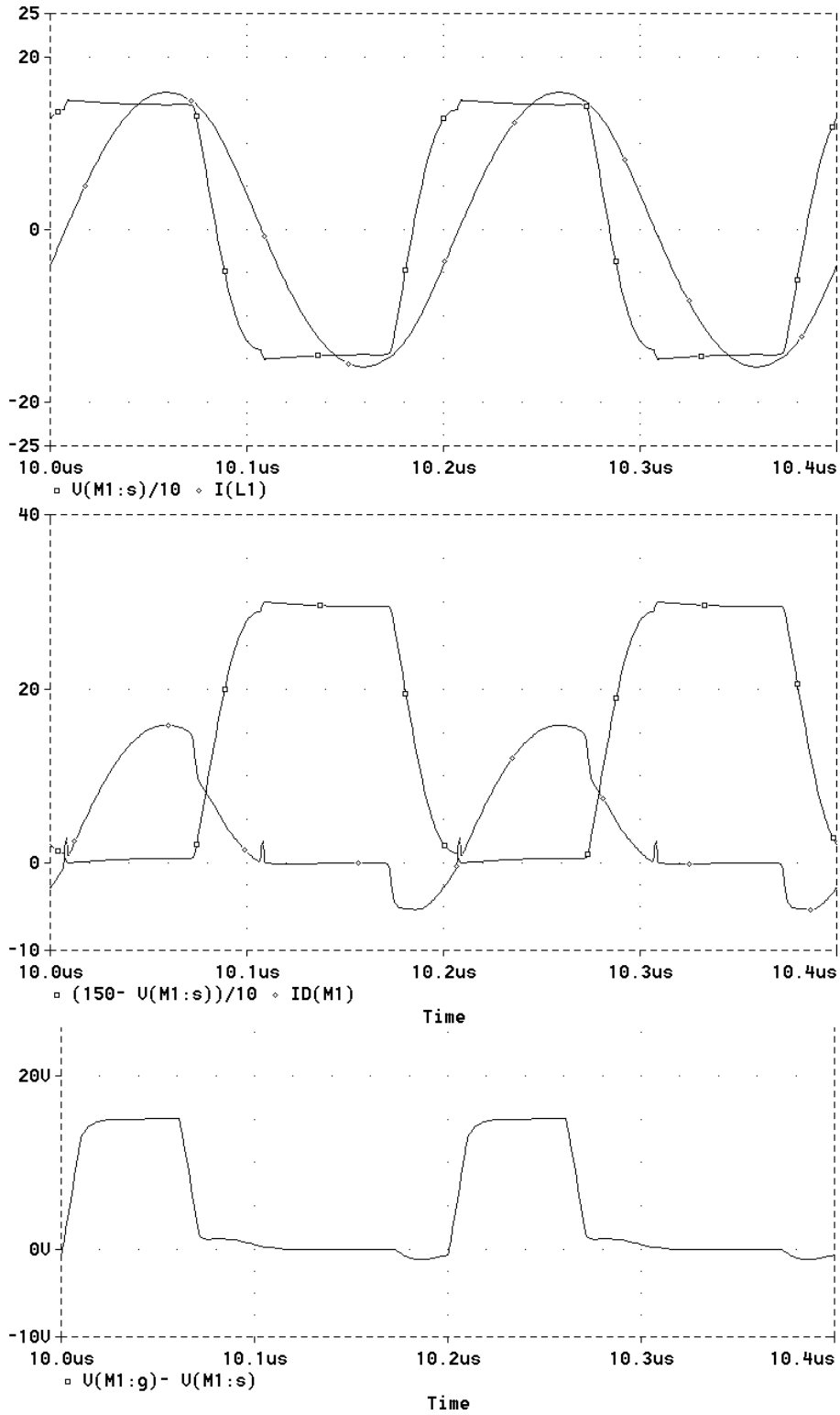


Figure 3.5 PSpice Schematic of the Class-DE inverter

The magnitude of the load current was lower than the designed 16 A because the MOSFETs are non-ideal and have a non-zero on-resistance. In order to increase the amplitude of the load current to the desired 16 A, the magnitude of the load resistance has to be lowered.



Input Power	= 1150 W	Peak Voltage Across C,L	= 500V, 650V
Output Power	= 1090 W	Irms per MOSFET	= 7.7 A
Power Dissipated	= 60 W	Power Dissipated	
Efficiency	= 94.7%	Per MOSFET	= 30W

Figure 3.6 Simulation Waveforms and Results of the Class-DE Inverter

To achieve the optimum Class-DE operation (i.e. zero-voltage and zero-load-current turn on), all that needs to be adjusted is the phase lag of the load current and the pulse width of the gate drive signal. To increase the phase lag of the load current, either a) the frequency can be increased making the load look more inductive, or b) the inductance and/or the capacitance of the LCR network can be increased, thus increasing its inductive reactance. In this simulation, the frequency is fixed at 5 MHz, and the inductance is varied to obtain the correct phase lag. The optimum Class-DE operation was achieved by a succession of adjustments to the inductive reactance and the duty-cycle of VPulse sources.

The three plots show the same voltages and currents as shown in the simulation waveforms of Figure 3.4 for a Class-D inverter. Again it should be noted that the current, ID(M1), is the total switch current and consists of the current through the MOSFETs conducting channel added to the current needed to charge/discharge its integral output capacitance. As in Figure 3.4, the various simulation calculations of power input, power output etc. are given below the simulation waveforms.

From the results of Figure 3.6, we can see that the MOSFETs now turn-on at almost zero voltage and zero-load-current. The output power has decreased slightly to 1090 W, but the efficiency has dramatically increased to 94.7%. The power dissipation in the MOSFETs has decreased to a more practical value of only 30 W. Thus from a power dissipation aspect, this inverter is practically more feasible. These simulation results also clearly illustrate that by operating the inverter in Class-DE mode, the capacitive switching losses of a classic Class-D inverter can be effectively eliminated. The simulation also shows that the PSpice model of the IRFP450 MOSFET is capable of operating at 5 MHz producing over 1 kW of power.

The PSpice simulation of the Class-DE inverter will predict a performance that is better than what can be expected in practice as the simulation performed has the following limitations;

- a) The PSpice model of the MOSFET is idealized and not entirely accurate,
- b) No MOSFET dv/dt failure of any kind is modeled,
- c) Thermal aspects, interference, ground loops and EMI are not considered,
- d) Additional parasitics due to the physical layout of the circuit have not been included.

The additional parasitics can be included to a certain extent but the actual values have to be obtained empirically off a fully constructed inverter or found approximately using calculations. This was considered not to be worthwhile for these simulations. Even with the above shortcomings, the PSpice simulation will give a reasonable evaluation of the how the inverter will perform, provided the MOSFETs are driven as required, and the results were encouraging. It was felt that if the practical problems of implementing such an inverter can be overcome, the inverter would have a good chance of working. As mentioned previously, the physical implementation of the half-bridge inverter in the MHz region presents some challenging practical problems associated with having two independent switches. These briefly are: the control, relative timing and gate-drive of two independent MOSFETs, of which one is floating, and finally the layout and physical construction of the inverter. These problems are dealt with in the following chapters.

CHAPTER 4. DRIVING THE INVERTER

The operation of a half bridge inverter requires the high and low-side switches to be alternately turned on and off at the desired frequency and with the required duty-cycle. The switch state (i.e. on or off) is controlled by the switch's *drive signal*. In a Class-DE inverter the switches will be driven at exactly the same frequency and duty cycle, but the drive signal for the high-side switch must be phase shifted exactly 180° degrees relative to the low-side switch's drive signal. The frequency and duty cycle required will depend on the values of LCR load network and the output capacitance of the switches. The duty cycle will be between 0% and 50%.

A half-bridge inverter is fundamentally a very broadband topology and its bandwidth can potentially extend from DC to its highest practically feasible operating frequency. In order to take advantage of this fact the inverter driving circuitry must be capable of driving the half-bridge inverter over the widest range of frequencies possible and with a variable duty cycle. If a means of varying the frequency and duty cycle of the inverter are provided, then the only circuit changes that would be needed for different operating frequencies are the inductance and capacitance of the tuned network. The inverter could then be tuned to Class-DE mode of operation by simply adjusting the switching frequency and duty cycle of the inverter. This would enable very quick modifications for different operating frequencies. The half-bridge inverter could then be used as a broadband RF power supply.

The switches in a half-bridge inverter are controlled by the high and low-side switch drive signals. Therefore, in order for the frequency and duty cycle of the inverter to be varied, a means of varying the frequency and duty cycle of the switch drive signals over the widest range possible must be provided. Generation of these drive signals is dealt with in the second section of this chapter. Operation of the inverter in a switching mode requires the MOSFETs to be turned on and off by the drive signals. Turning the MOSFET on and off involves charging and discharging the gate capacitance and this is dealt with in the next section.

4.1 DRIVING THE MOSFET GATE

4.1.1 Requirements of the Gate-driver

In a switch-mode topology, the amount of time it takes for the switch to turn on or off is relatively important. For reasonable performance in a Class-DE inverter, the switching devices should be capable of a switching in less than approximately 5% of the period (for conduction angles in the region of 80°-150°). If the MOSFETs are to switch in less than 5% of the period at 5 MHz, then their total time to switch on or off should be less than 10ns. Hence the MOSFET gate must be charged / discharged in less than 10ns.

The effective gate capacitance or input capacitance, C_{iss} , of MOSFET can be seen from Figure 3.2 to be comprised of the gate-source capacitance and the gate-drain capacitance (or Miller capacitance) [31]. The total gate charge, Q_g , required to charge the gate of an IRFP450 MOSFET from 0 V to 12 V is 120 nC. This total charge includes the (Miller) charge required to discharge the gate-drain capacitance when the MOSFET switches from the off-state, with a V_{DS} of 300 V, to the on state. If this entire charge is to be delivered in 10ns then the gate-driver must supply an average current of $I_g = 120\text{nC}/10\text{ns} = 12 \text{ A}$.

The loops around which the current will flow when charging and discharging the gate capacitance can be seen in Figure 4.1. The current required to charge/discharge the gate capacitance must increase in a few nanoseconds from zero to maximum of 12 Amps or more. If the rate of current rise is to be in the order of 4A/ns, then an inductance of 1nH in the charging/discharging loop will cause a 4V voltage drop across it, reducing the drive voltage available and slowing the rate of rise of the current [19,36]. It can be seen, therefore, that it is imperative to keep the inductance of the gate charging and discharging loop to a minimum. The source-lead inductance is part of the gate charging and discharging loop and in addition it has an induced voltage across it due the changing drain current which further reduces the gate-drive voltage available. Thus the source-lead inductance adversely effects the switching times and so it is desirable to keep it to an absolute minimum [19].

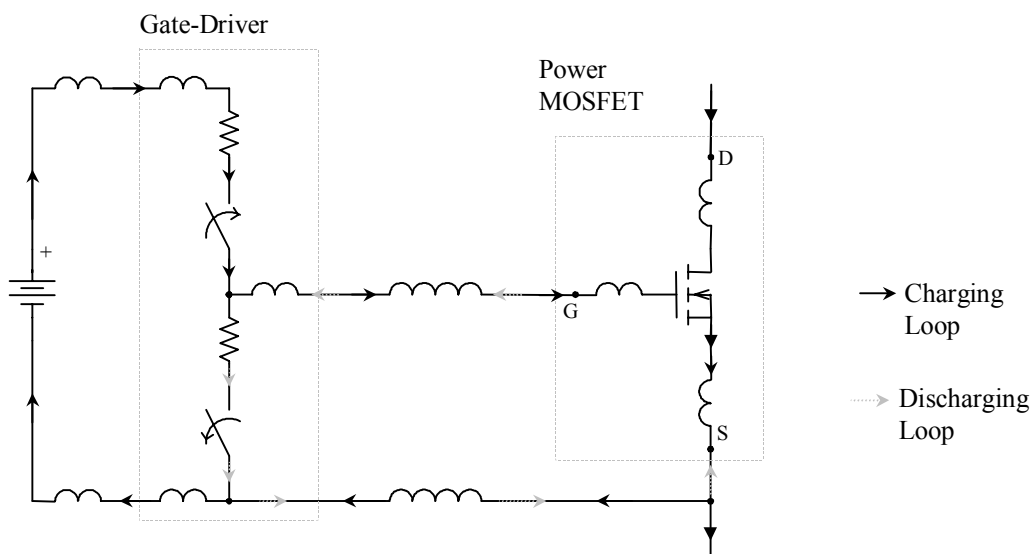


Figure 4.1 Direct Drive of the MOSFET gate

The gate-driver of Figure 4.1 can be considered to be a simple model of a commercial MOS-gate driver. If the gate is to be charged and discharged through a resistive path, as shown in Figure 4.1, then all of the energy supplied by the gate-driver will be dissipated in its internal resistances. The total power dissipated, P_d , in the gate-driver circuitry will then be dependent upon the total gate charge, Q_g , the gate-driver supply voltage, V_{dri} , and the operating frequency, f . Hence

$$P_d = Q_g V_{dri} f \quad (4.1)$$

Calculating the power dissipated in a gate-driver, with a 12 V supply voltage, driving the gate of a IRFP450 MOSFET at 5 MHz, we have $P_d = 110 \text{ nC} \times 12 \text{ V} \times 5 \text{ MHz} = 7.2 \text{ W}$. Hence the gate-driver must be capable of dissipating 7 W or more.

To summarize:

The MOSFET gate must be charged or discharged in less than 10ns, so the gate-driver must have rise and fall times of less than 10ns. The gate-driver must source and sink in excess of 12A and should have as low an output impedance as possible to prevent spurious turn on with high dV_{DS}/dt . The gate-driver must be able to dissipate in excess of 7 W. The charging and discharging loop must have the least inductance possible and its supply rails should be very well decoupled.

4.1.2 Choice of the Method Used to Drive the MOSFET Gates

There are two practical choices for driving the gate capacitance with a square wave at a few MHz. The first uses a gate-driver coupled to the gate through a transformer. The transformer is used to provide galvanic isolation and the level shifting required for the high-side switch. The advantage of this system is that the high-side gate-driver does not require a floating power supply as the power is coupled through the transformer. The disadvantage is that transformers inherently have leakage inductances and coupling capacitances associated with their construction. The leakage inductance of the windings makes it very difficult to obtain the rapid rise of current required and will cause excessive ringing. The coupling capacitances limit the dv/dt and noise immunity of the transformer. Transformer coupling also makes it complex to transfer DC information (i.e. duty ratio). Improved operation can be obtained by using a large sinusoidal drive, as the transformer does not require the high bandwidth needed for a square wave drive, and the leakage inductance of the transformer can be included into a resonant circuit topology, El-Hamamsy [5]. In a resonant circuit topology, the energy stored in the gate capacitance is resonated to an inductance and back again and hence much less power is dissipated than in a hard-switched system. The disadvantages of a resonant circuit topology are that it is a single frequency system and only a limited adjustment of the dead-time is possible. For the above reasons, a transformer-coupled gate drive was considered not to be the best solution for this application.

The second way of driving the gate capacitance is to drive the gate directly with a gate-driver as shown in Figure 4.1. This method will have the lowest loop inductances, provided the physical layout is designed correctly, and thus will have the fastest charge and discharge times. If the MOSFET gate-drivers are provided

with an independent power supply, they can then drive the MOSFET gates over the full bandwidth (DC-5 MHz), with any duty cycle. As fast switching times and a variable duty cycle are quintessential requirements of a Class-DE inverter, this method was considered to be the best solution.

However this method has two practical problems, the first being that the high-side gate-driver must be provided with a DC and RF isolated independent power supply. The high-side power supply's negative rail will be referenced to the source of the high-side MOSFET (the midpoint). The midpoint swings between ground and the supply voltage at the operating RF frequency with slew rates of more than 30V/ns. The high-side power supply should therefore have a minimum coupling capacitance from the point of connection at the high-side gate-driver to ground, as this effectively appears as a capacitance added to the midpoint. The high-side power supply should therefore appear as a very high impedance to ground at the operating RF frequency. The second problem of this method is that the high-side gate-driver drive signal reference must be transferred or level-shifted from the control circuitry's reference, so that it is referenced to the midpoint. This problem is dealt with in the following chapter.

4.1.3 The Gate-Driver

Incorporating the gate-driver directly onto the same die as the power MOSFET enables the lowest loop inductances to be achieved and hence the fastest rise and fall times [9,36]. This solution was beyond the scope and budget of this thesis and is left for future development. The next best solution is to mount the gate-driver directly from the gate to the source and design the charging and discharging loop with the minimum leakage inductance. This was the approach that was followed for this inverter.

For this application, the most feasible way to make the gate-driver, in terms of cost and development time, was found to be parallel four commercial MOS-gate drivers together. The most suitable commercial MOS-gate driver was found to be the EL7104 in a DIP14 package from élantec. These have rise and fall times of 10ns with 1nF load, can source and sink 4 A with 12 V supply voltage and have an output impedance of 3 ohms. Four of these drivers paralleled will have a source and sink capability of 16 A and an output impedance of 0.75 ohms. The power dissipation capability of the EL7104 is 1 W with the ambient at 25 °C. Four of them in parallel will therefore only have a power dissipation capability of 4 W, which is not high enough to dissipate the expected 7 W of power. However, the power dissipation capability was suitably increased by adding external heatsinking with some air-cooling and this is discussed further in Chapter 6.

4.1.4 High and Low-side Gate-Driver Power supplies

The most common way of providing a floating power supply for the high-side is to use a bootstrap capacitor and diode. The bootstrap diode in this inverter would have to withstand operation at 5 MHz, a blocking voltage 300 V, a forward current of more than 1 A and a recovery dv/dt of 30 V/ns. Operation at this frequency, voltage and current would mean the reverse recovery losses of any commercial diode currently available would be excessive. The reverse recovery current effectively adds more capacitance to the midpoint, which is undesirable.

For these reasons a bootstrap supply is unsuitable for this inverter. A better solution was to use an independent isolated power source. A 15 V, 1 A isolated DC-DC converter provided the floating power source and the DC isolation needed for the high side. A common mode choke between the power supply and MOSFET gate-drivers provided the RF isolation required. The common mode choke must be designed to minimize the coupling capacitance across it. The low side power supply was provided by a non-isolated 15 V, 1 A DC-DC converter. A 5 W, 8 Ω series resistance was included in both high and low-side 15 V power supply rails to limit the power dissipation in the gate-drivers to a maximum of 7 W. Figure 4.2 shows the supply voltage, the power dissipated and the current drawn by the gate-driver with an 8 Ω series resistance in the power supply rail.

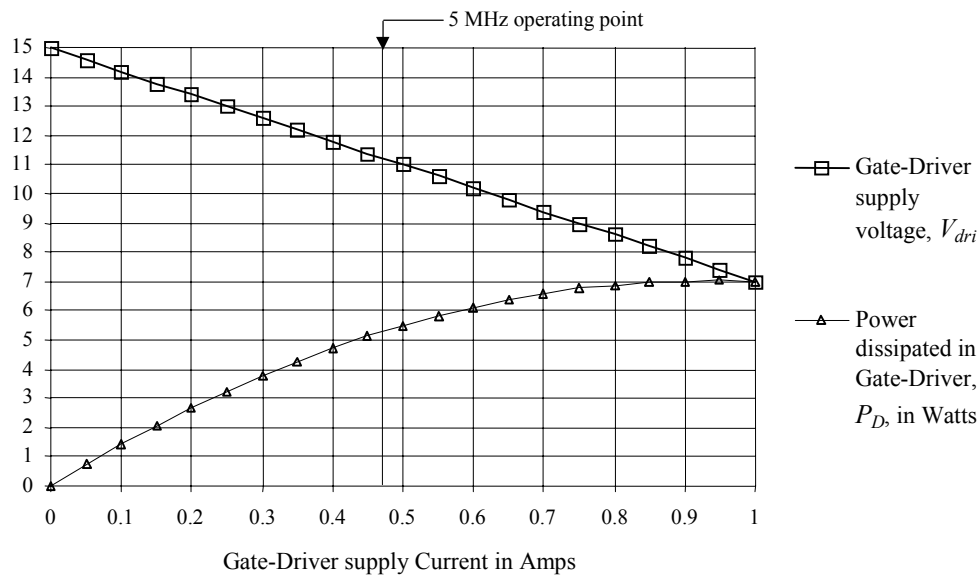


Figure 4.2 Load-line of the Gate-Driver Power Supplies

4.1.5 Final Gate-Drive System

Figure 4.3 shows an overview of the final gate-driver and power supplies for the high and low-side. The complete circuit can be found in Appendix C. High frequency layout techniques are imperative when designing the circuit board and this is discussed further in Chapter 6. Figure 4.4 shows the gate to source voltage of the high and low-side MOSFETs. The MOSFETs used are IRFP450LCs and waveforms were obtained with the supply voltage at zero volts, hence the gate to source voltage of the high side MOSFET could be measured directly. The main limitations of this system are the power dissipation, the leakage inductance, and the rise or fall times can not be reduced much below 10ns. This system will not work much above 5 MHz. At higher frequencies, new techniques such as those used by Leedham [36] and El-Hamamsy [5], will have to be implemented to drive the gate capacitance. Driving the gate capacitance of high power MOSFETs will be one of the main technical problems when implementing an inverter to work up higher frequencies such as 13.56 MHz or 27 MHz.

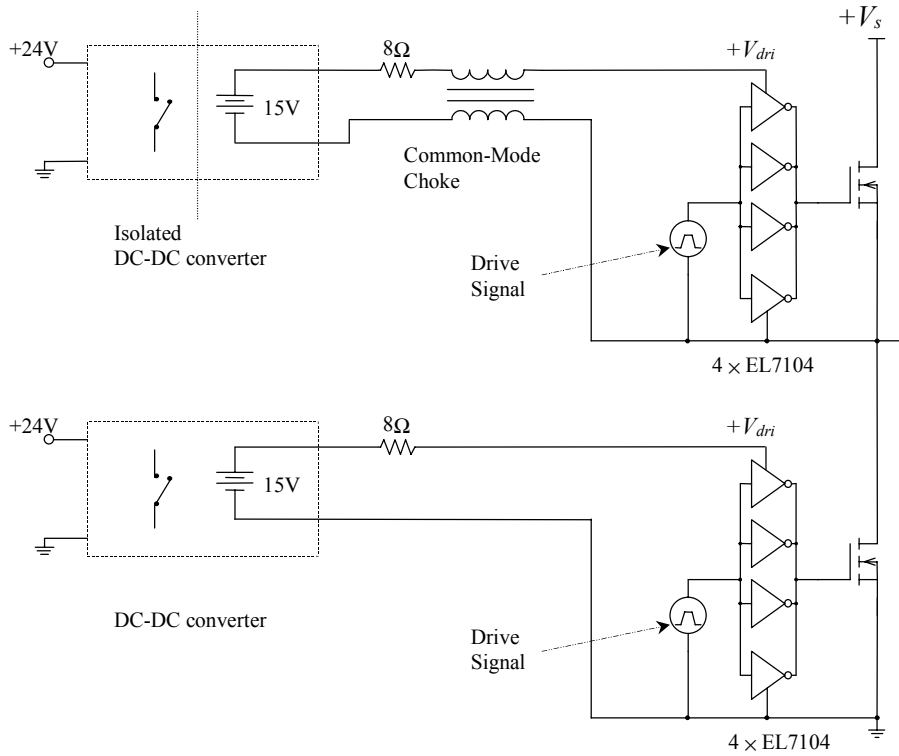


Figure 4.3 Final Gate-Drive system with Power Supplies

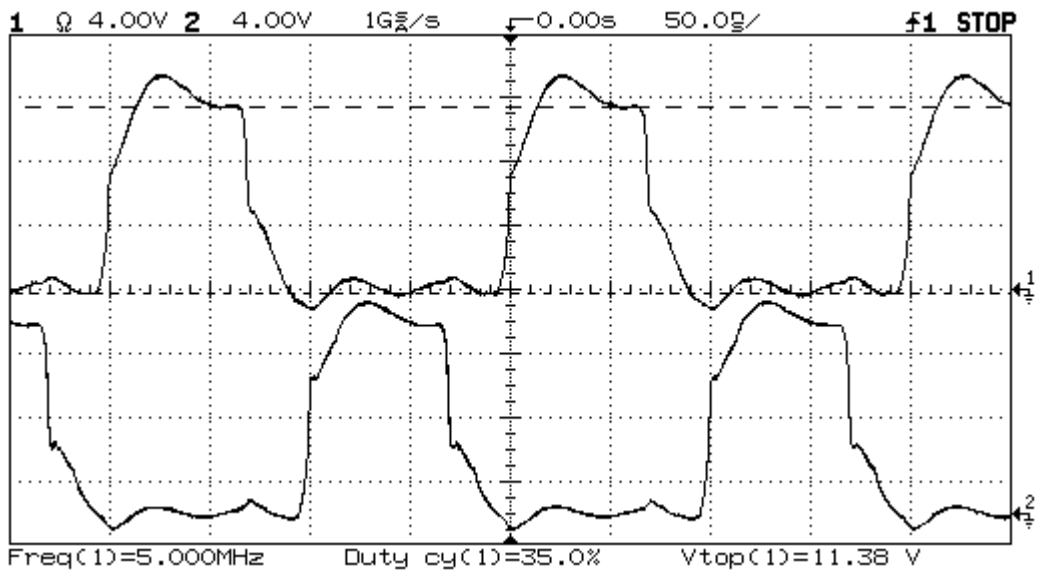


Figure 4.4 Gate to Source voltage of the high and low-side MOSFETS

4.1.6 MOSFET Gate Current when Operating in Class-DE Mode

If the inverter is operating in Class-DE mode then the entire gate charge will not have to be supplied all at once in order to turn the MOSFET on or off. The Miller charge due to the gate to drain capacitance will be sourced before the MOSFET is turned on and sunk after the MOSFET has turned off. This will lower the demand placed on the gate-driver in one switching instant. These effects of Class-DE operation on the gate-drive requirements can be seen in the waveforms of Figure 4.6. The voltage and current waveforms of Figure 4.6 are marked on PSpice schematic of Figure 4.5. They are the current into the MOSFET gate, $I_g(M1)$, the voltage across the MOSFET, $(150-V(M1:s))/10$, and the gate to source voltage of the MOSFET, $V(M1:g)-V(M1:s)$. The periods during which the gate-drain capacitance is being charged and discharged is marked on Figure 4.6 as the “Miller current”.

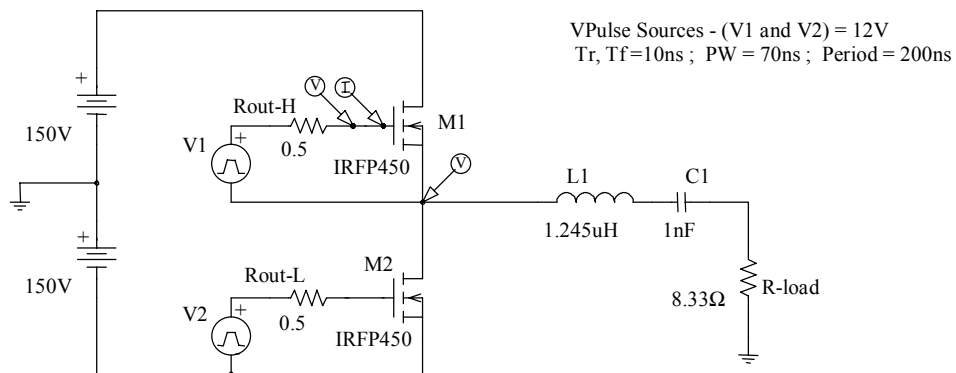


Figure 4.5 PSpice Schematic of the Class-DE inverter

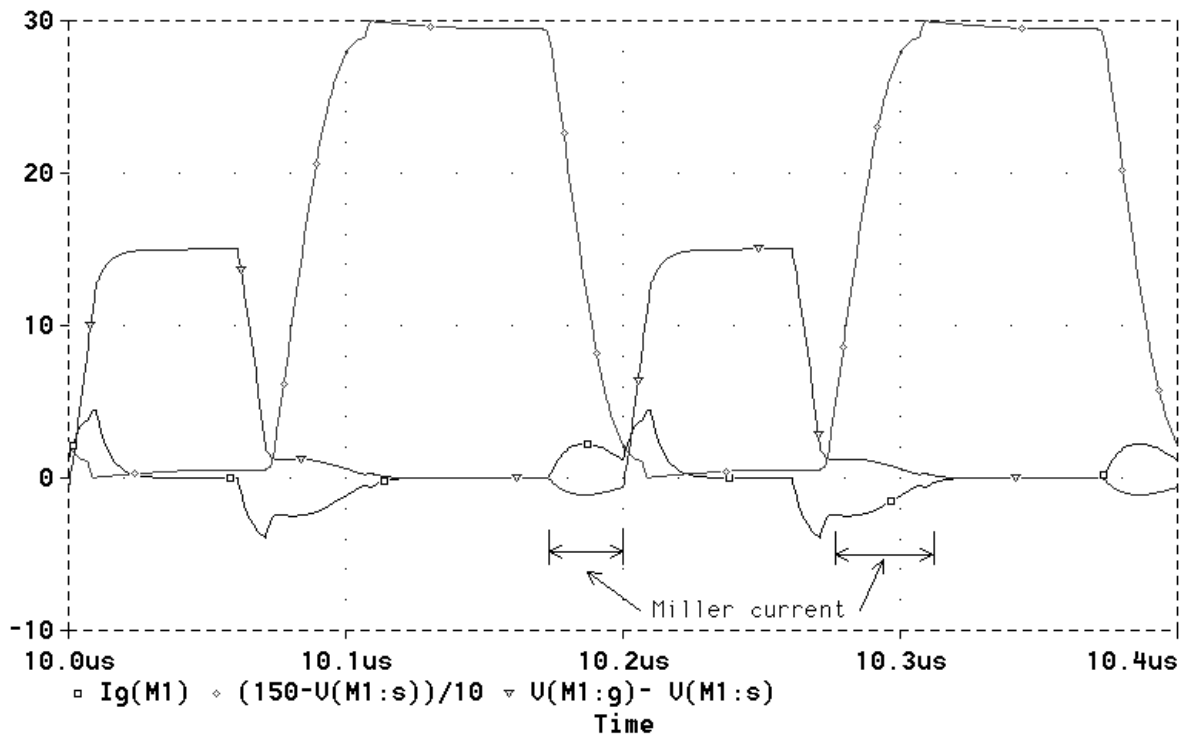


Figure 4.6 MOSFET Gate Current when operating in Class-DE mode

The mechanism of operation may be described by the following sequence of events. After the low-side MOSFET has turned off, the midpoint voltage will rise and the voltage across the high side switch will fall. The gate voltage of the high-side MOSFET will still be low, but as the voltage across the MOSFET is falling the high-side gate-driver must first source the current needed to discharge the gate-drain capacitance (Miller current). Once the voltage across the MOSFET has stopped falling and reached zero, the current needed to discharge the gate-drain capacitance will cease but the gate-driver must now source the current needed to charge the gate of the MOSFET to 12V (V_{dri}) to turn it on. Similarly, when the MOSFET is turned off the gate capacitance must be discharged from 12V (V_{dri}) to 0V first, turning the MOSFET off. The gate-driver must then sink the current injected into the gate terminal by the gate-drain capacitance as the voltage across the MOSFET rises (Miller current). The gate-driver must therefore have a low enough impedance to sink this current without the gate voltage rising high enough to turn the MOSFET back on.

4.2 DRIVE SIGNAL GENERATION

4.2.1 Requirements of the Drive-Signal-Generator

The first requirement of the drive-signal-generator is the ability to generate two drive signals of exactly the same frequency and duty cycle but are always phase shifted exactly 180° degrees relative to each other. The second requirement of the drive-signal-generator is the ability to vary the frequency and duty cycle of the drive signals. The duty cycle (or dead-time) of both the high and low drive signals should be adjusted simultaneously by a single adjustment method. This will ensure that both drive signals always have the same duty cycle. The frequency range of the inverter was desired to be 50 kHz to 5 MHz. Resolution of the drive signals should be at least 2% of period which at 5 MHz corresponds to rise and fall times of less than 4ns. The duty cycle should be adjustable over the range 25%-48%. At 5 MHz this means the dead-time will range from 4ns to 50ns. Lower frequencies will require longer dead-times, hence a dead-time range of 4 - 400ns was thought to be reasonable for testing purposes.

4.2.2 Conceptual Circuit of the Drive-Signal-Generator

Any circuit used to generate the drive signals should incorporate a divide by two circuit on the clock signal to obtain a 50% duty cycle (even symmetry of each half cycle). The path that the two drive signals take should also be of similar length and incorporate the same gates to ensure that the time skew between the two drive signals is minimized. The number of gates should also be kept to a minimum, as the delay variation of each gate will have a cumulative effect on the total delay variation of each drive signal. The dead-time for both drive signals should be generated by the same circuit to ensure that both signals have the same duty cycle. This will also enable the duty cycle of both drive signals to be adjusted simultaneously. The conceptual circuit used to generate the control circuit is given in Figure 4.7.

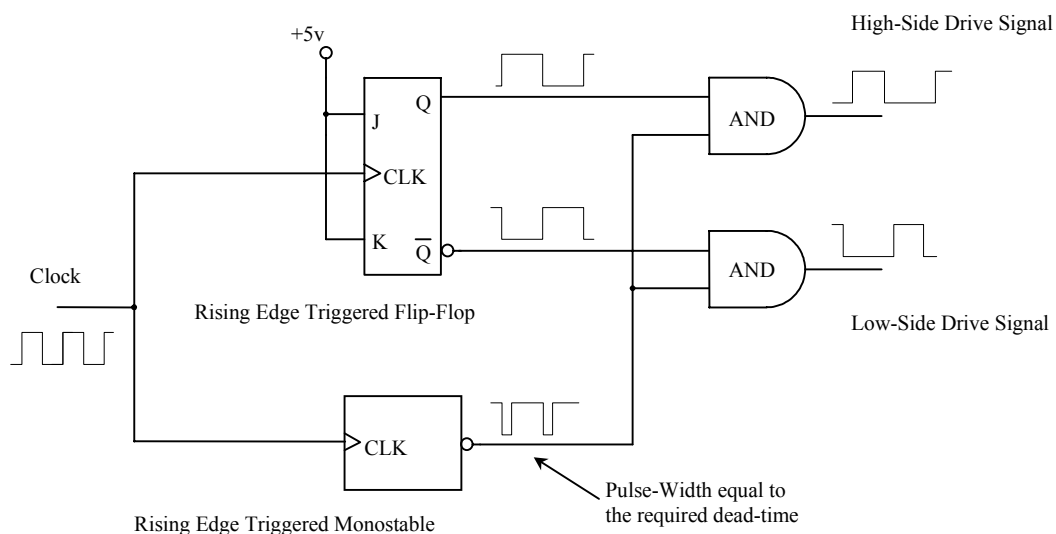


Figure 4.7 Conceptual Circuit of the Drive-Signal-Generator

The operation of the circuit in Figure 4.7 is as follows: The rising edge of the clock will trigger the flip-flop and the monostable. The outputs of the flip-flop will then invert and the monostable will generate a negative-going pulse. The pulse width should be equal to the required dead-time. The negative pulse of the monostable will keep the positive-going drive signal from going high until the dead-time period is complete. Exactly the same thing happens with the second drive signal on the next rising edge of the clock. To adjust the dead-time of both drive signals, only the pulse width of this one monostable needs be varied. As both drive signals use the same monostable to produce their dead-time, their respective duty cycles should then always be the same, even when the dead-time is being adjusted. As both the flip-flop and the monostable trigger on the rising edge of the clock signal it is in effect a divide by two circuit, giving the required symmetry to the two half periods of the drive signal. Varying the frequency of the clock signal will vary the frequency of the drive signals independently from the dead-time.

4.2.3 Final Drive-signal-Generator Circuit

The final circuit to generate the drive signals is given in Figure 4.8. AC CMOS logic devices were used for their fast rise and fall times and short delay times. High frequency layout techniques are imperative and were used through out the whole circuit. The clock signal was generated by a variable frequency oscillator which enabled the switching frequency to be adjusted without affecting the dead-time. The frequency range was from 50 kHz - 6 MHz, and the duty cycle range was from 25% to 48% (Duty cycle could not be adjusted this low at the lower frequencies). The maximum time skew between the two drive signals was in the order of 2ns. The duty cycle difference between the two drive signals was less than 0.5%. The drive signals for the high and low-side are shown in the waveforms of Figure 4.8.

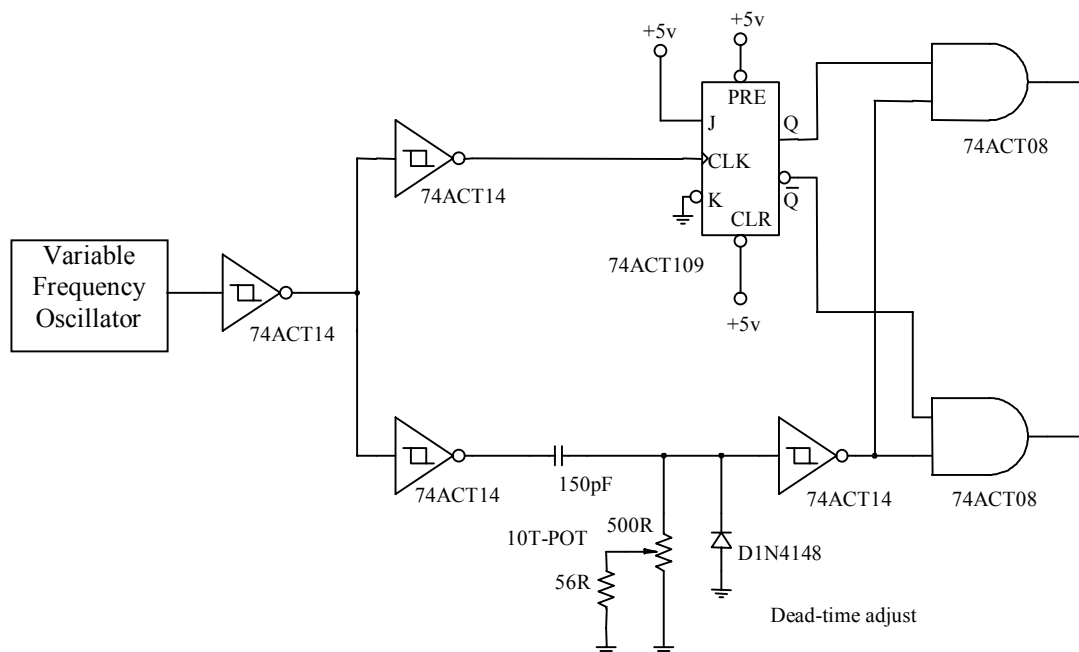


Figure 4.8 Final Circuit used to generate the Drive signals

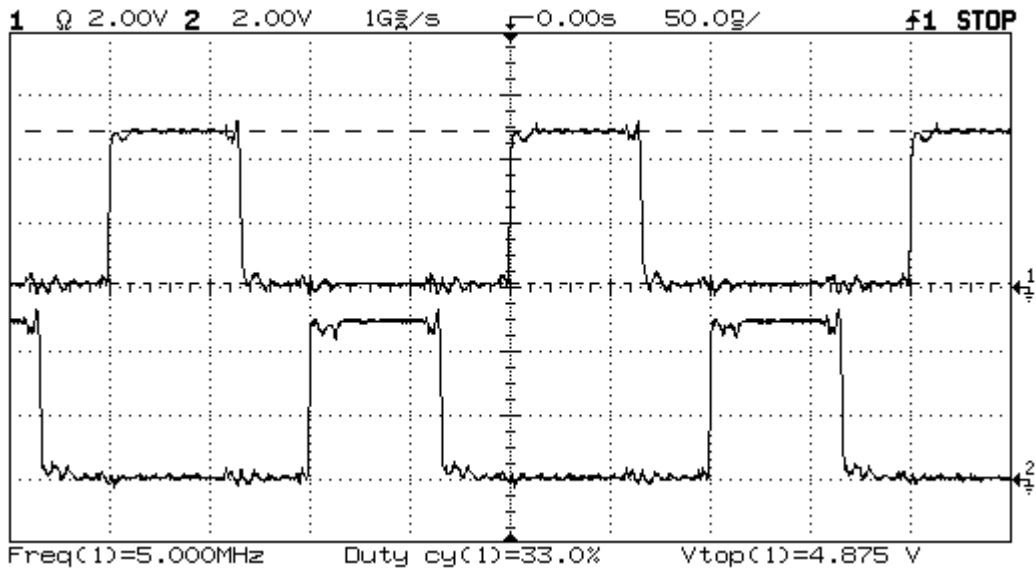


Figure 4.9 Drive signals generated by the Drive-Signal-Generator Circuit

A limitation of this circuit is that it has a minimum duty cycle of 25%, which may be limiting at higher frequencies. A second disadvantage of this circuit is that the dead-time is generated using an analog RC circuit. This is sensitive to noise and can cause timing jitter. A better solution would be to use a digital generated dead-time. A digital generated dead-time and a method of adjusting the duty cycle to less than 25%, are both recommended for use at higher frequencies. The remaining problem of controlling the inverter is sending the control information to the high side switch. This is the subject of the next chapter. The complete circuit of the Drive-signal-generator is given in Appendix-C. A possible future circuit that solves the above problems is given below.

4.2.4 Possible Future Circuit

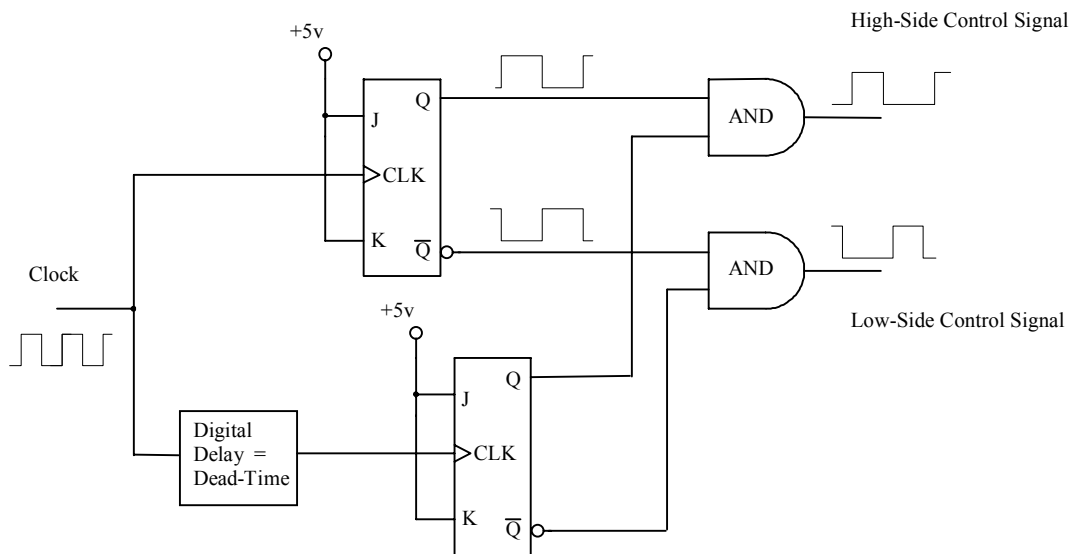


Figure 4.10 Possible Future Circuit

CHAPTER 5. COMMUNICATION-LINK TO THE HIGH-SIDE SWITCH

The two drive signals for the switches in the half-bridge inverter are generated by the control circuitry and are both referenced to a common potential (normally the same ground as for the inverter). The drive signals must now be transferred to the MOSFET gates via the MOSFET gate-drivers. This is illustrated in Figure 5.1. If the low-side MOSFET gate-source voltage is referenced to the same potential as the drive signals, then to transmit the drive signal to the gate is a simple matter, requiring only a direct connection. However, the high-side MOSFET gate-source voltage is referenced to the midpoint of the inverter. Thus the high side drive signal, which starts off referenced to ground, must be transferred so it is referenced to the midpoint voltage i.e. it floats on top of the midpoint voltage. The midpoint voltage swings between the two rails at the operating frequency and hence it is a dynamic potential reference. The transference of a signal reference from one potential to another is often called level-shifting. Another way of thinking about it is that the *on/off information* must be *communicated* to the high side switch across a potential difference. The means of transferring the drive signal is conventionally described in the literature as a level-shifter but the term '*communication-link*' is used here as communication is essentially the function that is performed and it embodies all the various methods of controlling the high-side switch. A major problem of operating a half-bridge inverter into the HF band and at relatively high powers (>500 W), is controlling the high-side MOSFET. The requirements of the communication-link (abbreviated as the *coms-link*), needed to control the high-side switch in such an inverter, are described in the following section.

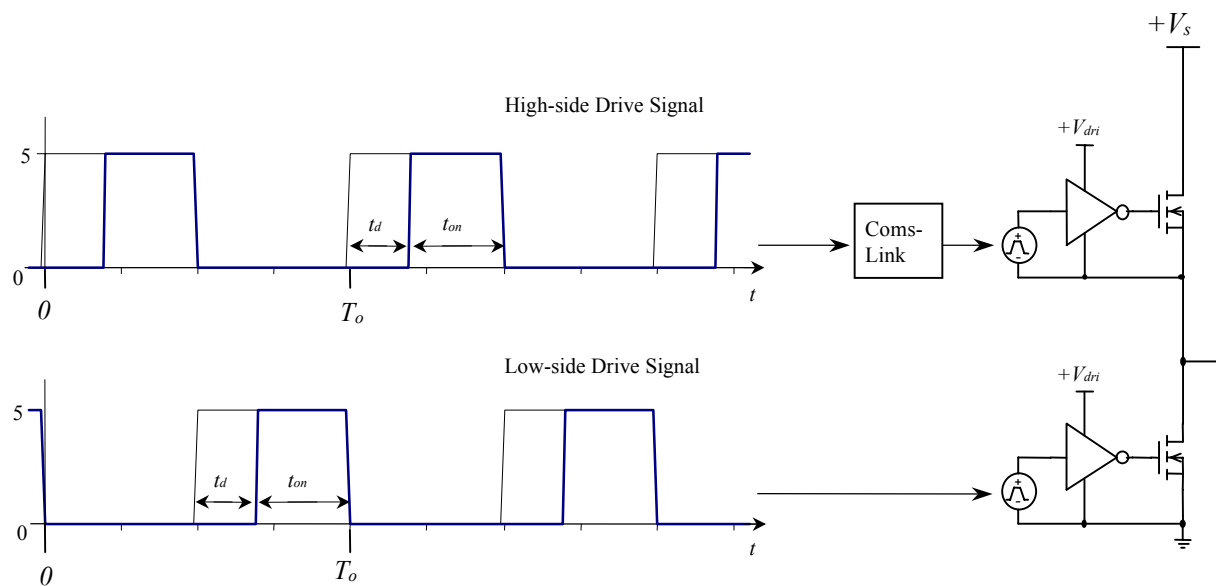


Figure 5.1 Transference of the Drive Signals to the high and low-side Switches

5.1 REQUIREMENTS OF THE COMMUNICATION-LINK

In order to operate a half-bridge inverter in Class-DE mode, the timing of the switch turn on and off is relatively important. For reasonably low noise, the resolution of the drive signal to the switch should be at least 2% of the period. To obtain this resolution, the bandwidth of the communication-link will have to be at least twelve times the required operating frequency. At 5MHz, the period is 200ns, hence the rise and fall times of the gate drive signal should be at most 4ns. The bandwidth required of the communication-link to achieve these rise and fall times will be 60MHz. The duty cycle of the drive signal will also be varying from approximately 10-50%. The communication-link must therefore also be capable of transferring DC information. As the relative timing between the two switches of the inverter is of fundamental importance to the operation of the inverter, the two drive signals must be received without any time skewing, loss of information, or pulse width distortion relative to the other sides drive signal.

When the high-side switch is on, the midpoint will be at the supply potential and the full supply voltage will be applied across the communication-link and hence it must have an isolation voltage rated accordingly. Another specification of importance is the dv/dt immunity of communication-link. During each switching transition, the midpoint voltage swings from one rail to the other. This causes a high dv/dt at the midpoint and hence across the communication-link. The higher the frequency, power and voltage, the higher dv/dt will be. The maximum dv/dt expected in the inverter when operating at 5MHz, with a 300V supply voltage and a 1kW power output, is in the region of 30V/ns. The communication-link must withstand these large voltage slew-rates without any false triggering occurring. When operating a half-bridge inverter at high frequencies, it is desired that the output capacitance from the midpoint to ground be kept to a minimum. The coupling capacitance across the communication-link appears as a capacitance from the midpoint to ground and thus this should also be kept to a minimum. In addition to the above conditions, the receiver side of the communication-link will be subjected to a large amount of EMI caused by the rapidly changing voltages and currents of the power output stage. The receiver should have a high immunity to this EMI and it should not cause any false triggering. In order for a half bridge to be useful over a large range of frequencies and loads, the frequency and duty-cycle of the drive signals should be variable over the largest range feasible. To this extent, the communication-link should not be the limiting factor and should therefore be capable of transferring the drive signal over the specified frequency range and for all the required duty-cycles.

5.2 METHODS OF CONTROLLING THE HIGH-SIDE SWITCH

5.2.1 Pulse Transformer

The circuit given in Figure 5.2 uses a pulse-transformer to provide the galvanic isolation and communication-link. The information is sent in a magnetic medium through the core of the transformer. A low power pulse-transformer would be used to obtain a large bandwidth, followed by a current buffer. Transformers, however, can not be built without inherent parasitic elements and will have an upper and lower frequency limit. There is also always a trade off to be made between high frequency and low frequency response. To reduce the rise and fall times, the primary and secondary windings should be tightly coupled. The tighter the coupling of the windings, the higher the coupling capacitance between the primary and secondary will be. This coupling capacitance will cause problems with a large dv/dt , inducing spurious signals into the windings. The capacitance will also appear across the output of the inverter, which is undesirable. The leakage inductance of the windings makes it difficult to obtain fast rise and fall times and will cause ringing. The windings of the transformer will also act as pick up coils and are prone to EMI. Transformer coupling also makes it complex to transfer DC information (i.e. duty ratios other than 50%). The close physical proximity of input and output restrict the layout options the designer has when physically constructing the inverter. To summarize, with a square wave drive, it will be difficult to obtain good signal fidelity using a transformer in a high power inverter operating in the HF band.

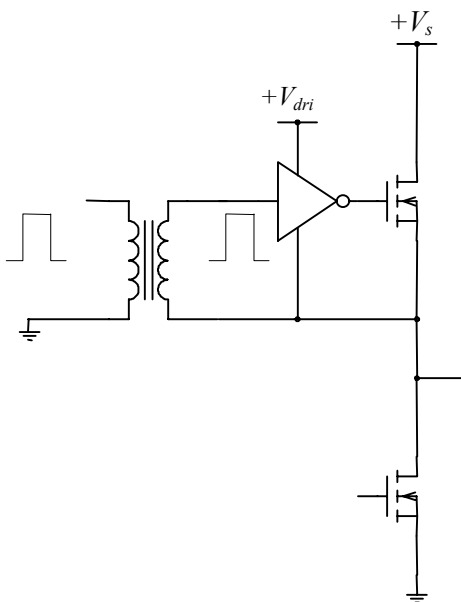


Figure 5.2 Pulse-Transformer Isolation

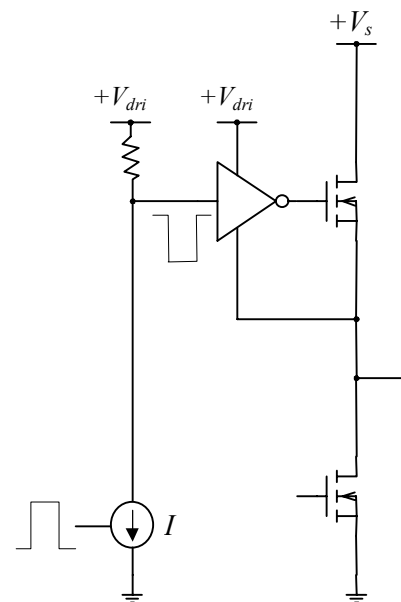


Figure 5.3 Electronic Level-shifter

5.2.2 Electronic Level-Shifters

An electronic level-shifter works on the principle of having a current source referenced to a fixed potential. The reference potential is usually that of the low side switch's source, hence they also called common source level-shifters. The drive signal causes a certain current to be drawn through a current source regardless of the voltage across it. The current is sensed by the receiving side and turned into on/off information. Electronic level-shifters do not provide galvanic isolation. A simple common source non-inverting level-shifter is given in the Figure 5.3. The output capacitance and the power dissipated by the current source, limit the frequency and voltage it can feasibly work at. A better solution, that decreases the amount of power dissipated, is to use a pulsed current source, which is then latched on the receiving side. Current Pulsed circuits are based on the following two topologies;

Dual Current Pulsed Latch

This topology employs two pulsed current sources. One pulsed current is used to set a flip-flop, which turns on the switch, the other is used to reset the flip-flop, which turns off the switch. Many commercial half-bridge drivers use this type of circuit. The problem with this circuit is that the reset current source has the full supply voltage across it when it conducts the current pulse, causing power dissipation during each switching transition. Hence the power dissipated by this topology increases with increasing frequency and becomes the limiting factor at higher frequencies [9,24].

Single-Ended Current Pulsed Latch

The single-ended current pulsed latch was developed by Carter [9,24]. This circuit solves the problem of the high power dissipation of the reset pulse by only having a single turn on current pulse. This pulse triggers a one shot timer with a pulse width equal to T_{on} , followed by a delay that incorporates the dead time. The circuit is relatively complex to implement and is most useful for fixed frequency power supplies of moderate power levels (100W). It is not as useful in a high power RF generator as it is limited in its frequency range and dead time adjustment.

The current source in all of the above circuits will have an output capacitance that appears across the level-shifter. This capacitance limits the bandwidth and decreases the noise immunity of the level-shifter. The dv/dt and isolation voltage is limited to the breakdown ratings of the current source transistor. Layout is difficult because of the close proximity of the input to the output. The EMI immunity is low compared to optical isolation.

5.2.3 Opto-couplers

Logic to logic opto-couplers are in principle very simple to use. A logic input appears as a logic output on the high side. They can transfer DC information and have static voltage isolation ratings of up to 5kV. They are commercially available of up to 20Mbd, with rise and fall times of 10-20ns. This is not fast enough for this application. Another problem of opto-couplers is that the propagation delay times change considerably with temperature causing pulse width distortion and time skewing. The maximum dv/dt that opto-couplers are rated for is in the region of 10V/ns which is below the required 30V/ns. The layout options are limited because of the close proximity of the input to the output.

5.2.4 Fiber Optic Link

A basic fiber optic communication system is given in Figure 5.4. The LED is current driven by the drive signal. The light emitted from the LED is sent down a length of fiber optic cable to the receiver. The receiver converts the received optical signal into an analog output voltage. The receiver consists of a PIN photodiode and a transimpedance amplifier. The output voltage of the amplifier is then level detected by a comparator and converted into logic signal.

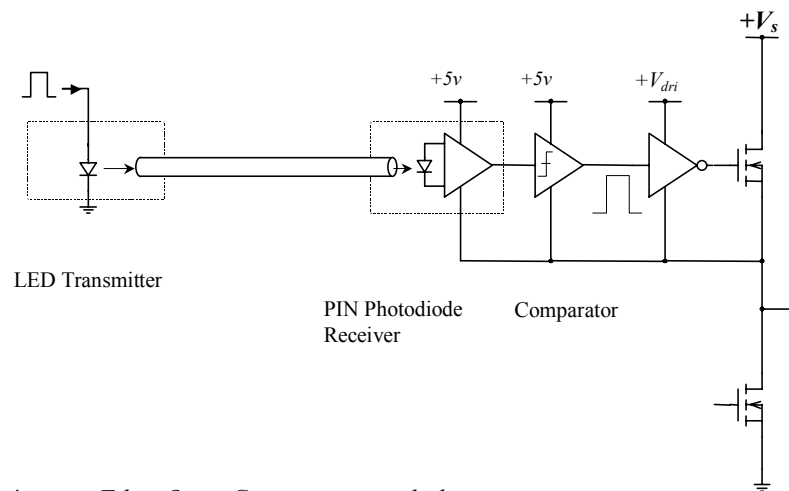


Figure 5.4 Fiber Optic Communication-link

The galvanic isolation and dv/dt rating of this communication-link can be increased to almost any desired value by simply lengthening the fiber optic cable. For a modest length of 10cm of fiber optic cable, the isolation voltage is approximately 100kV. The dv/dt rating is difficult to calculate but as the coupling capacitance is practically zero, even the highest realizable dv/dt will have little effect. The bandwidth available is an order of magnitude higher than needed for this application, but the higher the bandwidth the higher the cost. The fiber optic connection selected should have enough bandwidth to achieve the rise and fall times required. A fiber optic link's propagation delays are relatively constant over the working temperature range. Hence the pulse width distortion and time skew are not degraded due to temperature variations. The only external electrically conducting connections to the receiver side are the RF-isolated power supply connections. As the receiver-side

circuitry is referenced to the midpoint, it can thus be totally enclosed by a screen connected to the midpoint, offering excellent shielding from EMI. Electrical conductors are susceptible to electromagnetic fields and hence will radiate and pick up EM noise. Fiber optic links neither emit nor receive EM noise and pass through noisy environments unaffected. In addition to the above, when dealing with very rapidly changing currents, ground noise can become a problem. A fiber optic link practically eliminates any ground loop or common mode noise problems. To summarize, there are no fundamental limitations of a fiber optic system for this type of application. It has more than enough bandwidth, dv/dt and voltage isolation capabilities and can transfer DC information.

5.2.5 RF Modulated carrier signal

Another not well known method of communicating the on/off information is to use an RF modulated carrier signal at a suitably high frequency, of say 100MHz. The carrier signal could be transferred across the isolation barrier either magnetically (using, for example, a small poorly coupled transformer or a pair of loop antennas), or electrically (using small picofarad or sub- picofarad capacitances). This method was not explored in detail by the author but offers an interesting alternative method. Possible problems will be EMI susceptibility causing spurious turn-on/off, and dv/dt immunity during the actual switching transitions.

5.2.6 Summary

Summary table

	Usable frequency	Isolation Voltage	Dv/dt Capability	DC Information (Duty Ratio)	Coupling Capacitance	EMI immunity
Pulse Transformer	Limited to ~10 MHz	~ low kV	Limited	Difficult	Present	Low
Electronic Level-shifters	~<14MHz	~<1000V	Limited by current source	Yes	Cost of Current Source	Low
Opto-Couplers	<20Mbd	<5kV	<10v/ns	Yes	Very low	Good
Fiber optics	1GHz+	As high as Required	As high as Required	Yes	Negligible	Excellent

From the above table it can be seen that a fiber optic link is the only communication-link that is guaranteed to meet all the specifications needed for this application. A fiber optic link is relatively easy to implement and it can be expected to perform to its specifications. It is the only communication-link that will work to the upper end of the HF-band and is therefore the best method of controlling the high-side switch in a high power RF-inverter. The following section deals with the development of a fiber optic communications link that is suitable for a 5MHz, 1kW half-bridge inverter.

5.3 IMPLEMENTATION OF A FIBER OPTIC COMMUNICATION-LINK

A primary requirement of the inverter is that there must be no time skew between the high and low-side drive signals on reaching their respective switches. To solve this problem, identical fiber optic links were used to transfer both the high and low-side drive signals. This enabled identical circuits to be used for both sides, so the propagation delays of the drive signals would be the same, thus minimizing the time skew between them. Similar circuits for both high and low-side also increases the modularity of the inverter. Having fiber optic links to both sides means that the output stage can be galvanically isolated from all the control circuitry, which will protect the control board in the case of catastrophic failure of the output stage. It also enables the control circuitry to have a large physical separation from the power output stage and this creates many options for the design of the layout. This large physical separation, in fact, allows an entire faraday cage to be constructed between the control board and output power stage. This gives excellent isolation and shielding capabilities and hence good EMI immunity. The physical separation possible with fiber optic links was found to be a major advantage when designing and building a high frequency half bridge.

The fiber optic system selected was a 50Mbd link using cheap 1mm plastic fiber optic cable. The HFBR-1526 transmitter and HFBR-2526 receiver are used, and the fiber optic link has typical rise and fall times of 3.5ns. The price of these components is relatively cheap for the bandwidth available, and so these were a cost-effective solution. 1mm plastic fiber optic cable is readily available and easy to terminate. High frequency layout techniques must be used throughout the transmitter and receiver circuits, to obtain the best performance.

5.3.1 LED Transmitter Drive Circuit

To obtain the best performance from the LED transmitter, it is preferable for the LED driver to employ prebiasing and current peaking. To prebias the LED, it should be driven between a low and high current to represent low and high logic levels respectively, and never completely turned off. The prebias current prevents the junction and parasitic capacitances from discharging completely when the LED is in the “off” state, thus reducing the amount of charge that the driver must transfer to turn the emitter back on. The simple inverter circuit given in Figure 5.5 will provide a bi-level current drive to the LED. This circuit is used as the basis for the LED driver circuit, and the calculations of the values of the drive resistors, R_D and R_B , are given the following paragraph.

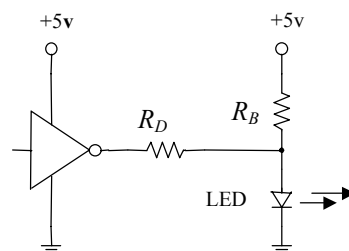


Figure 5.5 *Bi-Level Current Driver for the LED*

The most suitable high and low currents, I_{Fon} and I_{Foff} , through the LED transmitter for the respective on and off logic levels, must be chosen. From the data sheets of the LED, the forward voltage, V_{Fon} and V_{Foff} , at the high and low current levels respectively, can be obtained. For the circuit of Figure 5.5, two expressions can then be written relating the LED current and their forward voltage to drive resistors. Equation 5.3.1 shows the relationship of the high-level current, I_{Fon} , through the LED when the output of the inverter is high, to the drive resistors. Equation 5.3.2 shows the relationship of the low-level current, I_{Foff} , through the LED when the output of the inverter is low, to the drive resistors.

$$I_{Fon} = \frac{5 - V_{Fon}}{R_D} + \frac{5 - V_{Fon}}{R_B} \quad (5.3.1)$$

$$I_{Foff} = \frac{5 - V_{Foff}}{R_B} - \frac{V_{Foff}}{R_D} \quad (5.3.2)$$

A high current of 120mA and a low current of 2mA were selected as being suitable for the HFBR-1526 LED transmitter. From the data sheets, V_{Fon} and V_{Foff} for these two currents can be found. Equations 5.1 and 5.2 can now be solved for R_D and R_B , hence R_D was found to be 40Ω and R_B to be 91Ω. The actual values of R_D and R_B used are given in Figure 5.7. To practically implement this LED current driver, AC type CMOS inverters are used as they have the fast rise and fall times required, can sink and source up to 24mA continuously, and have a peak current rating of 75mA. The inverter of Figure 5.5 was implemented by paralleling four of the inverters from a 74AC14 hex inverter to give the required current rating. When the LED driver circuit of Figure 5.5 is used to drive the LED, slow rise and fall times are observed. This can be seen in Figure 5.6, where the upper trace shows the LED forward voltage and the lower trace shows the output of the fiber optic receiver. The fiber optic receiver output voltage varies between 1.8V and 2.8V giving a 1Vpp output voltage swing.

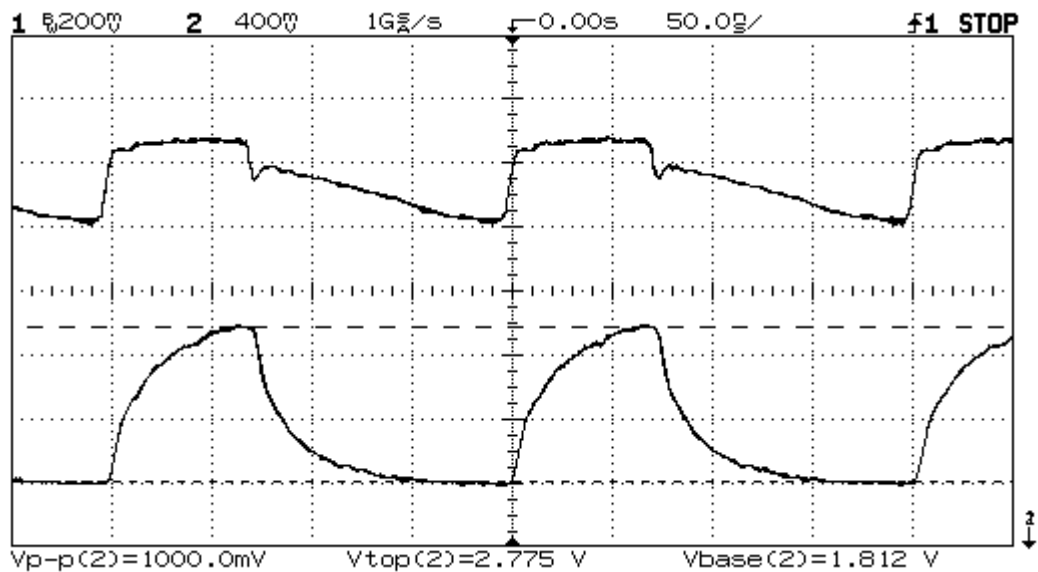


Figure 5.6 LED Forward Voltage and Fiber Optic Receiver Output Voltage

The slow rise and fall times observed in Figure 5.6 occur because the parasitic and junction capacitances of the LED have to be charged and discharged. The rise and fall times can be improved considerably by using current peaking. The addition of a simple RC speed-up network in parallel with the drive resistor, R_D , of the circuit given in Figure 5.5, was found to be highly effective. A series resistor-capacitor combination was found to be preferable to just a plain capacitor, as this induced too much ringing. The optimum RC values were found empirically and their values are given in the final LED driver circuit of Figure 5.7. The AC-CMOS inverters have a peak source/sink current rating of 75mA each, and so they can easily provide the peak currents required.

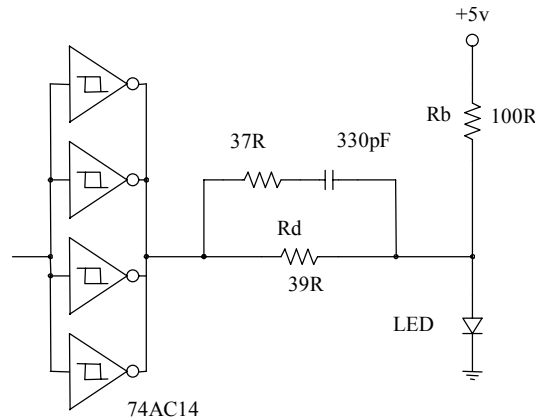


Figure 5.7 Final LED Driver Circuit

The waveforms obtained with the final LED driver circuit of Figure 5.7 can be seen in Figure 5.8. The circuit was found to be simple to implement and effective, achieving the fast rise and fall times required. The upper trace of Figure 5.8 shows the LED forward voltage and the lower trace shows the output of the fiber optic receiver.

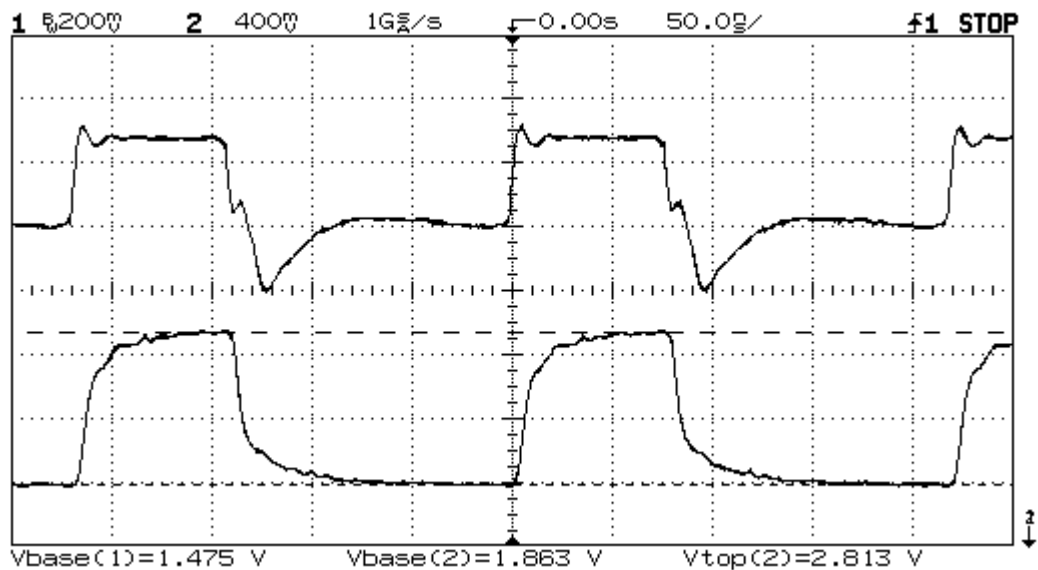


Figure 5.8 LED Forward Voltage and Fiber Optic Receiver Output Voltage with RC speed-up network

As mentioned before, fiber optic links of identical lengths with matching driver and receiver circuits are used to transfer the drive signals to both high and low-side MOSFETs. This was done to minimize the time skew and pulse width distortion between the signals, and as the two links are in close proximity to each other, the temperature effects on both links should be similar. Figure 5.9 shows the fiber optic receiver output voltage for both the high and low side. The time skew between the two received signals was observed to be less than 2 nanoseconds over the full range of duty-cycles and frequencies. The waveforms of Figure 5.9 were obtained with the supply voltage held at zero volts, so the high side signal could be measured relative to ground.

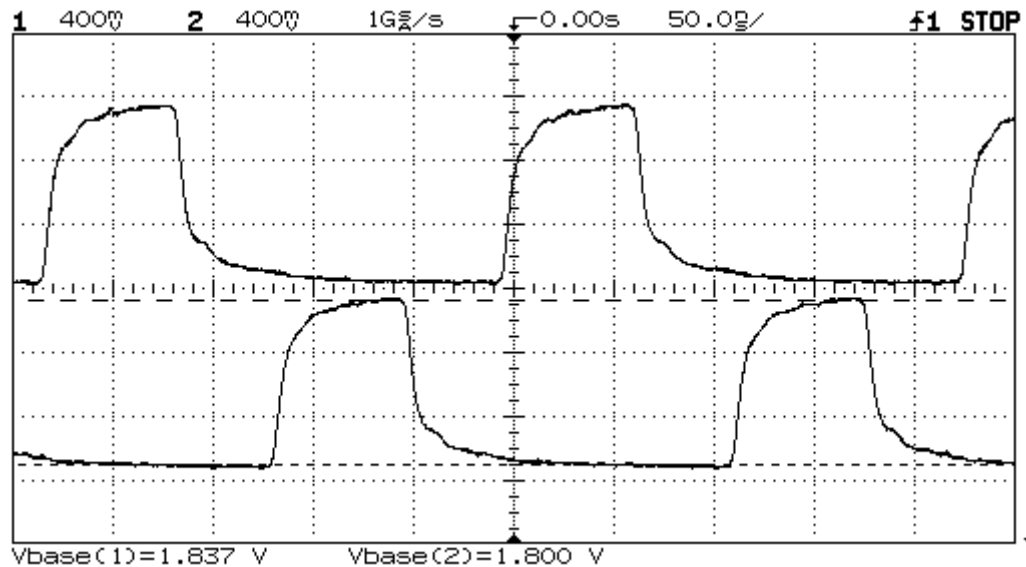


Figure 5.9 High and Low-side Fiber Optic Receiver Output Voltage

5.3.2 Comparator

The amplitude of the output signal from the fiber optic receiver is at best 1V peak to peak, and must be converted into a 5V on/off logic signal. However, converting this to a logic signal is complicated by the fact that the DC offset of the received signal can drift up to ± 1 V with changing temperature. Thus the received signal can not simply be compared to a set reference level. This problem could be solved by using capacitive decoupling, but then permanent on or off information would be lost, and MOSFETs could not be held on or off reliably for an indefinite amount of time. The problem was solved using an average DC-level crossing detector with hysteresis added (memory). This is done by combining two simple circuits, an inverting comparator with hysteresis and a DC-level crossing detector (also inverting). The two circuit diagrams of Figure 5.10 explain the development of the circuit. The idea is that the low pass RC filter of the DC level crossing detector will tend towards the average DC level of the incoming signal. However, with the correct hysteresis added, the DC level of the RC filter will be kept slightly above or below the average DC of the incoming signal, depending on the last state the comparator was in. Thus the hysteresis acts as a form of memory, keeping the comparator in its last state. The average DC-level crossing detector enables the comparator to track slow changes in the DC offset due to temperature effects and the hysteresis (memory) enables the comparator to stay in its last state for an

indefinite period of time. The approximate values of resistors can be calculated approximately using a simple circuit analysis and refined using a Spice simulation. The capacitor is attached to +5V instead of ground to ensure the correct start-up state i.e. the MOSFETs are off on start-up. The signals from the high and low side comparators are shown in Figure 5.11. The comparator used was an LT1016 and the complete circuit can be seen in Appendix C.

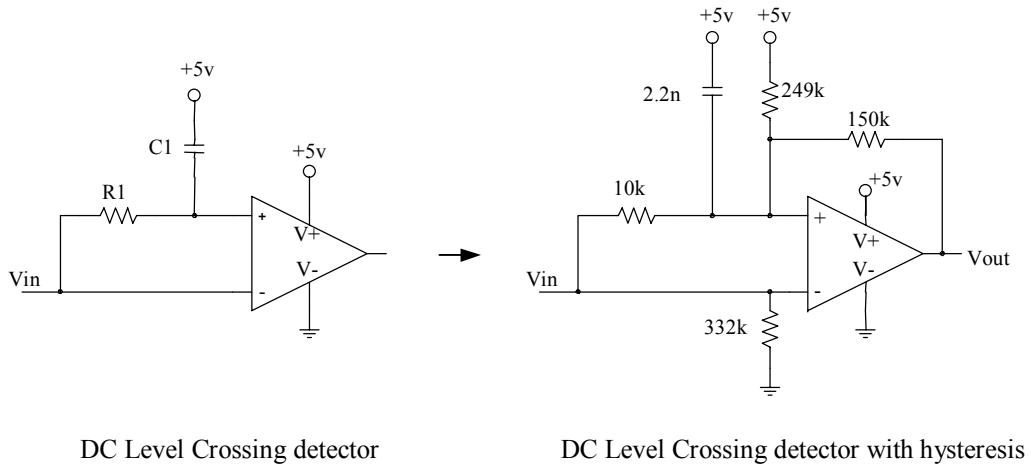


Figure 5.10 Development of the Comparator for the Fiber Optic Receiver

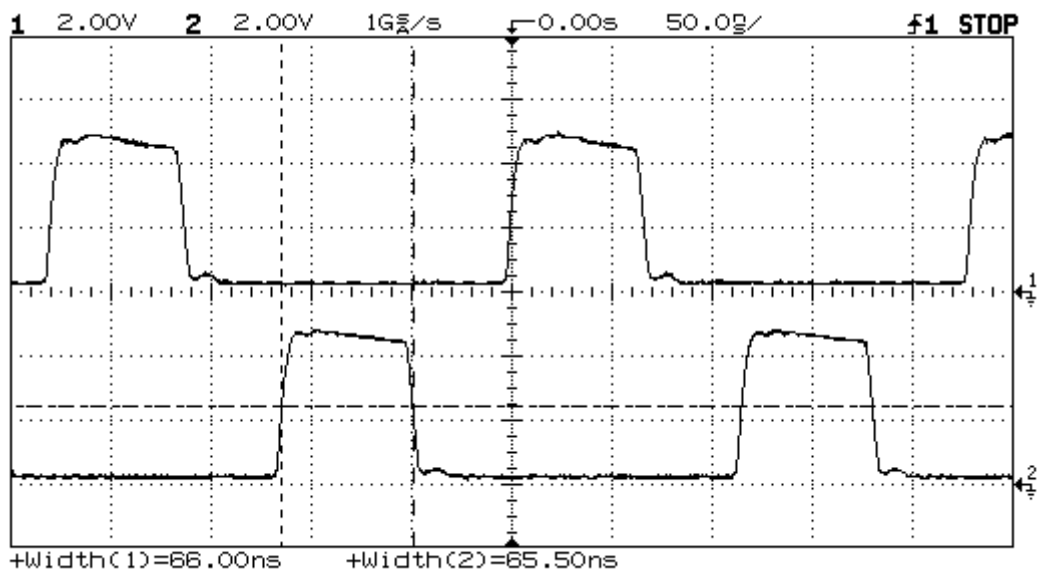


Figure 5.11 High and Low-side Comparator Outputs

5.4 CONCLUSIONS

This Fiber optic link was tested on a half bridge operating up to 1kW at 5MHz, with slew rates of up to 30V/ns. From the midpoint voltage of the half bridge, it could be ascertained that the MOSFETs were switching at the correct instants. The drive signal information must therefore have been transferred to the high and low side switches correctly, and it can be concluded that the fiber optic link is functioning as required. The Fiber optic communication-link proved to be a comprehensive solution that was relatively easy to implement has excellent EMI and dv/dt immunity. Its high bandwidth enabled reliable operation from DC up to 5MHz, with almost any duty cycle possible. To summarize, the fiber optic communication-link enabled a broadband, versatile and adaptable half-bridge inverter to be built.

5.5 DISCUSSION

A type of idealistic half bridge inverter would have two light activated switches, which require minimal input power and have infinitesimal switching times. To operate the inverter one would then simply direct light into the desired switch to turn it on. By using a fiber optic cable with a receiver, comparator and current buffer, we are in effect emulating such an ideal switch. The use of Fiber optic links in high power, high frequency inverters to control floating devices has not been fully explored and its advantages have not been fully realized. The cost and complexity of fiber optic links may have limited their use in the past but simple logic to logic fiber optic links using cheap plastic fiber are now available.

The fiber optic *communication-link* described in this chapter was used to drive n-channel MOSFETs. This is a switch with its on/off signal referenced to its cathode. A switching device may have its on/off signal referenced to either its cathode or anode. A fiber optic communication-link can easily be adapted for use on both these types of switches. Using Fiber optic connections to both high low side switches enables any combination of the above switches to be used. Another possible application of fiber optic communication-link is to drive power devices that have been stacked in series to increase their voltage rating. This would enable simultaneous switching of the power devices, which are all at different potentials. In microprocessor controlled converters where a communications link is required between the micro-board and the output stage, a fiber optic link could perform the communication and level shifting in one step.

A fiber optic communication-link should be an excellent solution in any demanding power electronic applications where frequency, voltage, dv/dt or EMI requirements preclude the use of more conventional methods. A fiber optic link will also improve greatly improve the ruggedness of less demanding applications and a 1mm plastic fiber link will provide a relatively inexpensive system.

CHAPTER 6. PHYSICAL CONSTRUCTION OF THE INVERTER

6.1 DESIGN CONSIDERATIONS OF THE INVERTER CONSTRUCTION

In order to obtain reliable operation of a Class-DE series resonant inverter and have clean waveforms, it is critical that the half-bridge inverter output stage be constructed correctly. The first consideration is that the decoupling-capacitor — inverter loop shown in Figure 6.1, must be designed to have the absolutely minimum inductance feasible. This low inductance loop is needed because at the instant of turn off, the current is commutated from one switch-leg to the other switch-leg (into its output capacitance). Also, the high-side switch requires a low RF impedance through the decoupling-capacitor to ground when it turns on. The decoupling capacitance should be large enough for operation at the lowest frequency and have the minimum ESR and ESL possible.

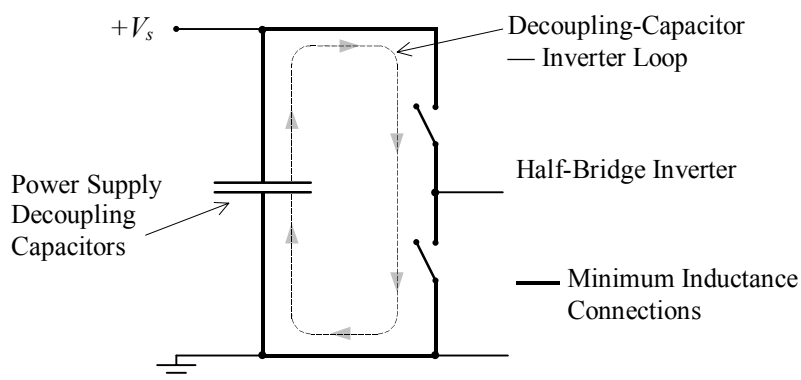


Figure 6.1 *The Decoupling-Capacitor — Inverter Loop*

The impedance of the decoupling-capacitor — inverter loop shown above in Figure 6.1 will increase linearly with frequency. Thus it becomes more critical as the frequency increases to minimize its inductance in order to obtain correct operation. As a rough guide, the impedance associated with the loop inductance should be at most 1/10 of the load impedance level the inverter is operating with. The load impedance of the inverter in this thesis is in the region of 10Ω and the operating frequency is 5 MHz. The loop should therefore have a maximum impedance of 1Ω , which at 5 MHz means the loop inductance must be less than 30 nH. If additional output capacitance is added to the switches, it should be connected directly across the switch terminals with minimal lead inductance. This will allow the current to easily commutate from the switch into its output capacitance. If the midpoint voltage measurement is to be made referenced to ground, then a very good RF ground plane should be provided for the low side switch. This will avoid ground loops and hence ground noise.

A second design consideration is that the stray capacitance added to the midpoint due to the physical construction of the inverter should be kept to a minimum. Lower midpoint capacitance means that there will be less power dissipation in the case of non-zero voltage switching, and that the conduction angle will not have to

6.2 ACTUAL CONSTRUCTION OF THE INVERTER

The IRFP450 MOSFETs used in this inverter are packaged in the industry standard TO-247AC case. This has a drain lead inductance of 5 nH between the center of the die contact and the point on the drain lead 6mm from the edge of the package. Similarly, it has a source lead inductance of 13 nH between the center of the die contact and the point on the source lead 6mm from the edge of the package. The back-tab of the package is bonded directly to the MOSFET die. The drain lead inductance can be practically eliminated by mounting each MOSFET directly onto its own aluminum heatsink and using the heatsink as the drain connection to the back-tab of the package. This required two isolated heatsinks, one of which would have the high-side MOSFET mounted on it and hence is at the supply potential, and the other would have the low-side MOSFET mounted on it and hence is at the midpoint potential. The midpoint heatsink was mounted so that it had enough physical separation from the surrounding ground enclosure to minimize the stray capacitance to an acceptable level. The separation of the two heatsinks from each other was optimized to obtain a compromise between added stray capacitance and connection inductances. The layout of the heatsinks can be seen in Figure 6.3.

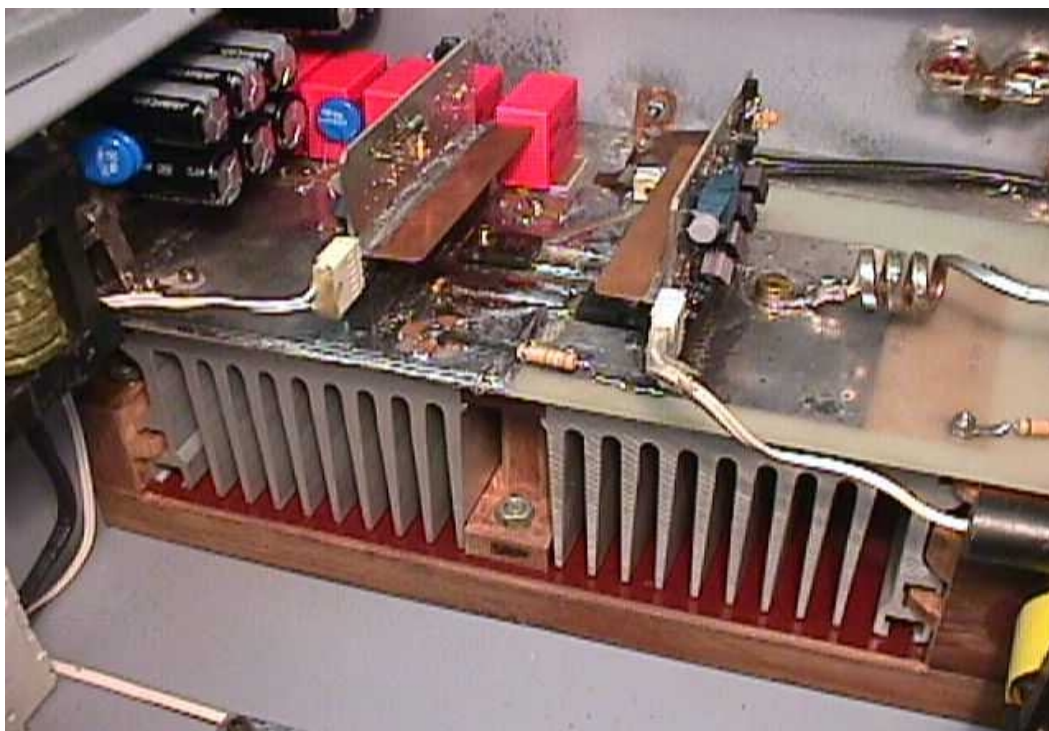


Figure 6.3 *Front View of Inverter Output Stage Showing the Isolation of the Heatsinks*

Low inductance connections must then be made from the source of the high-side MOSFET to the low-side MOSFET's heatsink, from the source of the low-side MOSFET to ground, and from ground through the decoupling power supply capacitors back to the high-side MOSFET's heatsink. These low inductance connections were achieved by mounting the two heatsinks in the same plane, enabling a PCB to be placed directly over the top of both heatsinks. This PCB is referred to as the main PCB board. The MOSFETs were mounted through the main PCB board onto the heatsinks. The topside of the main PCB board was then used to

provide the connections between the two heatsinks and to the gates of both MOSFETs. The center drain lead of the MOSFET was removed in order to allow wider gate and source tracks. The entire topside of the main PCB above the high-side heatsink was made a ground plane. This provided the low inductance connection from the ground plane, through the decoupling power supply capacitors and to the drain of the high-side MOSFET. The bottom side of the PCB was therefore connected directly to the heatsink and the decoupling capacitors were connected between the topside and bottom side of the PCB. The decoupling power supply capacitors were provided by twenty 68 nF, 500 V multi-layer ceramic capacitors paralleled with larger polypropylene capacitors. Multi-layer surface mount ceramic capacitors have very low ESR and ESL and are imperative for this application. The topside of the PCB over the midpoint heatsink was directly connected with plated feed-thru holes to the bottom side. The topside of the PCB was extended to make the connection to the source of the high side MOSFET. These connections can be seen in Figure 6.4, which shows the topside of the main PCB board.

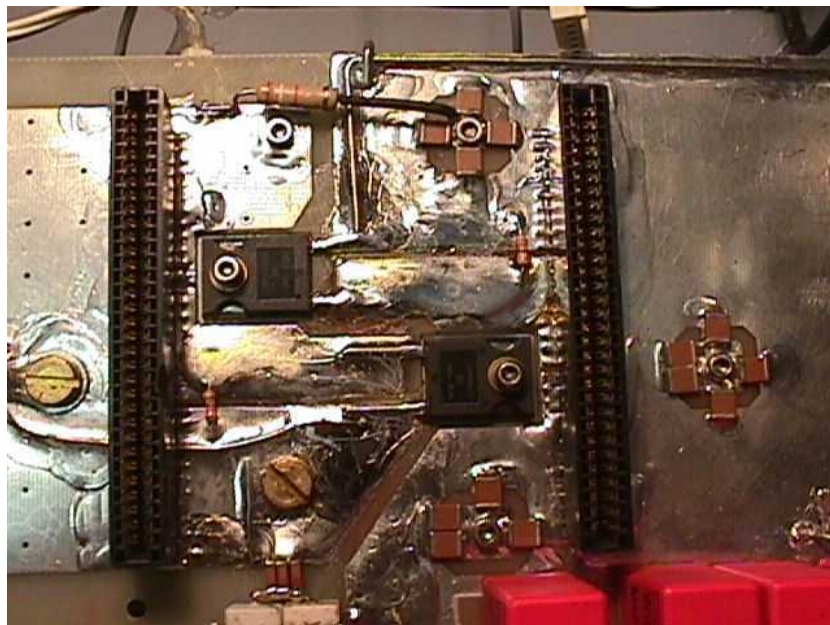


Figure 6.4 Top View of Main PCB Board Showing the Layout of the Power MOSFETs

The added stray capacitance to the midpoint due to the physical construction of this inverter was measured to be 90 pF. The inductance of decoupling-capacitor inverter loop is difficult to measure but is thought to be mainly comprised of the two source lead inductances, hence it will be in the region of 26 nH.

The gate-driver circuitry was mounted on a separate PCB referred to as the Gate-driver board. The two boards for the high and low side were mirror images of each other. These boards were mounted perpendicular to the main PCB board. This enabled the gate-driver to be physically close to the MOSFET without breaking up the low inductance connections to the sources of both MOSFETs. It also enabled low inductance gate charging and discharging loops to be made. Mounting the gate driver boards vertically means there will be a free air-flow over the boards, improving their thermal dissipation capabilities. The gate-driver boards will also be thermally isolated from the power MOSFETs. The gate-driver boards and the fiber optic connections can be seen in Figure 6.5.

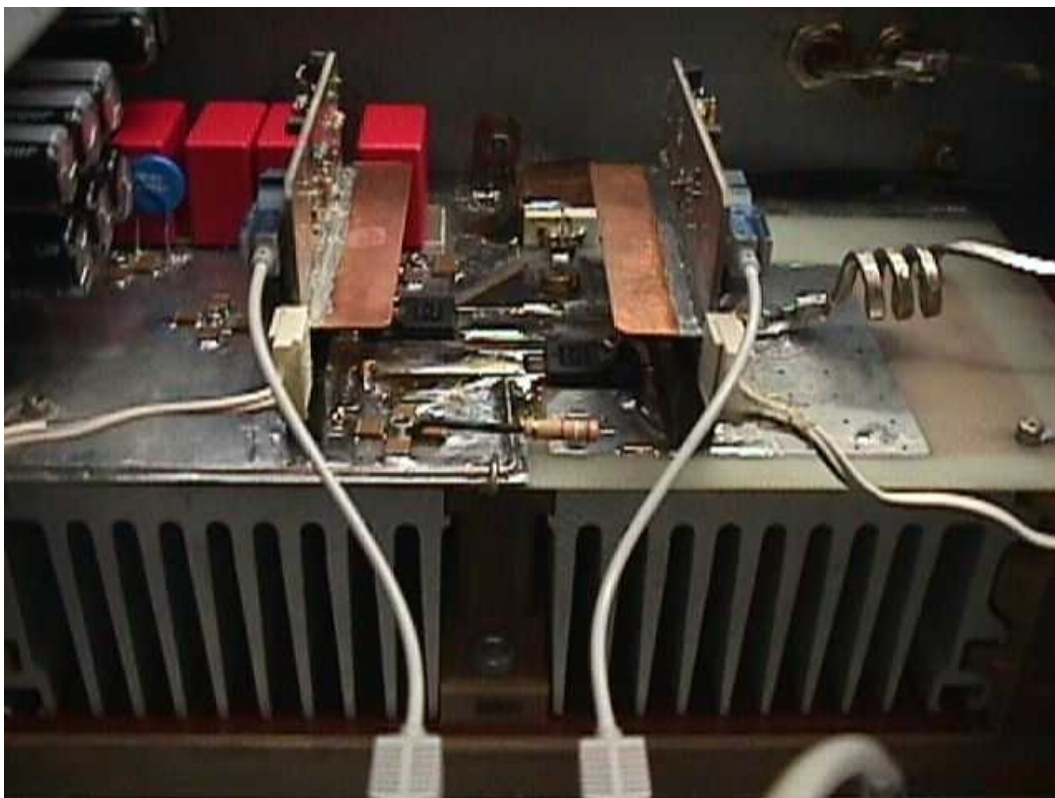


Figure 6.5 Front View of Inverter Output Stage Showing the Gate-driver boards and Fiber Optic Links

The whole output inverter stage has a large physical separation to the drive signal generator board and all other auxiliary circuit boards. This was made possible by use of fiber optic links to transfer both drive signals. All other auxiliary circuit boards should be made with good RF construction techniques and with a good ground plane as the inverter will generate a fair amount of RFI and EMI. It may prove necessary to provide additional shielding for the auxiliary circuit boards but this was not needed in this inverter.

The inverter construction described above is approaching its operational limit at 5 MHz. For operation at higher frequencies it will be necessary to employ a more suitable means of construction. A better solution would be to construct the entire half-bridge on a ceramic substrate. This method will enable lower loop inductance, less added stray capacitance and good power dissipation. With this technology, it should be possible to construct an inverter that has the potential to operate to higher frequencies such as 13.56 MHz, and possibly 27 MHz.

6.3 RESONANT LOAD NETWORK

The capacitor used in the LCR network will experience large voltages at Radio frequencies because of the Q of resonant network. It will therefore have to be an "RF power capacitor" of which the most commonly used type are the ceramic capacitors. RF power capacitors are usually rated by peak voltage, peak current and peak reactive power over a specified frequency range. The capacitor, C , used in the LCR network must therefore be selected to have adequate ratings for its particular application. The current through the capacitor is simply the same as the load current, hence the peak current through the capacitor will be I_p , and the peak voltage across the capacitor is then given by

$$V_C = \frac{I_p}{\omega_s C} \quad (6.3.1)$$

The reactive power, Q_n , handled by the capacitor is given by

$$Q_n = \frac{I_p^2}{2\omega_s C} \quad (6.3.2)$$

The series resonant capacitor used in the LCR network for operation at 5 MHz will have a peak current of 16A through it, a peak voltage of 510V across it, and it will handle a reactive power of 4070VA. The capacitor used was a 1nF 5kVA_r mica capacitor.

The inductance seen by the inverter will be the inductance of the whole LCR loop, which is difficult to measure, but it will be larger than the measured inductance of the inductor in the LCR network. Hence, the inductor of LCR network should be designed to have a value slightly less than the desired inductance. It should also be constructed in such a way that there is minimal coupling capacitance across it. The inductor used for operation at 5 MHz was constructed of a single layer of 4 widely spaced turns, 30mm in diameter. The measured inductance was $1.1\mu H$. The inductance and capacitance should be mounted in such away that they have minimal stray coupling capacitance to any surrounding ground conductors.

The required load resistance for this inverter was calculated in the design example of section 2.2.5 to be 9.4Ω . Spice simulations showed the actual resistance required will be less than this because of the on-resistance of the MOSFETs, and hence should be in the region of approximately 8Ω . The load resistance should also have minimal stray inductance and capacitance, (i.e. it should be a well-behaved RF load), as stray parasitics can lead to stray resonances. The load resistance must also be capable of dissipating 1 kW of power. The final load resistance was constructed of six 50Ω 250W RF dummy load resistors connected in parallel and mounted on a water cooled heatsink. This gives an effective load resistance of 8.33Ω . The connections between the resistors were made with the least inductance possible. The second load resistance of 12.5Ω was made by paralleling the 4 250W RF dummy load resistors and water cooling the heatsink with iced water. 12.5Ω was chosen as it lends itself to matching to 50Ω with 1:4 transmission line transformer.

6.4 MEASUREMENTS

Two principal measurements are made on the inverter while it is in operation. These are the midpoint voltage and load current. The midpoint voltage is measured using a 100:1 resistor voltage divider. A 10W 5k resistor provides the first resistor which is attached between the midpoint and the inner conductor of a 50ohm coaxial cable. The outer conductor of the coaxial cable is grounded. The coaxial cable is then fed to the scope and is terminated with 50Ω at the scope input.

The current is measured using a toroidal current transformer placed between the midpoint and the load network as shown in Figure 6.7. The first current transformer used a 1:18 turns ratio, the secondary being terminated with two 2W 22 Ω resistors in parallel with a 50 Ω coaxial cable. The coaxial cable is fed to the scope and is terminated with 50Ω at the scope input. The effective secondary resistance is therefore 9 Ω , which gave sensitivity of 0.5V per 1A. Various physical implementations of the current transformer were attempted. The first attempts had one of the secondary terminals of the current transformer grounded, together with the outer conductor of the coaxial cable. This method had a lot of ringing and noise caused by the rapidly changing midpoint voltage coupling through the stray capacitances to the secondary windings. Shielding the secondary helped reduce this ringing but was not entirely effective.

A better solution was found to make the entire current transformer floating i.e. not grounding either secondary terminal or the outer conductor of the coaxial cable. The coaxial cable feeding the scope can then be made into a transmission line balun, (acts as a common mode choke), by passing it through a toroidal core and grounding it a suitable length away from the current transformer. This is illustrated in Figure 6.6. The coaxial cable is still terminated with 50Ω at the scope input. The final current transformer used a 1:25 turns ratio, feeding a 50 Ω resistance in parallel with a 50 Ω coaxial, giving an effective resistance of 25 Ω , and a sensitivity of 1V per 1A. The transformer still some required shielding to reduce the pick-up noise caused by EMI emitted when the inverter was non-zero voltage switching. The shielding was placed around the secondary without completing the loop, with one end of the shield being connected to one of the secondary terminals.

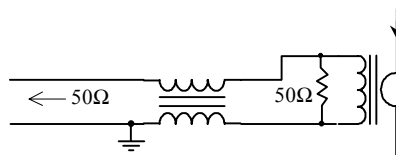
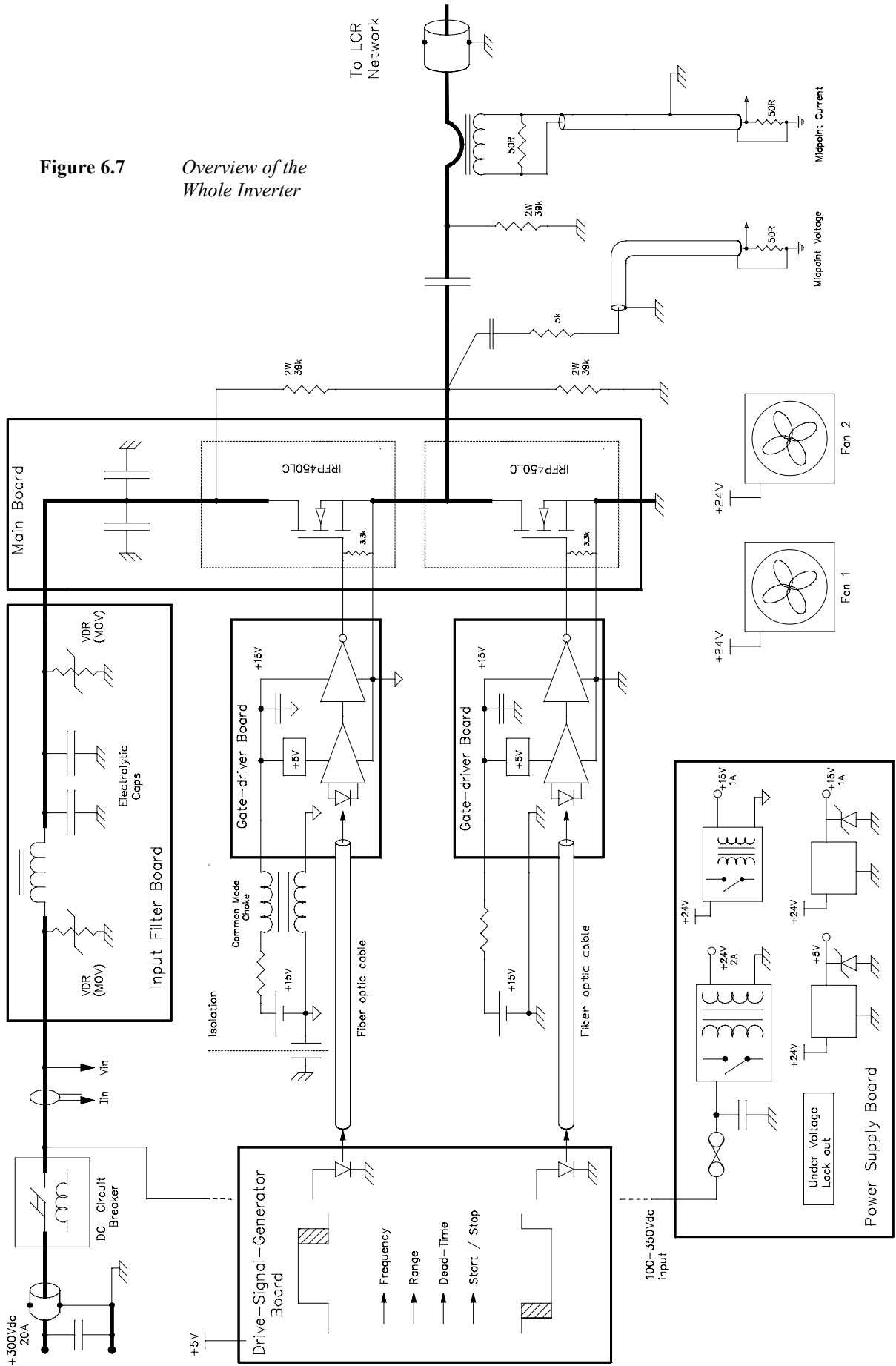


Figure 6.6 Current Transformer

The power output was measured by recording the midpoint voltage and load current on a digital oscilloscope and importing the waveform data into a spreadsheet. Here the two waveforms are multiplied together and averaged over one period to obtain the power output. The power measurements were confirmed by measuring the voltage directly across each individual 50 Ω resistor of the load resistance, and using a digital scope to find the true RMS voltage. A final overview of the whole inverter can be seen in Figure 6.7.

Figure 6.7 Overview of the Whole Inverter



CHAPTER 7. EXPERIMENTAL RESULTS

The broadband design of the control circuitry, communication-link and gate-drive enabled the half-bridge output stage to be driven from 50 kHz through to 6 MHz. The only circuit changes needed for the different operating frequencies are the inductance and capacitance of the tuned network. The calculation of the values of the inductance and capacitance for tuned LC network is simple and fast. The tuning procedure for Class-DE mode of operation is relatively simple and can be done without any circuit changes. This enabled very quick modifications for different operating frequencies. When operated in the Class-DE mode, the inverter was found to be capable of delivering a power output of over 1 kW from 50 kHz to 5 MHz with an efficiency of over 90%.

The inverter used IRFP450LC MOSFETs, as these have a lower input, reverse transfer and output capacitance. This lower output capacitance means the switches can be operated with a larger conduction angle for a given frequency, and hence will output more power. Thus, at a operating frequency of 5 MHz, a supply voltage of 300 V and with load resistance of 8.33 ohms, the inverter can be expected to output slightly more power than shown in the simulation of Section 3.3.3, which used IRF450 MOSFETs. The lower gate charge required for the IRF450LC also lowered the power dissipated in the gate-drivers and allowed for a higher gate-drive voltage.

Tests on the inverter started at a low frequency and power and both were systematically increased. The inverter could be operated in normal Class-D operation up to approximately 1 MHz. Up to this frequency, the inverter operation was as good as could be expected using non-ideal switches and little problems were experienced. Above 1 MHz, the inverter should be operated in such a way that the capacitive switching losses are reduced. Above 3 MHz and at power levels greater than 500 W, the inverter must be operated as close as possible to true Class-DE type of operation. When the inverter was operated in a non-zero voltage-switching mode, (i.e. the switches were turning on with a non-zero voltage across them), the ringing noise and EMI emitted were very apparent. Operating the inverter in the Class-DE mode reduced the ringing noise and EMI to a level that was barely noticeable.

When operating below 3 MHz in Class-DE mode, the only significant loss in the inverter was due to the on-resistance of the MOSFETs. The efficiency of the inverter at full output power for all frequencies up to 3 MHz was therefore in the region of 94%. The results up to 3 MHz were close to perfect and do not give the designer much practical information. The test results presented in this thesis are therefore from 3 MHz upwards. Above 3 MHz, the efficiency begins to decrease which is thought to be due to a number of reasons. These are:

- a) Some turn-off loss will occur due to non-instantaneous switching,
- b) Higher RMS currents will be experienced because of the smaller conduction angle required,
- c) Loss associated with the drift resistance of the MOSFET when charging/discharging the output capacitance
- d) Some capacitive discharge loss will occur at turn-on.

7.1 TUNING PROCEDURE FOR CLASS-DE OPERATION

The process of obtaining Class-DE operation starts by making the inductance and capacitance of the LC tuned network with values as close as possible to the calculated ones. The conduction angle of the switches should then be set to a value smaller than what was calculated (i.e. a larger dead-time). The supply voltage to the inverter should be set at a relatively low value, which in this case was 100 V. The approximately correct phase lag of the load current to the midpoint voltage should then be obtained. This is done by increasing the driving frequency of the inverter above the resonant frequency of the LCR network until the midpoint voltage is seen to swing almost to the opposite rail after turn-off. This effect can only be observed if the dead-time is larger than required. The dead-time must then be adjusted until the switches turn on at the instant where the voltage across them is the lowest. This process can then be repeated with smaller adjustments until optimum Class-DE operation is obtained. The inductance and/or the capacitance of the tuned network can now be appropriately adjusted to increase or decrease the operating frequency. The process described above is then repeated until the inverter operates in Class-DE mode at the desired frequency. As the supply voltage is increased above 100 V, slightly less dead-time and phase lag are required to obtain optimum Class-DE operation due to the non-linear output capacitance of the MOSFETs.

The following section (Figure 7.1 to Figure 7.4) shows four cases of oscilloscope waveforms obtained while tuning the inverter for Class-DE operation. The supply voltage in all four cases is 100 V and the LCR tuned network remains unchanged. The only parameters that are varied are the switching frequency of the inverter and the conduction angle of the switches. The oscilloscope waveforms shown for each case are the midpoint voltage, the load current and the gate-source voltage of the low-side MOSFET. The waveforms are captured on a HP54615B 500 MHz digital oscilloscope. For each case, the first oscilloscope screen capture shows the midpoint voltage on channel-1 and the load current on channel-2. The voltage and current scale are both 1:1. The second oscilloscope screen capture shows the gate-source voltage of the low-side MOSFET. Both of the screen captures are triggered on the midpoint voltage and hence they have the same time line. Relative timing comparisons between the two screen captures can thus be performed. Figure 7.5 shows how the efficiency varies over the tuning procedure.

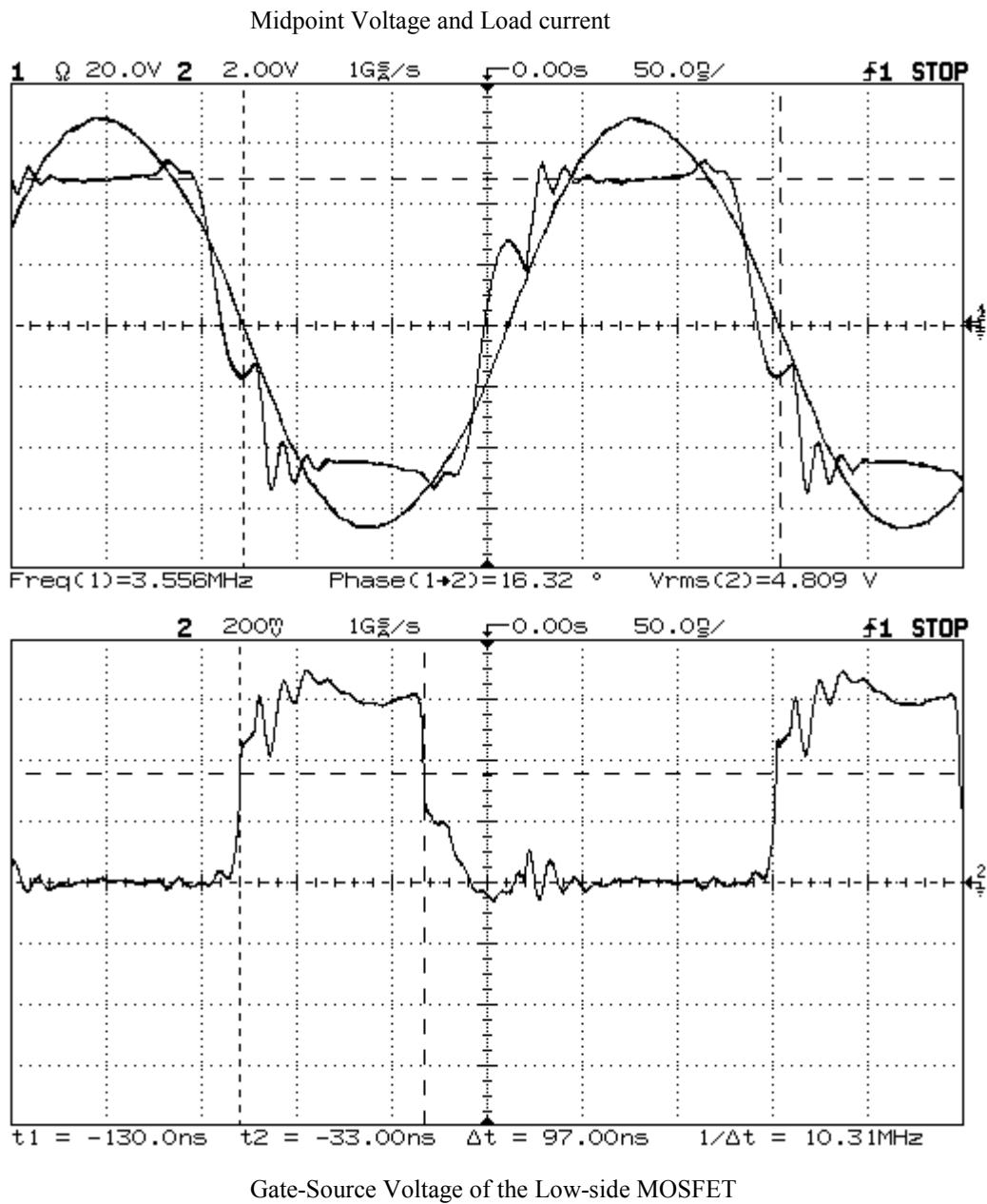


Figure 7.1 Case 1. *Too Little Phase Lag*

From the oscilloscope waveforms of Figure 7.1, it can be seen that non-zero voltage switching is occurring. This is because in the period between the switch off instant and the point where the load current reaches zero, the midpoint voltage does not swing all the way across to the opposite rail. This means that not enough charge is removed from the midpoint by the load current before it reverses direction. To increase the charge removed from the midpoint, the phase lag of the load current to the midpoint voltage must be increased. This is achieved by increasing the switching frequency of the inverter and the effect of this can be seen in the following waveforms of Case 2, Figure 7.2.

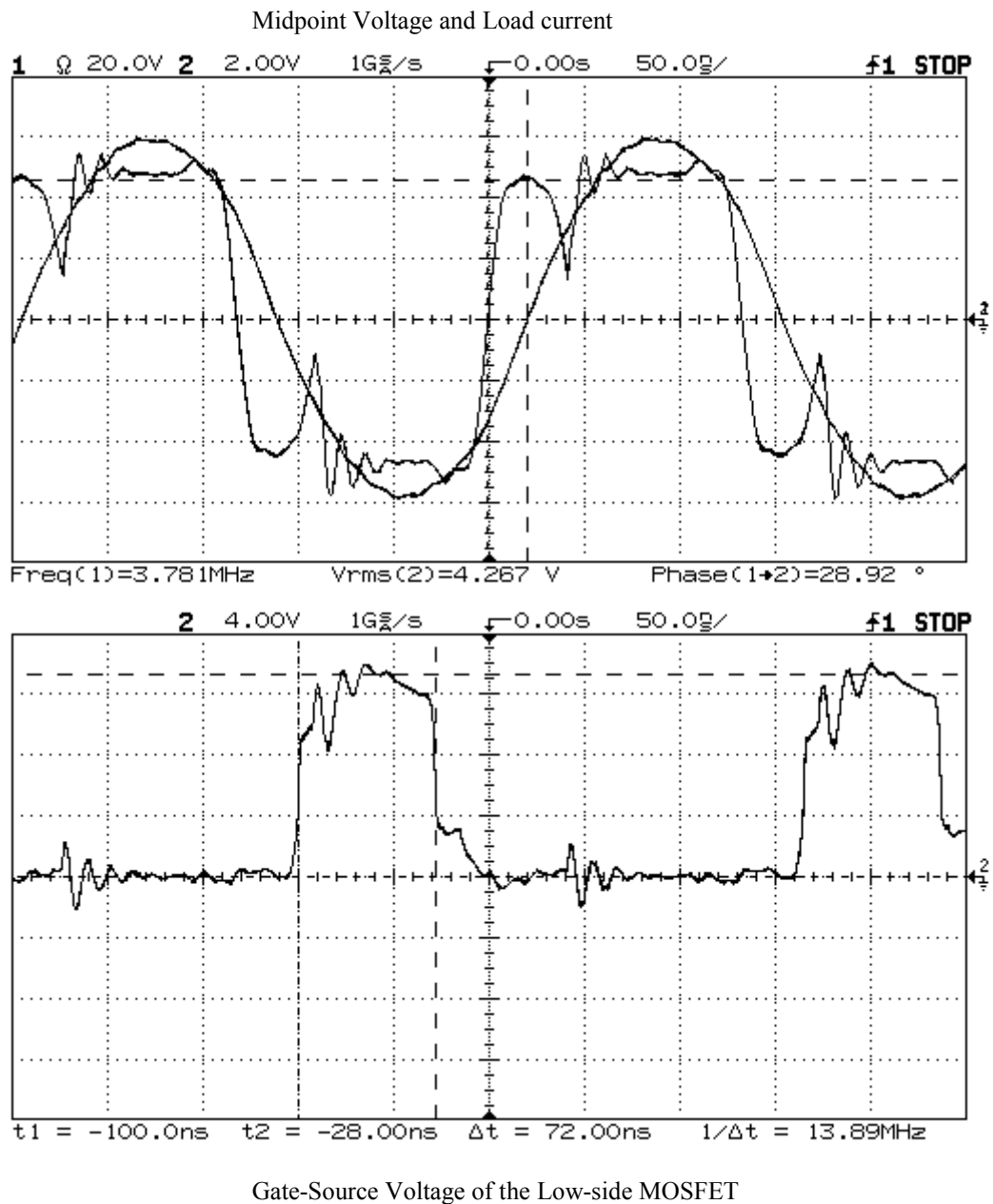


Figure 7.2 Case 2. *Too Much Dead-Time*

From the oscilloscope waveform of the midpoint voltage in Figure 7.2, it can be seen that after the switch-off instant the midpoint voltage swings almost all the way to the opposite rail before the load current reaches zero. The opposing switch however does not turn on at this instant and so when the current reverses direction the midpoint voltage starts to swing back towards its original rail. The opposing switch only turns on after the midpoint voltage has swung almost half way back to original rail. This means that the phase lag of the load current is correct but the conduction angle is too small (i.e. the dead-time is too large) and the switch is turning on too late. To remedy this the conduction angle simply has to be increased and the effect of this can be seen in the following waveforms of Case 3, Figure 7.3.

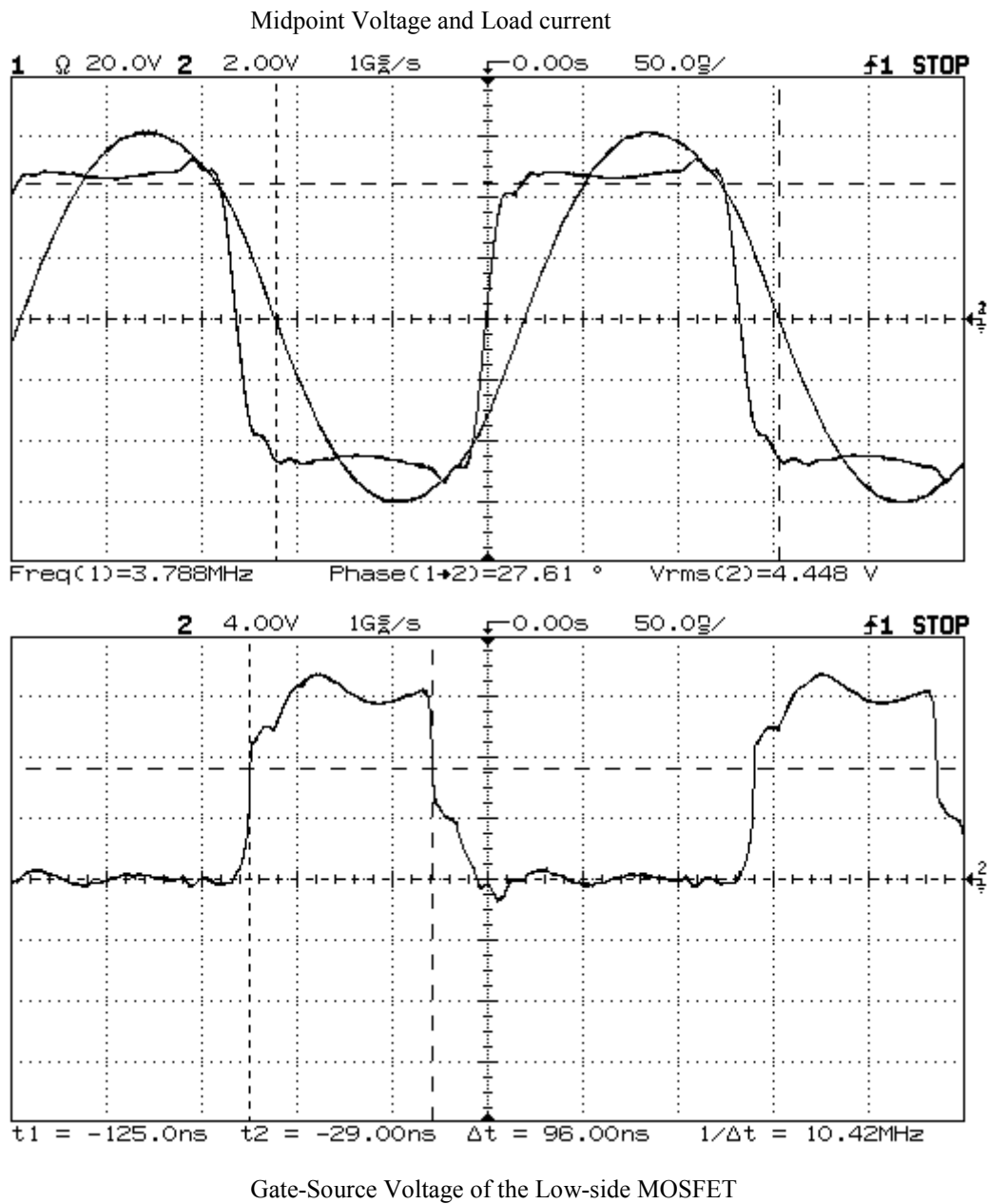


Figure 7.3 Case 3. Optimum Class-DE Operation

The oscilloscope waveforms of Figure 7.3, show optimum Class-DE operation. The midpoint voltage swings almost all the way to the opposite rail before the load current reverse direction and the opposing switch turns on at this instant. Thus the switches are turning on at zero-voltage and zero-load-current (zero dv/dt). This considerably reduces the amount of ringing caused by the switching transitions and the EMI emitted. These effects can be observed in the clean waveforms above as compared to the previous cases. If the conduction angle is increased further still then the switches will turn on before the midpoint voltage has reached the opposite rail (i.e. they will turn on too early). The effect of increasing the conduction angle too much can be seen in the following waveforms of Case-4, Figure 7.4.

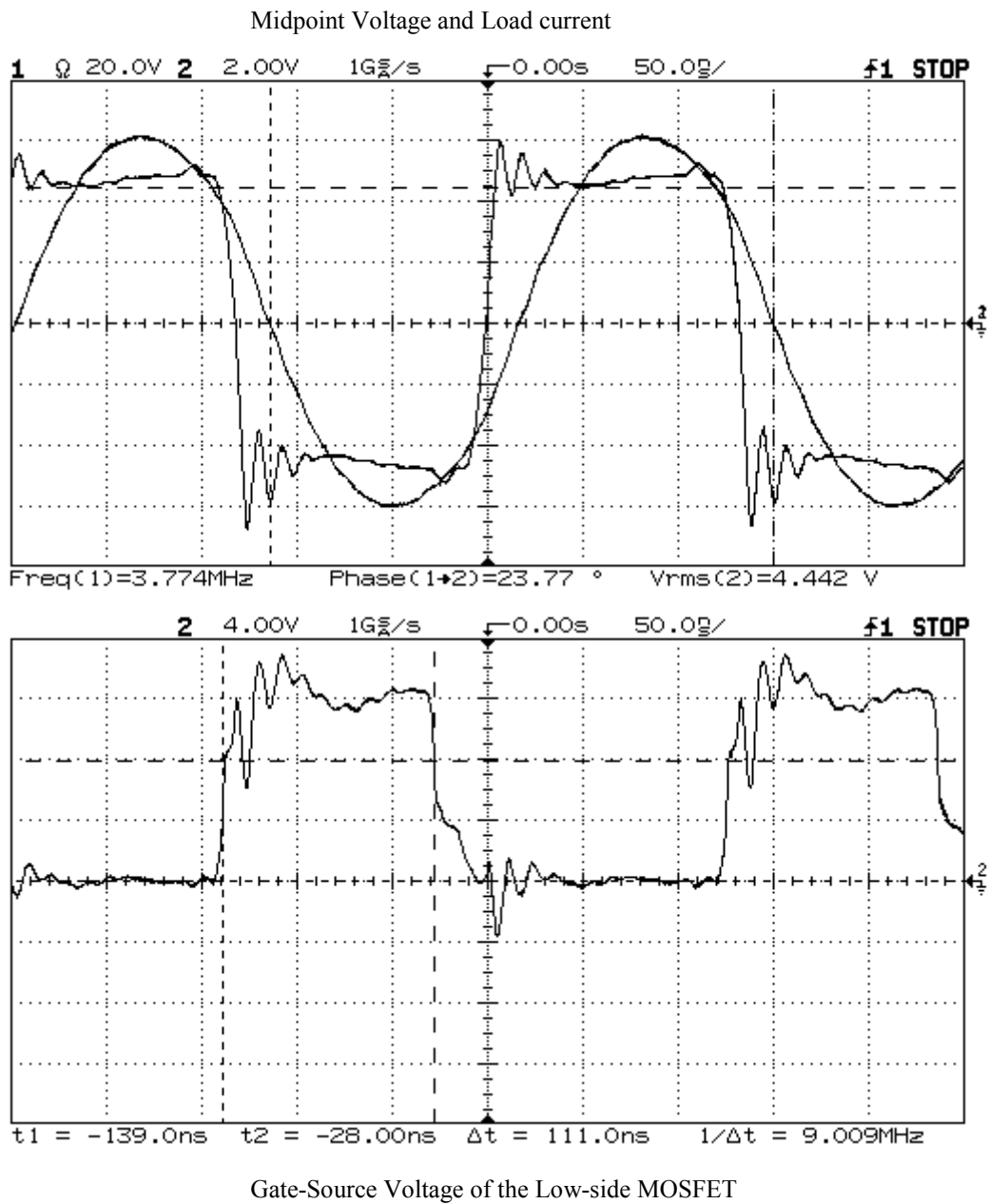


Figure 7.4 Case 4. *Too Little Dead-Time*

From the oscilloscope waveforms of Figure 7.4, it can be seen that the switches are turning on before the midpoint voltage has swung all the way to the opposite rail and there is still a voltage across the switches. It can also be observed that the switches turn on before the load current has reached zero, which means that they are turning on too early. The conduction angle has therefore been increased too much and should be reduced until the waveforms of case-3 are again observed.

Figure 7.5 shows how the efficiency of the inverter varies with switching frequency for a specific LCR network. The LCR network has a natural resonant frequency of 3.60 MHz, and the load resistance is 12.5 Ω . For this test, the inverter was first adjusted for optimum Class-DE operation with the supply voltage set at 100V. Optimum Class-DE operation occurred at a frequency of 3.90 MHz. The supply voltage (100V) and the dead-time were then kept constant, while the switching frequency was varied. The power input and output were then measured the efficiency calculated. The results can be seen in Figure 7.5.

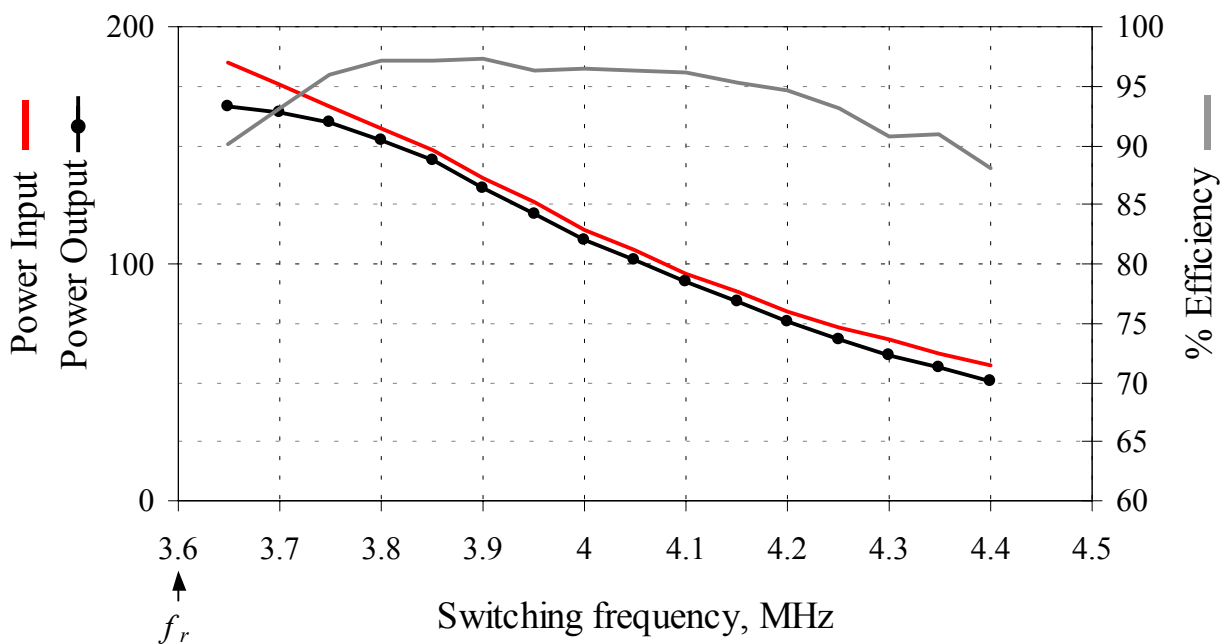
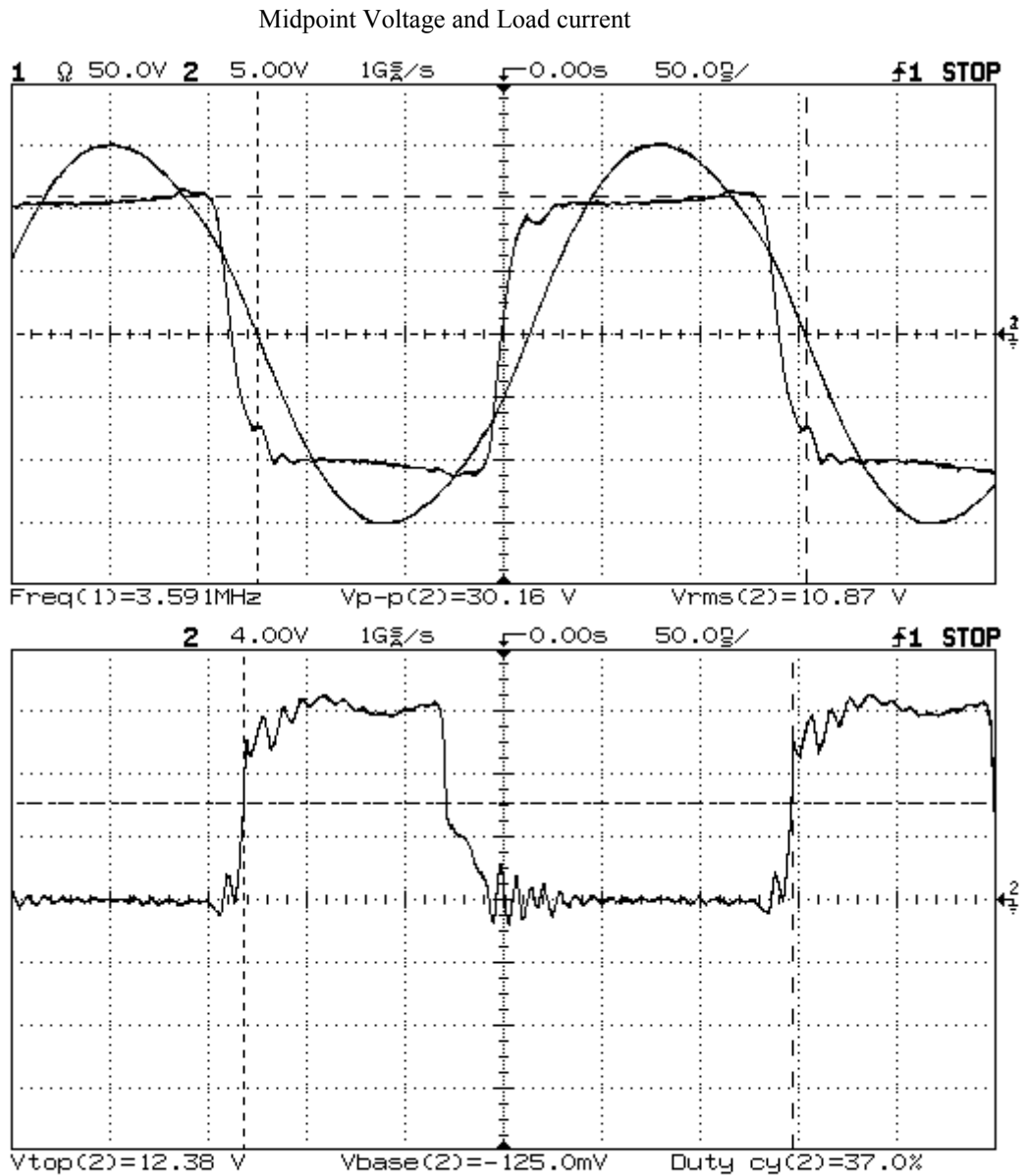


Figure 7.5 Plot of Efficiency versus Switching Frequency for a specific LCR Network

7.2 OPERATING WAVEFORMS, POWER OUTPUT AND EFFICIENCY OF THE INVERTER

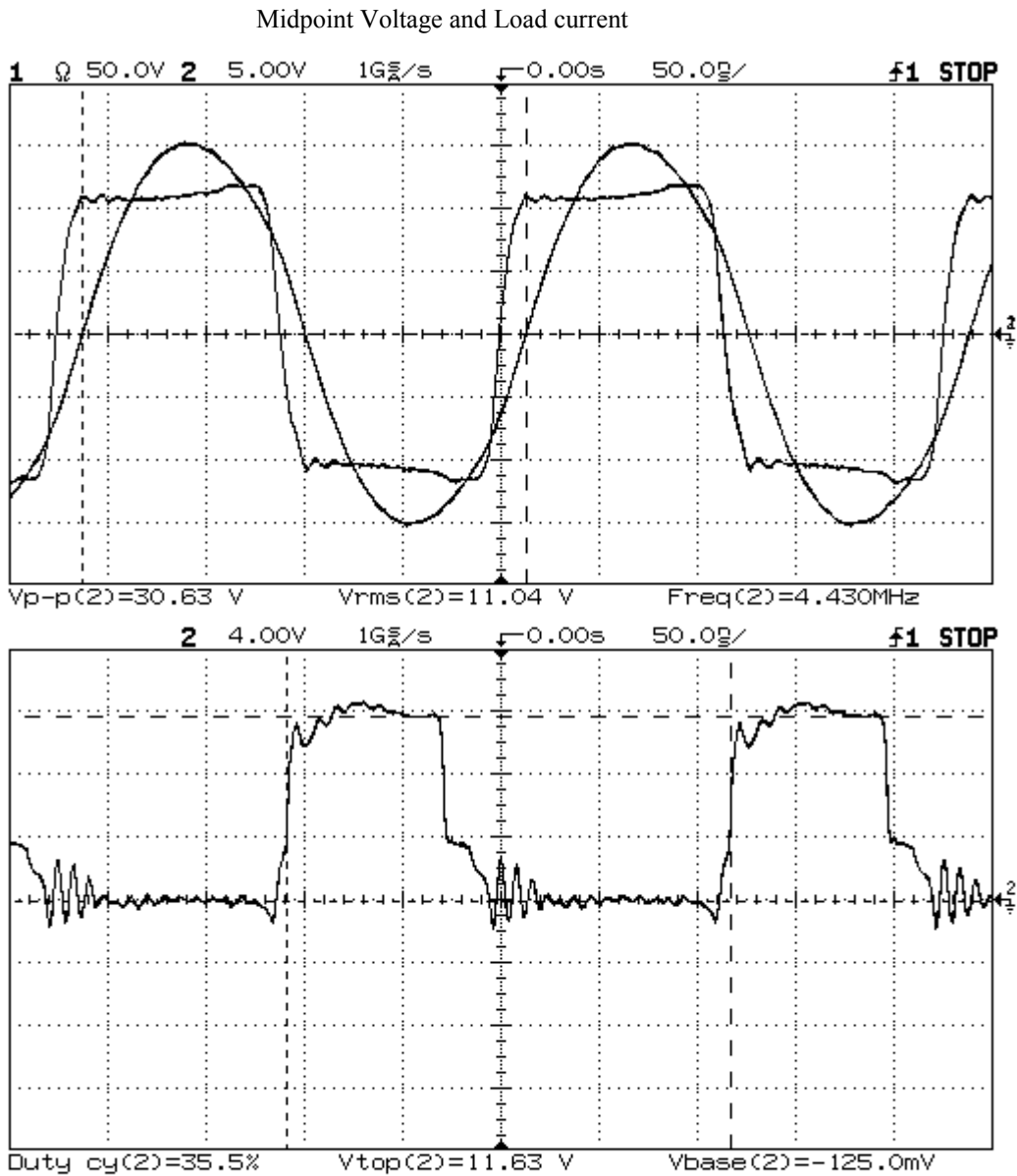
The results presented in this section show the operating waveforms of the inverter at various tests ranging from 3 to 6MHz, together with the corresponding power and efficiency calculations. The waveforms shown for each test are the same as in section 7.1 with the first oscilloscope screen capture showing the midpoint voltage on channel-1 and the load current on channel-2. The voltage and current scale are both 1:1. The second oscilloscope screen capture shows the gate-source voltage of the low-side MOSFET. The various power measurements are given below the oscilloscope waveforms. Three methods of measuring power output are used. The first uses the RMS value shown on the digital oscilloscope of the output voltage measured directly across the load resistance. The power output is then simply V_{rms}^2 / R , where R is the load resistance, and hence is labeled as the "RMS Load Voltage, P_{out} ". The second method uses the RMS value of load current as shown on the digital oscilloscope. The power output is then simply $I_{rms}^2 R$, where R is the load resistance, and hence is labeled as the "RMS Load current, P_{out} ". The third calculation is done by importing the midpoint voltage and load current waveform data into a spreadsheet where they are multiplied together and averaged over one period to obtain the power output. Both of first two methods have inaccuracies and are only used as a comparison to confirm the spreadsheet power output calculation, which the value taken as the actual output power. The auxiliary power is the power used by the ancillary circuits such as the gate-driver circuit boards, fans etc. The output stage efficiency is then simply the power output over the DC power input. The total system efficiency is calculated by adding the auxiliary power to the DC input power. The first set of tests was performed with the load resistance equal to 8.33Ω. Further tests were performed with the load resistance equal to 12.5Ω and 16.7Ω. However, the 50Ω load resistances were not capable of dissipating more than 300W each and their resistance increased considerably at these powers. Hence the RMS current power calculation is not valid for these tests.

The IRFP450LC MOSFETs have a maximum voltage rating of 500V and a maximum RMS current rating of 14A. If they were to be operated in a Class-D topology at this voltage and current level, the theoretical power output would be over 4kW. Operating the MOSFETs at a more realistic voltage of say 450V and 10A RMS current would give 3kW of output power in a Class-D topology. The MOSFETs should definitely be able to produce close to this amount of power in a Class-DE mode up to 1MHz. However, as the frequency is increased from 1 to 5MHz the power output capability will decrease. How much it will be decreased by is unknown as it is not clear how the voltage, current, dv/dt , die temperature and switching stresses will effect the MOSFET performance at these frequencies. Unfortunately the author did not have the time or resources to test the MOSFETs to their absolutely full potential but the results presented here were thought to be good enough to show the effectiveness of a Class-DE topology. The results also give a good indication of the switching performance of the MOSFETs at MHz frequencies. It is the authors opinion that the power output of the inverter using two IRFP450LC MOSFETs can possibly be extended to 2kW at 5MHz. It should be noted though, that if the devices are operating close to their limits, their tolerance to mismatches will be considerably reduced.



Frequency	= 3.59MHz	DC Voltage Input	= 230V	RMS Load Voltage, P_{out}	= 1024W
Load Resistance	= 8.33Ω	DC Current Input	= 4.71A	RMS Load current, P_{out}	= 985W
Auxiliary Power In	= 24W	DC Power Input	= 1083W	Spreadsheet, P_{out}	= 1007W
Total System Efficiency	= 91%	Inverter Output Stage Efficiency	= 93%		

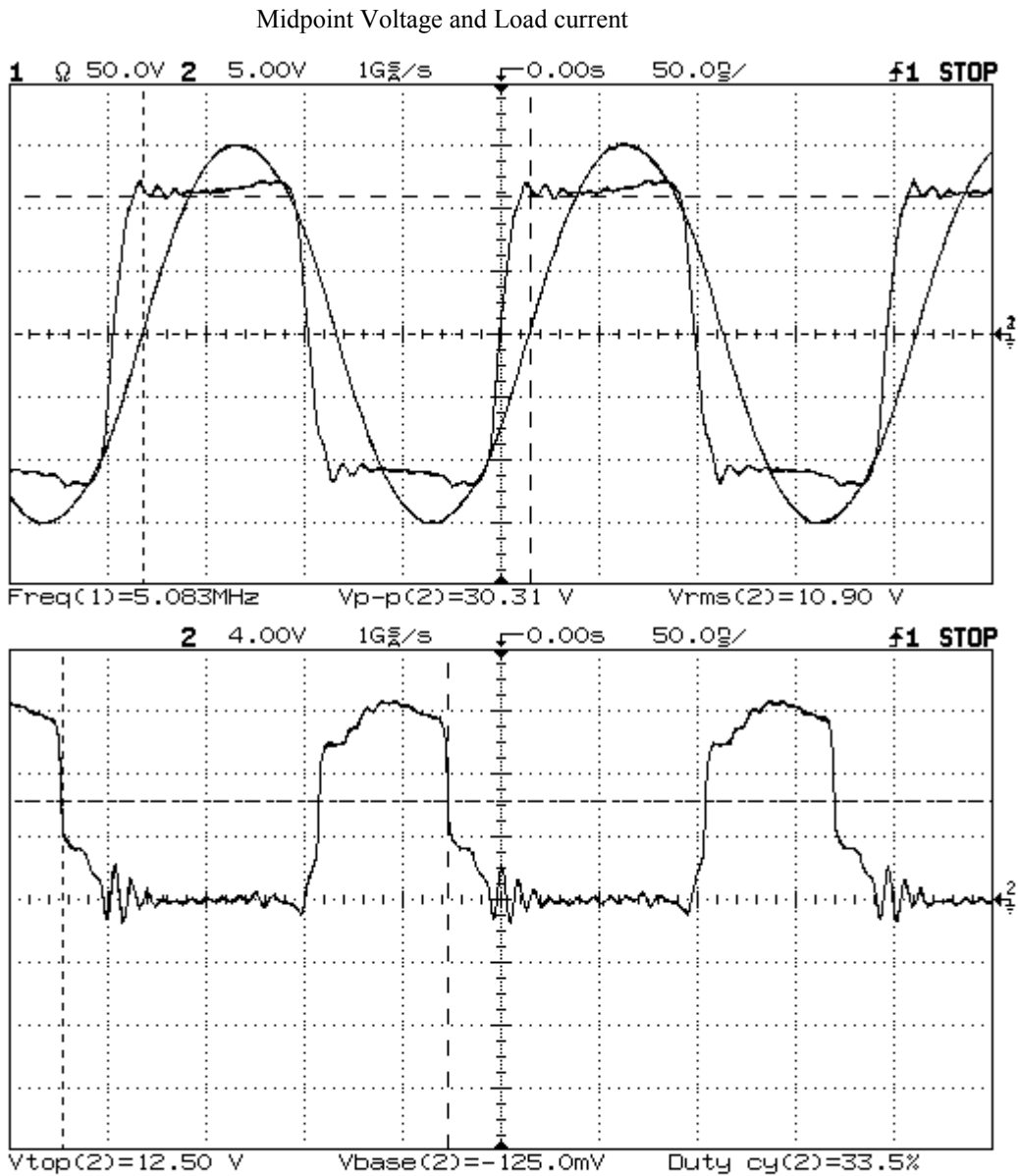
Figure 7.6 *Test 1.* 3.59MHz 1kW $R = 8.33\Omega$



Gate-Source Voltage of the Low-side MOSFET

Frequency	= 4.43MHz	DC Voltage Input	= 240V	RMS Load Voltage, P_{out}	= 1060W
Load Resistance	= 8.33Ω	DC Current Input	= 4.70A	RMS Load current, P_{out}	= 1016W
Auxiliary Power In	= 24W	DC Power Input	= 1128W	Spreadsheet, P_{out}	= 1025W
Total System Efficiency	= 89%	Inverter Output Stage Efficiency	= 91%		

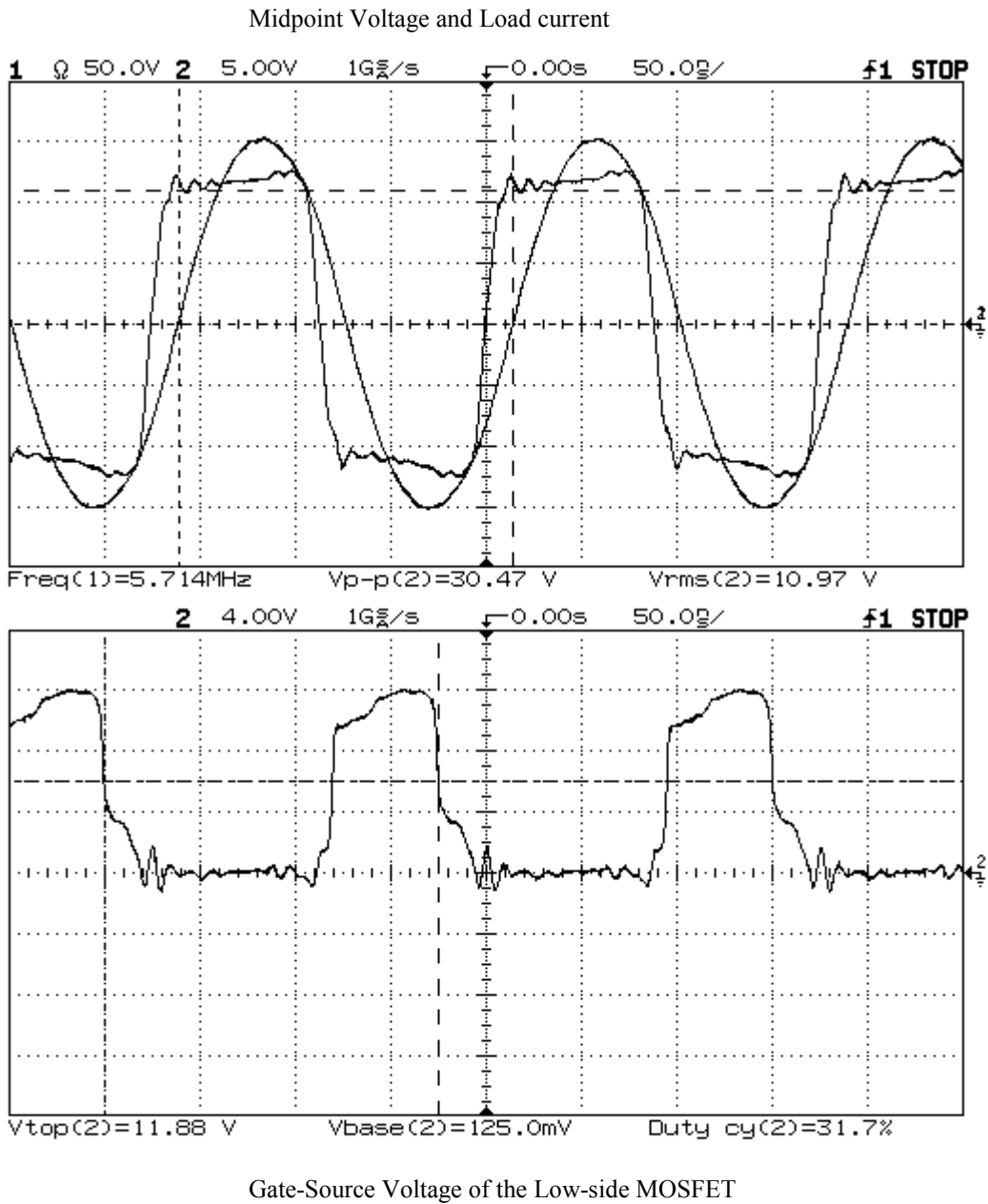
Figure 7.7 *Test 2.* 4.40MHz 1kW R = 8.33Ω



Gate-Source Voltage of the Low-side MOSFET

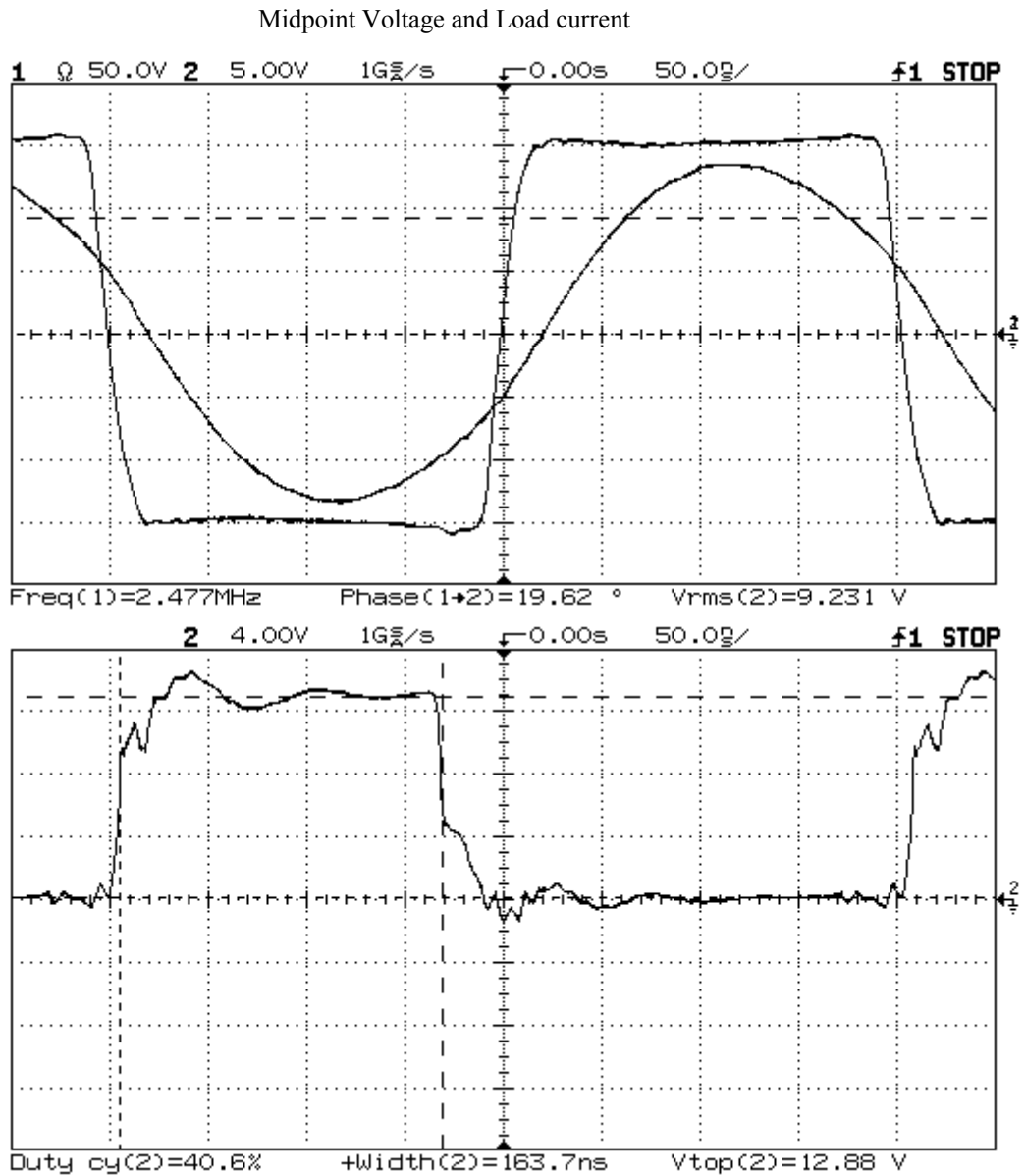
Frequency	= 5.08MHz	DC Voltage Input = 250V	RMS Load Voltage, P_{out}	= 1011W
Load Resistance	= 8.33 Ω	DC Current Input = 4.41A	RMS Load current, P_{out}	= 990W
Auxiliary Power In	= 25W	DC Power Input = 1102W	Spreadsheet, P_{out}	= 997W
Total System Efficiency	= 88.5%	Inverter Output Stage Efficiency	= 90.5%	

Figure 7.8 Test 3. 5.08MHz 1kW R = 8.33 Ω



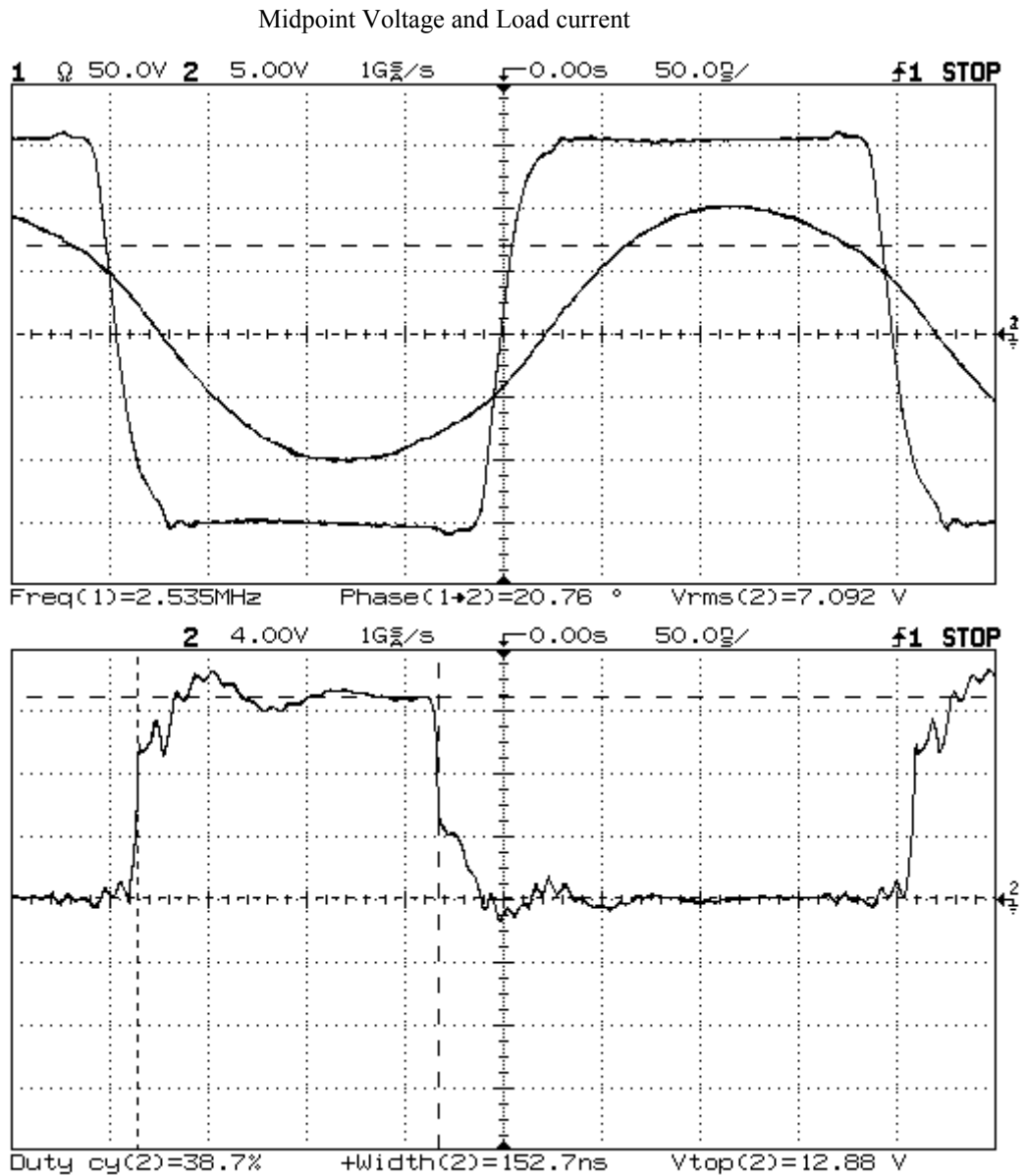
Frequency	= 5.71MHz	DC Voltage Input	= 260V	RMS Load Voltage, P_{out}	= 1044W
Load Resistance	= 8.33Ω	DC Current Input	= 4.40A	RMS Load current, P_{out}	= 1003W
Auxiliary Power In	= 26W	DC Power Input	= 1144W	Spreadsheet, P_{out}	= 1006W
Total System Efficiency	= 86%	Inverter Output Stage Efficiency	= 88%		

Figure 7.9 *Test 4.* 5.71MHz 1kW R = 8.33Ω



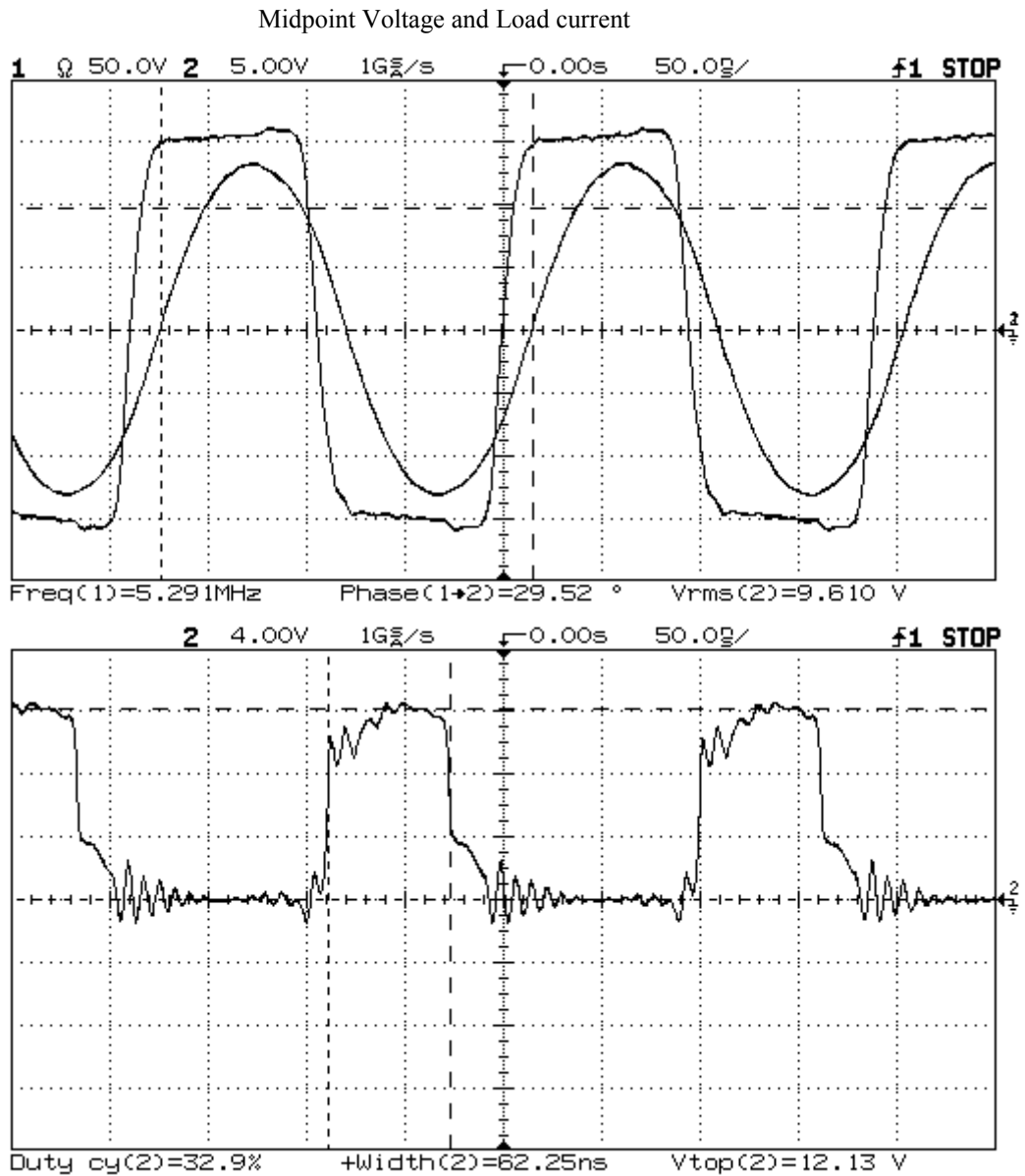
Frequency	= 2.48MHz	DC Voltage Input	= 321V	RMS Load Voltage, P_{out}	=
Load Resistance	= $\sim 12.5\Omega$	DC Current Input	= 4.17A	RMS Load current, P_{out}	=
Auxiliary Power In	= 23W	DC Power Input	= 1340W	Spreadsheet, P_{out}	= 1257W
Total System Efficiency	= 92%	Inverter Output Stage Efficiency	= 93.8%		

Figure 7.10 *Test 5.* 2.48MHz 1.25kW $R \sim 12.5\Omega$



Frequency	= 2.53MHz	DC Voltage Input	= 322V	RMS Load Voltage, P_{out}	=
Load Resistance	= $\sim 16.7\Omega$	DC Current Input	= 3.15A	RMS Load current, P_{out}	=
Auxiliary Power In	= 23W	DC Power Input	= 1017W	Spreadsheet, P_{out}	= 959W
Total System Efficiency	= 92%	Inverter Output Stage Efficiency	= 94.3%		

Figure 7.11 *Test 6.* *2.53MHz* *960W* *R ~ 16.7Ω*



Gate-Source Voltage of the Low-side MOSFET

Frequency	= 5.29MHz	DC Voltage Input	= 330V	RMS Load Voltage, P_{out}	=
Load Resistance	= 12.5 Ω	DC Current Input	= 3.84A	RMS Load current, P_{out}	= 1154W
Auxiliary Power In	= 25W	DC Power Input	= 1267W	Spreadsheet, P_{out}	= 1154W
Total System Efficiency	= 89%	Inverter Output Stage Efficiency	= 91%		

Figure 7.12 *Test 7.* 5.29MHz 1.15kW $R = 12.5\Omega$

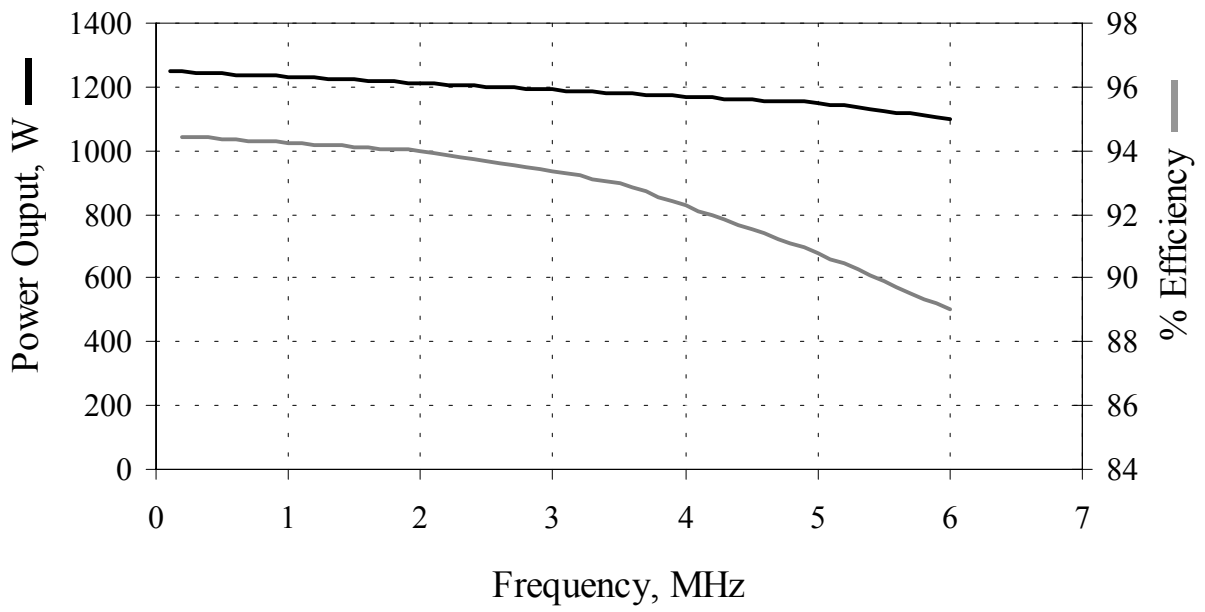


Figure 7.13 Measured Power Output and Efficiency of the Inverter when operating in Class-DE mode

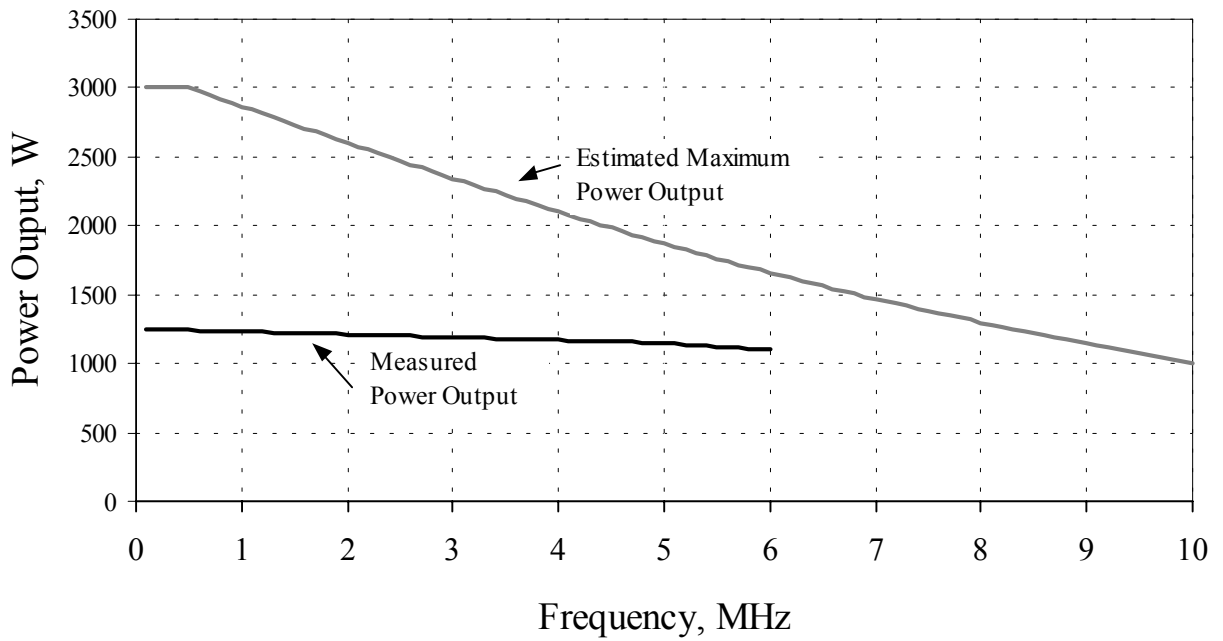


Figure 7.14 Estimated Maximum Power Output of the Inverter using two IRFP450LC MOSFETs

CHAPTER 8. MISMATCHED LOAD TOLERANCE

Many real industrial RF loads are not constant with time and cannot be represented by a fixed impedance. For example, the load could vary with time over a heating cycle or it could exhibit brief instabilities for reasons such as arcing in a plasma chamber. The tolerance of an RF power source to the variation of the load impedance is therefore of interest to the designer and the end user. The tolerance of a Class-DE inverter will depend on the matching network used but only a simple LCR network, as shown in Figure 8.1, is considered here.

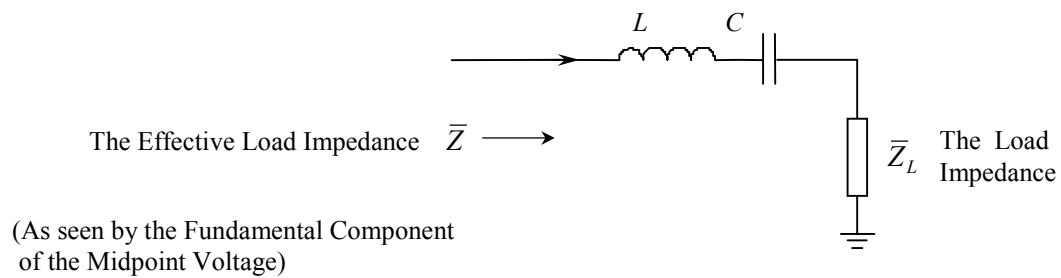


Figure 8.1 LCR Series Resonant Network Showing the Load Impedance

Figure 8.1 shows a LCR series resonant network consisting of a series resonant inductance, L , a series resonant capacitance, C , and a load impedance, \bar{Z}_L . The *load impedance* is defined by

$$\bar{Z}_L = R_L + jX_L \quad 8.1$$

This investigation will only consider an inverter operating at a *fixed* frequency and duty cycle designed for optimum Class-DE operation into a specific LCR network. Hence for optimum operation the load impedance must simply be the *nominal load resistance*, R , for which the inverter is designed to operate into. The *normalized load impedance* is then defined by,

$$\bar{Z}_L' = \frac{\bar{Z}_L}{R} = R_L' + jX_L' \quad 8.2$$

where R is the nominal load resistance. The normalized nominal load impedance is therefore simply equal to 1.

If the LCR resonant network is driven by a voltage fed inverter, then the frequency and/or the duty cycle of the inverter could be adjusted to obtain optimum or close to optimum Class-DE operation for a very wide range of load impedances. However, automatic control of the frequency and duty cycle of the inverter to maintain high efficiency operation with various loads represents a large area of further research and is not investigated here. This should be possible but it will become increasingly difficult with higher frequencies, particularly above 1 MHz. If the load impedance, \bar{Z}_L , deviates from the nominal load resistance, R , the inverter will no longer be operating in optimum Class-DE mode. The effect the deviation of the load impedance has on the operation of the inverter and the extent to which the inverter can tolerate this mismatched load is now investigated.

8.1 IDEAL CLASS-D INVERTER

To investigate the effect of the load impedance, we will first consider an ideal Class-D voltage-fed series resonant inverter. This drives the LCR circuit at resonance and the switches have no output capacitance and an ideal reverse diode. The load current will simply be given by the fundamental component of the midpoint voltage (always square) divided by the load impedance [3]. The only limitation of the load current in this case is that it should not exceed a maximum value given by I_{max} . The load impedance should therefore not be less than the value that gives rise this maximum load current, thus

$$I_m = \frac{2V_s}{\pi |\bar{Z}_L|} \leq I_{max} \quad \text{Hence} \quad |\bar{Z}_L| \geq \frac{2V_s}{\pi I_{max}} \quad 8.1.1$$

The region that this condition excludes can be seen on the normalized load impedance plane of Figure 8.2. For an ideal Class-D inverter, the load impedance can therefore take on any value up to infinity (open circuit) except for the shaded region shown in Figure 8.2. The power dissipated will always be zero and the efficiency will always be 100%. The voltage stress on each switch will always only be the supply voltage, V_s . It can therefore be seen that it is fundamentally a very robust topology.

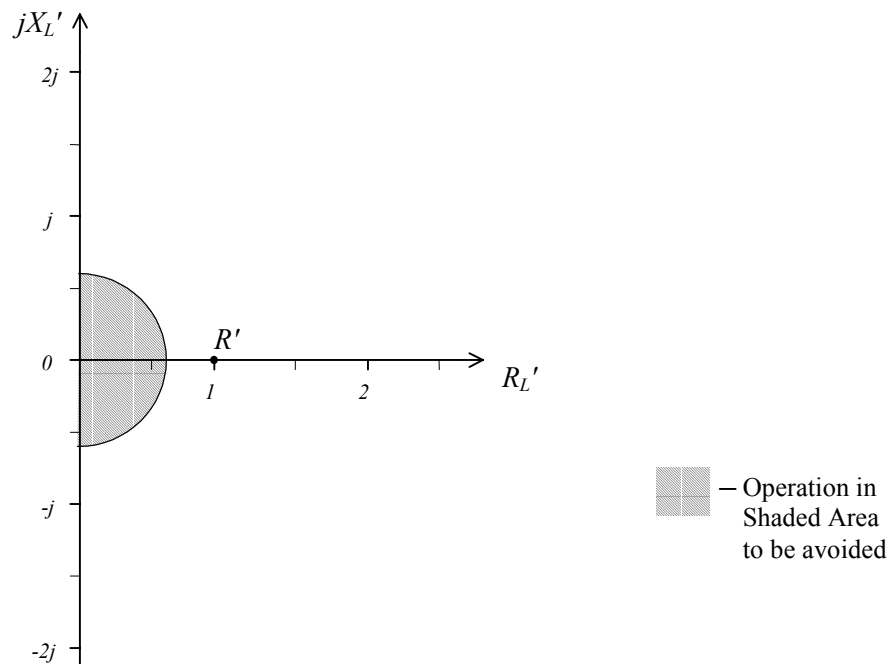


Figure 8.2 Normalized Load Impedance Plane showing the Range of Load Impedances Tolerated by an Ideal Class-D Inverter

8.2 PRACTICAL CLASS-D INVERTER

To feasibly operate an inverter in the conventional Class-D mode, the output capacitances of the switching devices must have a negligible effect on the operation of the inverter. This will only happen if the switching frequency is low enough so that the CV^2f losses are negligible, even with no load. Using currently available MOSFETs, a half-bridge voltage-fed series resonant inverter can feasibly operate in the conventional Class-D mode up to approximately a few hundred kHz. At higher frequencies, the capacitive switching loss will have to be considered. However, even at low frequencies, a practical Class-D inverter using MOSFETs will have a failure mode associated with the MOSFET's reverse integral diode. This diode has a maximum reverse recovery dv/dt rating that cannot be exceeded as it will cause device failure. This will occur if the inverter is operating in the capacitive mode and the MOSFETs are being hard switched. In the capacitive mode the inverter will be driving the LCR network below resonance and have a leading load current. Hence the switch's diode will be conducting at the end of the conduction period. If the MOSFETs are being hard-switched, then the dv/dt rating of the integral reverse diode will be exceeded when the opposing switch turns-on and the device will fail. The load impedance can therefore not have any capacitive reactance. In practice, however, the inverter will be operating slightly above resonance and so some capacitive reactance will be tolerated, but this is not shown in Figure 8.3. The load current may also not exceed a maximum value and so the same condition as with an ideal Class-D inverter applies. Except for the shaded regions shown in Figure 8.3, all other reactive load impedances will be tolerated up to infinity (open circuit). The voltage stress on each switch will always only be the supply voltage, V_s . Assuming the capacitive switching losses are small, then the power dissipated should remain close to the normal operating value for all the allowed load impedances. The tolerated range of load impedances can be seen in the normalized load impedance plane of Figure 8.3.

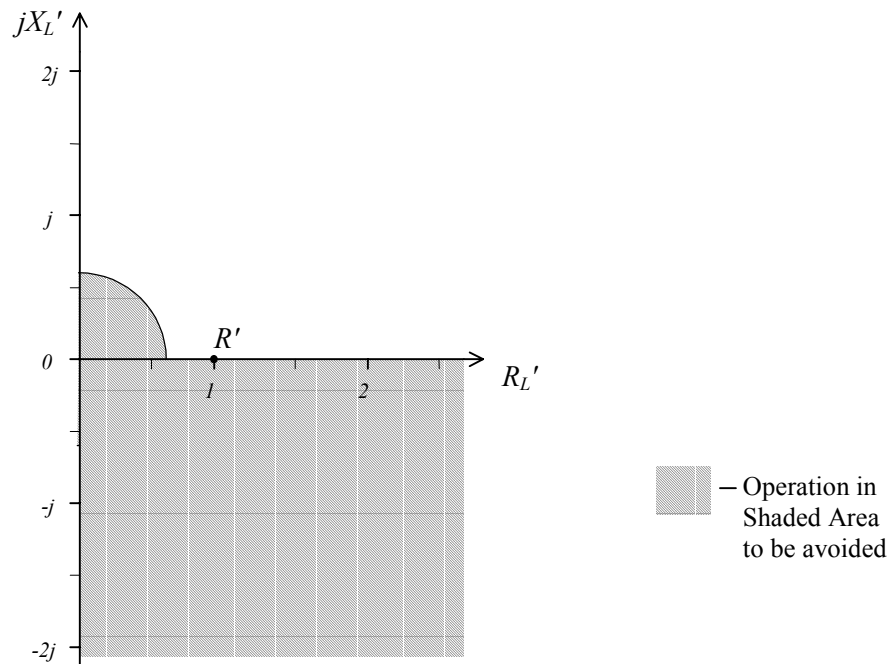


Figure 8.3 Normalized Load Impedance Plane showing the Range of Load Impedances Tolerated by a Practical Class-D Inverter using MOSFETs

8.3 THE CLASS-DE INVERTER

The term "Class-DE" is applied here to an inverter where the output capacitance cannot be neglected. It is also referred to in the literature as a zero-voltage-switching (ZVS) Class-D series resonant inverter [54]. These inverters must employ some means of reducing the capacitive switching losses. The mismatched load tolerance of a Class-DE inverter will depend on a number of parameters and follows certain trends described below;

- A higher output capacitance \Rightarrow Decreases the tolerance of an inverter as the capacitive switching losses will be increased,
- Increasing the switching frequency \Rightarrow Decreases the tolerance of an inverter as the capacitive switching losses will be increased,
- Increasing the impedance levels \Rightarrow Decreases the tolerance of an inverter as the higher supply voltage implies increased capacitive switching losses,
- Decreasing the conduction angle \Rightarrow Decreases the tolerance of an inverter as this implies either or all of the following; a high output capacitance, a high switching frequency, or high impedance levels.

The actual range of load impedances a Class-DE inverter can tolerate is difficult to specify exactly but general guidelines can be investigated. This investigation will only consider a Class-DE inverter using MOSFETs. A Class-DE inverter operating into its designed nominal LCR network will see an *effective load impedance*, as defined in Section 2.2.3, defined by

$$\bar{Z} = R + jX \quad 8.3.1$$

where R and X are given by equation (2.2.27) and equation (2.2.28) of Section 2.2.3. As the load impedance varies away from its nominal load resistance, R , then the effective load impedance that the fundamental component of the midpoint voltage will see is given by

$$\bar{Z} = \bar{Z}_L + jX \quad 8.3.2$$

The effect of the variation of the load impedance can now be investigated. If the load impedance's resistance increases, then the load current will be decreased and the midpoint voltage will not swing all the way to the opposite rail and capacitive switching losses will occur. This is illustrated in Figure 8.4 that shows the power dissipation increasing with increasing load resistance. If the load impedance's resistance decreases, the load current will increase and the midpoint voltage will swing past the opposite rail causing the diode to conduct at the beginning of the conduction period (ZVS turn-on will occur). Assuming that the diode conduction at the beginning of the conduction period has no adverse affects, then there will be no power dissipated in this region of operation.

The effect of load reactance on the inverter is not so clear. As the reactance of load impedances varies it will change the phase and magnitude of the load current. However, the actual shape of the midpoint voltage will be

complicated due to the fact that the switches are operating with a duty cycle of less than 50%. The first consideration is that as in a practical Class-D inverter, the dv/dt reverse recovery rating of the diode means the inverter must not operate in the capacitive mode (diode conducting at the end of the conduction period). From equation 8.3.2, we can make the intuitive deduction that the load impedance can have a capacitive reactance of least up to $-jX$ before the inverter will be operating in the capacitive mode. As the capacitive reactance of the load impedance increases from zero to $-jX$, the capacitive switching losses will gradually increase reaching a maximum at some point. At this point the MOSFETs will be turning on with the full supply voltage across them and this represents the worst case of capacitive switching losses. The amount of capacitive reactance the inverter can tolerate therefore depends on its power dissipation capability and this is illustrated in Figure 8.4. If the load impedance's inductive reactance increases then the phase lag of the load current will increase and this will cause the diode to conduct at the beginning of the conduction period (ZVS turn-on will occur). However, the magnitude of an inductive load impedance may only increase to certain amount before the magnitude of the load current is too small to swing the midpoint voltage all the way to the opposite rail. As in an ideal Class-D inverter, the magnitude of load impedance cannot be less than a specific value, but this magnitude will include the reactance jX , hence this circle will be centered around $-jX'$. These conditions are illustrated by the shaded regions of Figure 8.4 which shows the range of load impedances tolerated by a Class-DE inverter in the normalized load impedance plane.

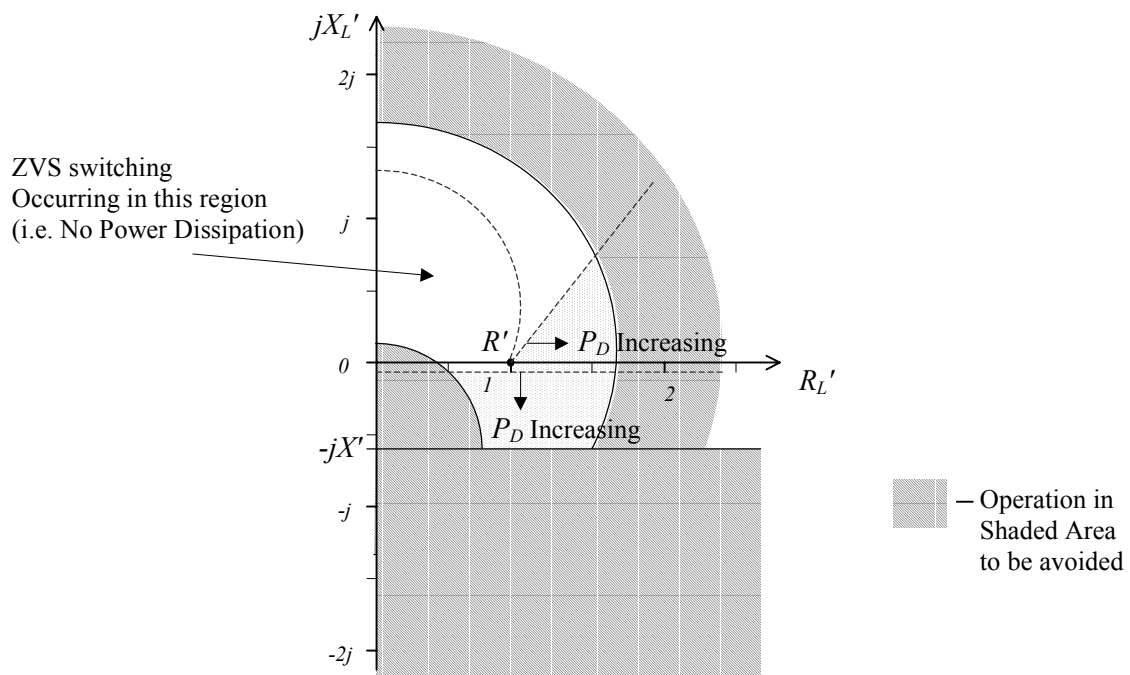


Figure 8.4 Normalized Load Impedance Plane showing the Range of Load Impedances Tolerated by a Class-DE Inverter using MOSFETs

From Figure 8.4 we can see that the inverter will tolerate a fairly large range of inductive load impedances while still maintaining ZVS and hence have no power dissipation. Capacitive reactance will increase capacitive switching losses and hence power dissipated. As in a Class-D inverter, the voltage stress on each switch will

always only be the supply voltage, V_s , for all load impedances. It should also be noted that mismatched load tolerance depends to large extent on the power dissipation capability of the inverter. As a Class-DE inverter should be operating very efficiently, it should have ample power dissipation capability in reserve. From this fact, together with the results of Figure 8.4, it can be deduced that a Class-DE inverter should have a very good mismatched load tolerance. However, Figure 8.4 only serves as a guide and more quantitative information can be obtained by simulation on a program such as HB-Plus [57]. Ultimately the load tolerance of the inverter will have to be determined experimentally.

CHAPTER 9. CONCLUSIONS

This thesis investigated the various aspects of the theory, design and construction of high frequency and high power Class-DE type DC/AC inverters. From the analysis presented in Chapter 2 it can be seen that a Class-DE inverter has a theoretical power advantage over a Class-E inverter up to approximately 6 MHz using standard switch-mode type MOSFETs. The practical aspects of implementing a Class-DE inverter to work up to this frequency were then investigated. It was found that a half-bridge type inverter was the most suitable topology, as it does not fundamentally limit the operating power or frequency. The limiting factor will actually be the switching devices themselves. The main practical problems of implementing a half-bridge inverter were found to be the gate-drive, the physical construction of the inverter output stage, the generation of the control signals and the communication-link to the high-side switch. The use of a fiber optic link as communication-link to the high-side switch proved to be an excellent solution, enabling the inverter to be controlled from DC - 5 MHz. A fiber optic communication link will not be a limiting factor to the maximum feasible operating power and frequency of a Class-DE inverter. Generation of the control signals was suitably achieved for Class-DE type operation from 50 kHz to 5 MHz. The implementation of a digital dead-time should enable suitable control signals to be generated for Class-DE type operation over the entire HF band. The physical construction of the inverter becomes more difficult with increasing frequency and power (i.e. less tolerance of stray impedance). An innovative construction of the output stage of the inverter enabled very clean and discernible Class-DE type operation to be achieved up to 5 MHz at a power level of 1 kW (with an operating impedance level of 10 Ω). Hybrid circuit technology using ceramic substrates should enable a half-bridge inverter to be constructed with low enough stray impedances for operation up to 13.56 MHz, and possibly for power levels of up to 10 kW. Driving the gate capacitance directly with a suitably low impedance driver enabled the required rise and fall times to be achieved, and for the MOSFETs to be driven from DC-5 MHz with any duty cycle. However, power dissipation and the physical size of the gate-driver were problems. For higher operating frequencies new techniques will have to be investigated to reduce the rise and fall times, increase the power dissipation capability and reduce the physical size of the gate-driver circuitry.

The broadband design of the control circuitry, communication-link and gate-drive enabled the half-bridge inverter output stage to be driven from 50 kHz through to 6 MHz. The half-bridge topology proved to be an excellent solution as it enabled very clean and discernible waveforms to be observed that clearly showed Class-DE operation. It also enabled the mechanism of the operation of the inverter to be ascertained for various operating conditions. The broadband capability of the half-bridge enabled the inverter to produce RF power from 50 kHz to 6 MHz with the only circuit changes needed for the different frequencies being the inductance and capacitance of the tuned network. The design equations developed in Chapter 2 enabled simple and fast calculation of the values of the inductance and capacitance. The ability to change the frequency and duty cycle of the inverter made the tuning procedure for Class-DE operation relatively simple and as it could be achieved without any circuit changes.

When operated in the Class-DE mode, the inverter was found to be capable of delivering a power output of over 1 kW from 50 kHz to 1 MHz with an efficiency of 94%. This is fairly close to the theoretical maximum efficiency determined by the on-resistance of the MOSFETs. The efficiency decreased slightly with increasing frequency from 1 MHz to 5 MHz. The last test of the inverter produced 1.15kW of output power at 5.3 MHz with an efficiency of 91%.

A comparison of the performance of various topologies is given below. All the topologies are using only two IRFP450 MOSFETs and they experience the same peak voltage and current stresses. If the operating frequency is 5 MHz, the peak voltage stress is 330V, and the peak current is 12.7A, then we have

- Class B and C $P_{out} = \sim 450W$ $\eta = \sim 60\%$ $P_D = \sim 200W$
(Power output limited by power dissipation capability)
- Class-DE $P_{out} = 1150W$ $\eta = 91\%$ $P_D = 113W$
- Class-E $P_{out} = \sim 750W$ $\eta = \sim 87-90\%$ $P_D = \sim 100W$

Where P_{out} is the output power, η is the efficiency and P_D is the power dissipated. It can be seen from the above results that a Class-DE inverter is capable of producing a higher combination of power and efficiency than any other current topology up to a frequency of 5 MHz and at power levels of 1kW.

As the MOSFETs are being used as switching devices they may be connected in parallel relatively easily and the variation of device parameters will have no adverse effects. Paralleling the switching MOSFETs can increase the power output of a Class-DE inverter, but increasing the power will decrease the operating impedance level and hence place tighter restrictions on the construction of the inverter. It is the author's opinion that it should be possible to parallel more than five sets of MOSFETs at 5 MHz, thereby increasing power levels to approximately 10kW. It is also the author's opinion that the operating frequency of a voltage-fed half-bridge Class-DE inverter can be extended to cover the 13.56 MHz ISM band. The main practical problems will be the gate-drive and physical construction. Above this frequency the advantages of a Class-DE topology over a Class-E topology are limited and the development difficulties increase considerably.

A Class-DE type inverter could be used for many applications requiring RF power in the HF band, such as AM or SW radio transmitters, induction heating and plasma generators. The information presented in this thesis will be useful to designers wishing to implement such an inverter. A Class-DE type inverter also offers great potential for use in a DC-DC converter. However a method of regulating the power flow (and hence output voltage) while still maintaining zero voltage switching transitions (or as close as possible to optimum Class-DE operation) remains to be investigated. Many principles of a Class-DE topology are similar to a Class-E topology and hence the theory and information presented in this thesis will give a good introduction towards understanding the more complex operation and equations of a Class-E topology.

9.1 CLASS-DE VERSUS CLASS-E

The differences between Class-DE and Class-E are subtle compared to linear topologies, and the most suitable topology will depend on mainly on the operating frequency; but factors such as the application, power levels and development time also have to be considered. Class-D is most suited to frequencies from DC to a few hundred kHz, Class-DE from above a few hundred kHz to a few MHz, and above this Class-E. The exact cross-over points are somewhat ambiguous and will change with new technology. However, some general guidelines are given below.

From the analysis of a Class-DE topology, it can be seen that it has a theoretical power advantage over a Class-E topology for switch conduction angles greater than 104.4° (duty cycle of 29%). For a duty cycle of 29%, a Class-DE topology has the same switch utilization factor as a Class-E topology (i.e. the same power output for a given switch voltage and current stress). Thus if the duty cycle in a Class-DE inverter is required to be less than 29% it would produce less power than a Class-E. The duty-cycle required in a Class-DE inverter depends on the output capacitance of the switches used and it decreases with increasing operating frequencies. One may then calculate at what frequency the duty cycle required in a Class-DE inverter equals 29%.

However, the physical construction and practical problems of implementing a two switch Class-DE topology are considerably larger than the single switch Class-E topology. Hence the duty cycle should be at least 35% or more to in order justify the extra power gained through the use of a Class-DE topology over a Class-E topology. The frequency at which the required duty cycle is 35% appears to be in the region of 10 to 15 MHz using the high voltage and high power RF MOSFETs now offered by some manufacturers. Above this frequency the switch utilization factor approaches that of a Class-E and there is little to be gained from a Class-DE topology over a Class-E topology.

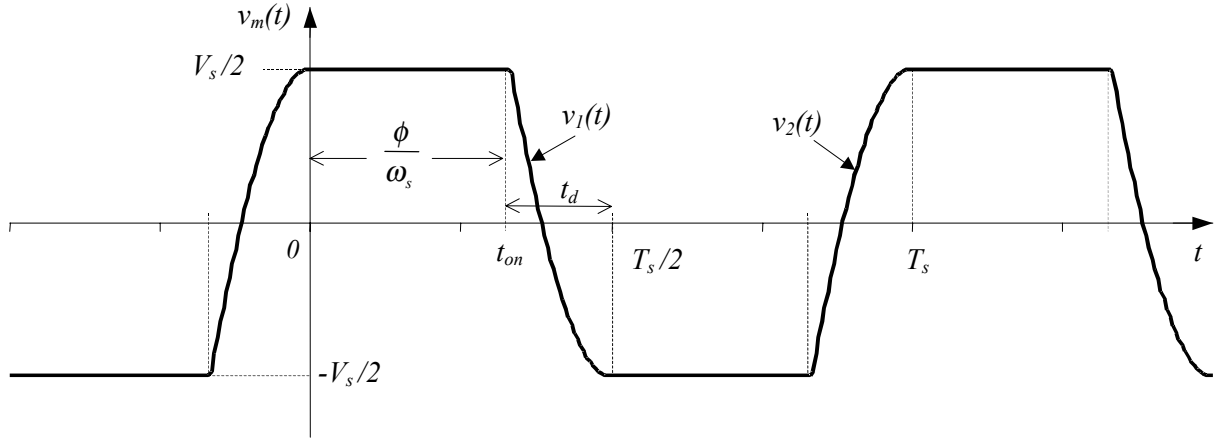
From the results of this thesis it can be seen that from 100kHz to 6 MHz a Class-DE topology is the best means of producing raw RF power. Over this frequency range it offers the highest combination of output power and efficiency and has a good mismatched load tolerance. It also preserves normal operating waveforms over a wide range of load impedances. It is the author's opinion that this frequency can be extended to cover the 13.56 MHz ISM band. However, it should be noted that a two switch Class-DE topology will require more development time and effort than a single switch Class-E topology.

9.2 ORIGINAL WORK

A summary of the original work presented in this thesis is given below.

- An analysis and description of Class-DE operation in a half-bridge inverter is presented. The concept of a conduction angle is introduced which enables a more intuitive understanding of the analysis equations and design equations developed thereafter. The effect of a non-linear output capacitance was studied and equations are modified to take this effect into account. The design equations enable the conduction angle required, power output and the circuit element values of the LCR network to be calculated simply and quickly.
- The results of an investigation into the practical problems of implementing a high power and high frequency Class-DE inverter, and guidelines to solving these problems, is presented. Some novel solutions to these problems are developed and these solutions were implemented in a prototype voltage-fed half-bridge inverter. These solutions enabled the feasible operation of a high power half-bridge inverter to be extended up to 5 MHz, and were found to work very effectively. It is concluded that the practical problems of implementing a half-bridge Class-DE inverter can be overcome with further development for operation up to 13.56 MHz.
- The use of a fiber optic link as the means of communicating the drive signal to floating switches at high frequencies and high powers is shown to be very feasible.
- Class-DE operation of a voltage-fed half-bridge series resonant inverter at various frequencies up to 5 MHz and at power levels of 1kW is clearly shown.
- The results of this thesis prove that a Class-DE topology is capable of producing RF power up to a frequency of 5 MHz with a higher combination of power and efficiency than any other current topology operating with the same switch voltage and current stresses.
- A brief investigation of the mismatched load tolerance of a Class-DE inverter is presented.

APPENDIX A. Fundamental Component of the Midpoint Voltage



Conduction Angle = ϕ , Duty Cycle, $D = \frac{\phi}{2\pi}$, $t_{on} = \frac{\phi}{\omega_s}$, $T_s = \frac{2\pi}{\omega_s}$

$$v_m(t) = \begin{cases} V_s/2 & t \in [0, t_{on}] \\ v_1(t) & t \in [t_{on}, T_s/2] \\ -V_s/2 & t \in [T_s/2, T_s/2 + t_{on}] \\ v_2(t) & t \in [T_s/2 + t_{on}, T_s] \end{cases}$$

Where $v_1(t) = -\frac{1}{2C_o} \int I_p \sin(\omega_s t) dt + K$ $t \in [t_{on}, T_s/2]$

Integrating and using the boundary condition that $v_1(t_{on}) = \frac{V_s}{2}$, then we have

$$v_1(t) = \frac{V_s}{(1 + \cos \phi)} \cos(\omega_s t) + \frac{V_s}{2} \left[\frac{1 - \cos \phi}{1 + \cos \phi} \right] \quad t \in [t_{on}, T_s/2]$$

Similarly $v_2(t) = \frac{V_s}{(1 + \cos \phi)} \cos(\omega_s t) - \frac{V_s}{2} \left[\frac{1 - \cos \phi}{1 + \cos \phi} \right] \quad t \in [T_s/2 + t_{on}, T_s]$

The midpoint voltage may be expressed as a sum of the Fourier series of complex exponentials

$$v_m(t) = \sum_{n=-\infty}^{n=\infty} \bar{V}_n e^{jn\omega_s t}$$

Where the complex Fourier series coefficients, \bar{V}_n , can be found using

$$\bar{V}_n = \frac{1}{T_s} \int_0^{T_s} v_m(t) e^{-jn\omega_s t} dt$$

The first coefficient of the fundamental can be found by evaluating this integral for $n=1$.

Thus setting $n=1$, and expanding the integral

$$\bar{V}_1 = \frac{1}{T_s} \left[\int_0^{t_{on}} \frac{V_s}{2} e^{-j\omega_s t} dt + \int_{t_{on}}^{T_s/2} v_1(t) e^{-j\omega_s t} dt + \int_{T_s/2}^{T_s/2+t_{on}} -\frac{V_s}{2} e^{-j\omega_s t} dt + \int_{T_s/2+t_{on}}^{T_s} v_2(t) e^{-j\omega_s t} dt \right]$$

Evaluating the integral, we have

$$\bar{V}_1 = \frac{V_s}{2\pi(1+\cos\phi)} [(\pi - \phi + \sin\phi \cos\phi) - j \sin^2\phi]$$

\bar{V}_1 can be expressed in polar form as

$$\bar{V}_1 = |\bar{V}_1| e^{j\beta}$$

Where

$$|\bar{V}_1| = \frac{V_s}{2\pi(1+\cos\phi)} \sqrt{(\pi - \phi + \sin\phi \cos\phi)^2 + \sin^4\phi}$$

$$\text{and } \beta = \tan^{-1} \left(\frac{-\sin^2\phi}{\pi - \phi + \sin\phi \cos\phi} \right)$$

The fundamental component, $v_{m1}(t)$, of the midpoint voltage $v_m(t)$, is given by

$$v_{m1}(t) = \bar{V}_1 e^{j\omega_s t} + \bar{V}_{-1} e^{-j\omega_s t}$$

But for real functions of time, $\bar{V}_{-1} = \bar{V}_1^*$, and so using the polar form of \bar{V}_1 , we have

$$\begin{aligned} v_{m1}(t) &= |\bar{V}_1| e^{j\beta} e^{j\omega_s t} + |\bar{V}_1| e^{-j\beta} e^{-j\omega_s t} \\ &= 2 \operatorname{Re} \left[|\bar{V}_1| e^{j(\omega_s t + \beta)} \right] = \operatorname{Re} \left[2 \bar{V}_1 e^{j\omega_s t} \right] \\ &= 2 |\bar{V}_1| \cos(\omega_s t + \beta) \end{aligned}$$

APPENDIX B. HB-PLUS SIMULATION RESULTS OF THE DESIGN EXAMPLE

Half-Bridge power amplifier/converter (HB) Jan. 10, 1999 12:55
Simulation of The Design Example

ENTER CIRCUIT PARAMETERS and TITLE SCREEN-1

Switching frequency (f).....[Hz]:	5E+06
DC supply voltage (Vcc or Vdd).....[volts]:	300
Fraction of period, turn-on of Sw1 to Sw2....:	0.5
Switch 1 parameters	
Duty ratio of switch 1.....:	0.345
Ron1.....[ohms]:	0.01
Roff1.....[ohms]:	1E+06
Cout1.....[farads]:	3.67E-10
Cout1 series resistance (Rcout1)..[ohms]:	0.001
Saturation offset voltage (Vo1)....[volts]:	0
Switch 2 parameters	
Duty ratio of switch 2.....:	0.345
Ron2.....[ohms]:	0.01
Roff2.....[ohms]:	1E+06
Cout2.....[farads]:	3.67E-10
Cout2 series resistance (Rcout2)..[ohms]:	0.001
Saturation offset voltage (Vo2)....[volts]:	0

ENTER CIRCUIT PARAMETERS SCREEN-2

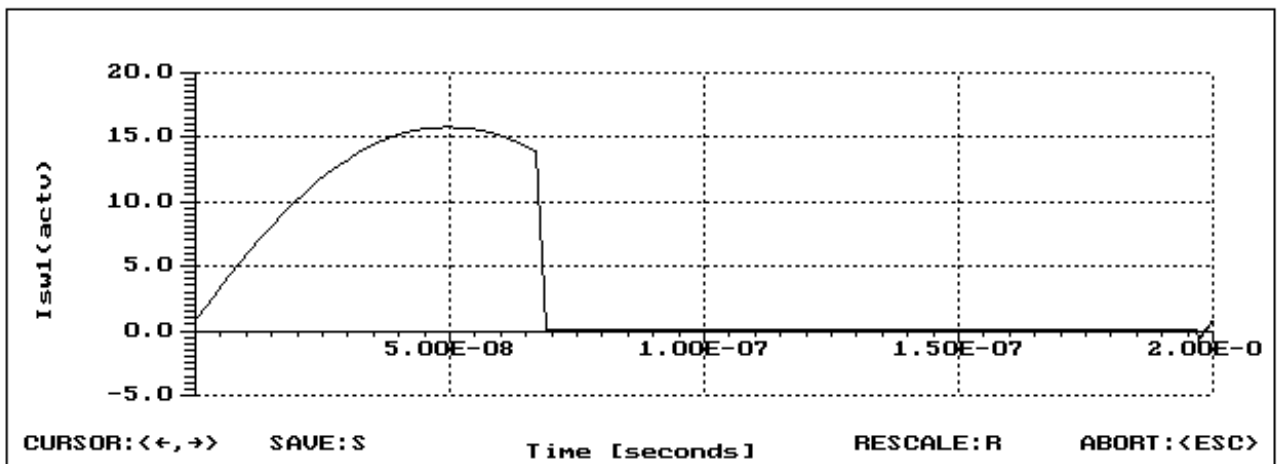
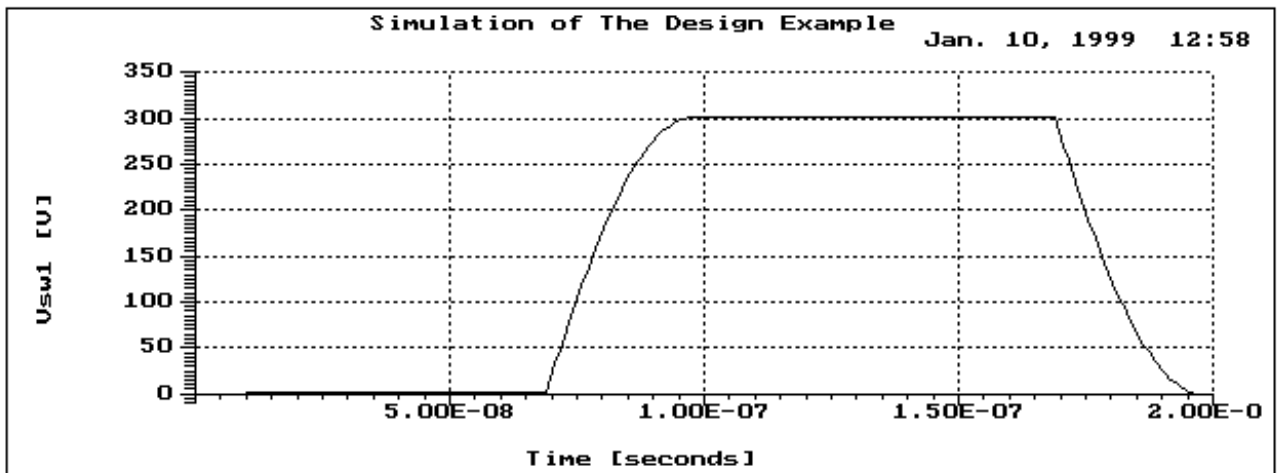
Load resistance (Rload).....[ohms]:	9.37
L2.....[henries]:	1.23E-06
ESR_L2.....[ohms]:	0.001
C2.....[farads]:	1E-09
ESR_C2.....[ohms]:	0.001

SELECTION: <□,□> ENTRY: ALPHANUM. EXECUTE: <PgDn> ABORT: <ESC>

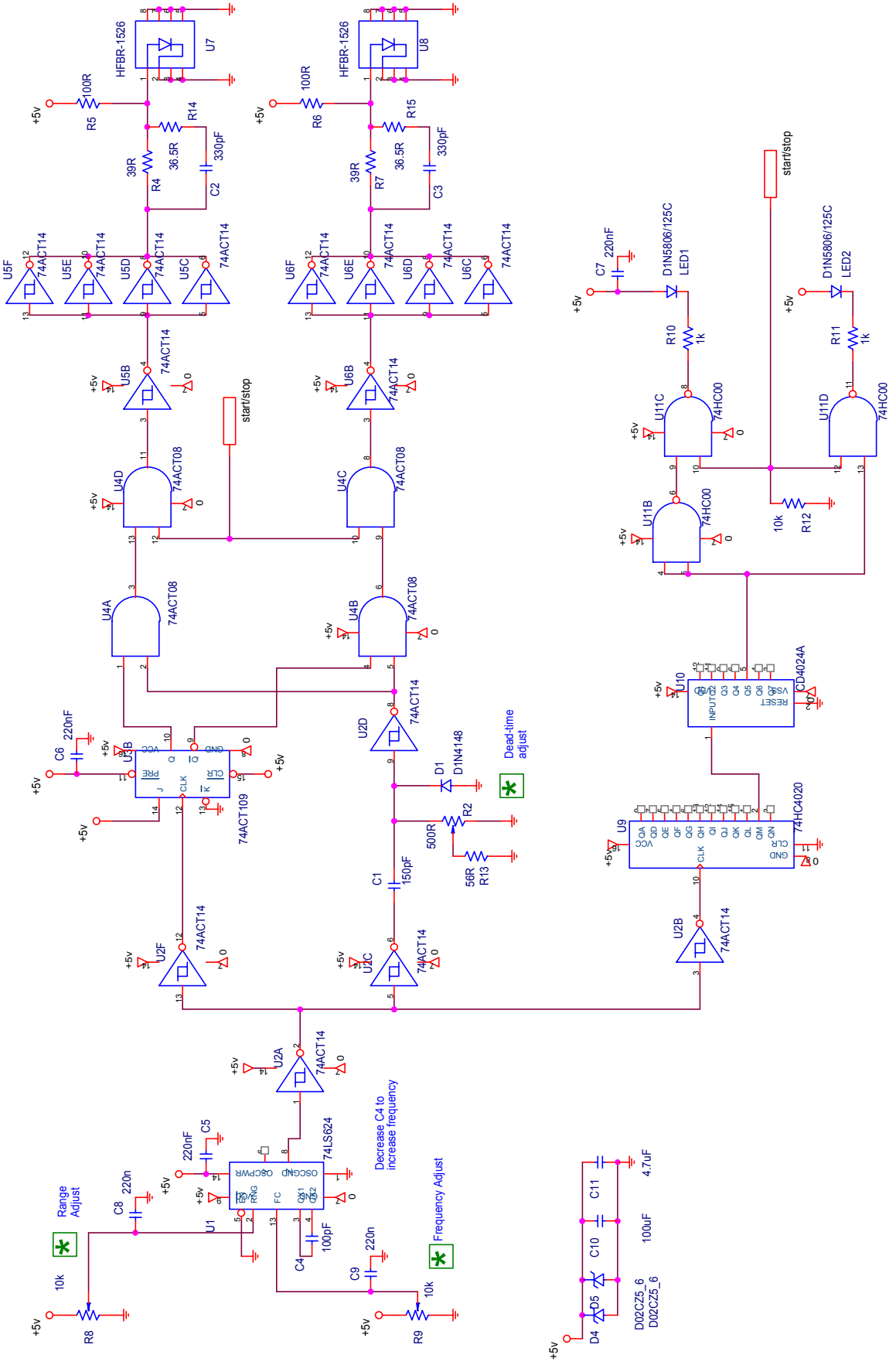
Half-Bridge power amplifier/converter (HB) Jan. 10, 1999 12:56
 Simulation of The Design Example

EFFICIENCY AND POWERS

Collector/drain efficiency (Pout/Pin).....[%]	99.882
Collector/drain ineff'y (Pin-Pout)/Pin.....[%]	0.11813
DC power input (Pin).....[watts]	1204.2
Power output (Pout).....[watts]	1202.8
Power loss in L2.....[watts]	0.12837
Power loss in C2.....[watts]	0.12837
Power loss in Ron1.....[watts]	0.57754
Power loss in Rcout1.....[watts]	0.0054026
Power loss in Ron2.....[watts]	0.57754
Power loss in Rcout2.....[watts]	0.0054026



APPENDIX C. Drive-Signal-Generator Circuit



APPENDIX D. Design Equations of a Half-Bridge Class-DE Inverter

A summary of the equations used and procedure followed when designing a Half-bridge Class-DE inverter is given below. The designer must first specify the desired supply voltage, V_s , the peak current through the devices, I_p , the output capacitance of the devices, C_o , and the switching frequency, f_s . Alternatively, if the output capacitance is non-linear, then the total charge Q_T required to charge the output capacitance to V_s must be specified. The effective output capacitance can then be found as, $C_{o-eff} = \frac{Q_T}{V_s}$. The required conduction angle can then be calculated using the appropriate equation below (where $\omega_s = 2\pi f_s$)

$$\cos \phi = \frac{2\omega_s C_o V_s}{I_p} - 1 \quad \cos \phi = \frac{2\omega_s Q_T}{I_p} - 1 \quad \cos \phi = \frac{2\omega_s C_{o-eff} V_s}{I_p} - 1$$

The required duty cycle of the switches and power output of the inverter will then be given by

$$D = \frac{\phi}{2\pi} \quad P_{out} = \frac{V_s I_p}{2\pi} (1 - \cos \phi)$$

The phase lag, α , between the fundamental component of the midpoint voltage and the midpoint current can be found using the expression

$$\tan \alpha = \left(\frac{\pi - \phi + \sin \phi \cos \phi}{\sin^2 \phi} \right)$$

The designer must now select the desired value of the Q of the resonant LCR network (usually in the region of 3 to 5). The natural resonant frequency of the LCR network can then be found using

$$f_r = \frac{f_s}{2} \left[\sqrt{\left(\frac{\tan \alpha}{Q} \right)^2 + 4} - \frac{\tan \alpha}{Q} \right]$$

Using this value of the natural resonant frequency, the value of the resistance, inductance and capacitance in the LCR network can be found using the following three expressions (where $\omega_r = 2\pi f_r$)

$$R = \frac{V_s}{\pi I_p} (1 - \cos \phi) \quad L = \frac{Q R}{\omega_r} \quad C = \frac{1}{\omega_r^2 L} = \frac{1}{\omega_r Q R}$$

The Average current and RMS current through each switch will be

$$I_{S-avg} = \frac{I_p}{2\pi} (1 - \cos \phi) \quad I_{S-rms} = \frac{I_p}{2} \sqrt{\frac{(2\phi - \sin 2\phi)}{2\pi}}$$

The maximum dv/dt experienced by each switch and the switch utilization factor will be

$$\frac{dv}{dt}_{MAX} = \frac{I_p}{2C_o} \sin(\phi) \quad U = \frac{1}{4\pi} (1 - \cos\phi)$$

If a more complex matching circuit is to be used other than a simple LCR network, such as tapped inductor or tapped capacitor network, then the effective load impedance required by the inverter can be used to calculate the circuit element values. The effective load impedance that the fundamental component of the midpoint voltage must see is given by

$$\bar{Z} = R + jX$$

where R is the real part of the effective load impedance and X is the reactive part (inductive). R and X can be found using the following expressions

$$R = \frac{V_s}{\pi I_p} (1 - \cos\phi)$$

$$X = \frac{V_s}{\pi I_p} \left[\frac{\pi - \phi + \sin\phi \cos\phi}{1 + \cos\phi} \right]$$

REFERENCES

- [1] P.J. Baxandall, "Transistor sine-wave LC oscillators", *Proceedings of the IEE*, vol. 106, part B, supplement 16, pp.748-758, 1959
- [2] H.L. Krauss, C.W. Bostian and F.H. Raab, *Solid State Radio Engineering*. John Wiley & Sons, 1981.
- [3] M.K. Kazimierczuk, "Class-D voltage switching MOSFET power amplifier", *IEE Proceedings-B*, Vol. 38, No. 6, Nov. 1991.
- [4] N.O. Sokal and A.D. Sokal, "Class-E – A New Class of High-Efficiency Tuned Single-Ended Switching Amplifier", *IEEE J. Solid-State Circuits*, vol. 10, no. 3, pp.168-176, June 1975
- [5] Sayed-Amr El-Hamamsy, "Design of High Efficiency RF Class-D Amplifier", *IEEE Transactions on Power Electronics*, Vol. 9, No. 3, pp. 297-308, May 1994.
- [6] D.C. Hamill, "Impedance Plane Analysis of a Class-DE Amplifier", *Electronics Letters*, Vol. 30, No. 23, pp. 1905-1906, 10th November 1994.
- [7] H. Koizumi, T. Suetsugu, M. Fujii, K. Shinhoda, S. Mori and K. Ikeda, "Class-DE High Efficiency Tuned Power Amplifier", *IEEE Trans. on Circuits and Systems*, Part I, vol. 43, no. 1, pp.51-60, Jan. 1996.
- [8] D.C. Hamill, "Class-DE Inverters and Rectifiers for DC-DC Conversion", *Power Electronics Specialists Conference*, Baveno, Italy, June 1996.
- [9] D.R.H. Carter, *Aspects of High Frequency Half-Bridge Circuits*. Ph.D. thesis, Cambridge University, Electrical Engineering Department, 1996
- [10] F.H. Raab, "Idealized Operation of the Class-E Tuned Power Amplifier", *IEEE Trans. on Circuits and Systems*, Vol. CAS-43, no. 12, pp.725-735, Dec. 1977.
- [11] B.J. Baliga, "Power Semiconductor figure of Merit for High-Frequency Applications", *IEEE Electron Device Letters*, Vol. 10, No. 10, pp. 455-457, October 1989.
- [12] D.A. Grant and J. Gower, *Power MOSFETS: Theory and Applications*. Wiley Interscience, 1989.
- [13] M.J. Chudobiak, "The Use of Parasitic Nonlinear Capacitors in Class-E Amplifiers", *IEEE Trans. on Circuits and Systems*, Part I, vol. 41, no. 12, pp.941-944, Dec. 1994.
- [14] M.K. Kazimierczuk and T. Nandakumar, "Class-D voltage switching inverter with a tapped resonant inductor", *IEE Proceedings-B*, Vol. 140, No. 3, May. 1993.
- [15] N.O. Sokal and I. Novak, "Resonant Power Converters: Computer-aided Predication of Voltage-Control Function, Transfer Functions and Avoidance of control-loop lock-up", *High Frequency power Conversion conference, Toronto, ON, Canada*, June 1991.
- [16] S. Hinchliffe and L. Hobson, "Review of solid state devices and circuits for HF electric process heating applications – Part I: devices", *Int. J. of Electronics*, Vol. 61, No. 2, pp. 143-167, 1986.
- [17] S. Hinchliffe and L. Hobson, "Review of solid state devices and circuits for HF electric process heating applications – Part II: circuits ", *Int. J. of Electronics*, Vol. 61, No. 3, pp. 261-279, 1986.
- [18] S. Hinchliffe, L. Hobson and R.W. Houston, "A high power Class-E amplifier for high frequency process heating", *Int. J. of Electronics*, Vol. 64, No. 4, pp. 667-675, 1988.

- [19] S. Hinchliffe and L. Hobson, "High frequency switching of power MOSFETS", *Int. J. of Electronics*, Vol. 65, pp. 127-138, 1988.
- [20] S. Hinchliffe and L. Hobson, "High-frequency (>1MHz) converters for induction heating applications", *Electronics Letters*, Vol. 24, No. 11, pp. 697-698, 26th May 1988.
- [21] S. Hinchliffe and L. Hobson, "High Power Class-E amplifier for high frequency induction heating applications", *Electronics Letters*, Vol. 24, No. 14, pp. 697-698, 7th July 1988.
- [22] S. Hinchliffe, K. Thomas and L. Hobson, "High efficiency power source for HF electric process heating applications", *Int. J. Electronics*, Vol. 63, No. 1, pp. 117-122, 1987.
- [23] M.K. Kazimierczuk, "High-Speed Driver for Switching Power MOSFETS", *IEEE Trans. on Circuits and Systems*, vol. 35, no. 2, pp.254-256, Feb. 1988
- [24] D.R.H. Carter and R.A. McMahon, "Electronic level shifter for use in half-bridges operating at 13.56MHz", *Electronics Letters*, Vol. 31, No. 16, pp. 1301-1302, 3rd August 1995.
- [25] D.C. Hamill, "Half-Bridge Class-DE Rectifier", *Electronics Letters*, Vol. 31, No. 22, pp. 1885-1886, 26th October 1995.
- [26] I.D. de Vries, J.H. van Nierop and J.R. Greene, "Solid-State Class-DE RF Power Source", *In Proceedings of ISIE'98, Pretoria, South Africa*, vol. 2, pp. 524-529, July 1998.
- [27] S.A. Zhukov and V.B. Kozyrez, "Push-pull switching generator without switching loss" (in Russian), *Poluprovodnikovye Pribory v Tekhnike Electrosvyazi (Semiconductor Devices in Electrical Communication Technology)*, vol. 15, pp. 95-107, 1975.
- [28] N. Dye and H. Granberg, *Radio Frequency Transistors: Principles and Applications*. Butterworth-Heinemann 1994.
- [29] *IR Application Note AN-937: Gate Drive characteristics and Requirements for HEXFETS*. International Rectifier Corporation , 1995.
- [30] S. Clemente and A. Dubashi, *IR Application Note AN-978: HV Floating MOS-Gate Driver ICs*, International Rectifier Corporation, 1995.
- [31] *HEXFET Designers Manual HDM-1*, International Rectifier Corporation, 1993.
- [32] W.J. Chudobiak and D.F. Page, "Frequency and Power limitations of Class-D Transistor Amplifiers", *IEEE Journal of Solid-State Circuits* , Vol. SC-4, no. 1, pp.25-37, Feb. 1969.
- [33] P. Senak, "Amplitude Modulation of the Switched-Mode Tuned Power Amplifier", *Proceedings of IEEE*, vol. 53, pp.1658-1659, October 1965.
- [34] R. Severns and J. Armijos, *MOSPOWER Applications Handbook*, Siliconix Inc., 1985.
- [35] N. Morrison, *Introduction to Fourier Analysis*, John Wiley and Sons Inc., 1994.
- [36] R.J. Leedham, *High Frequency Switching with Power MOSFETs*. Ph.D. thesis, Cambridge University, Engineering Department, 1995.
- [37] F. H. Raab, "The Class BD High-Efficiency RF Power Amplifier", *IEEE Journal of Solid-State Circuits*, vol. SC-12, no. 3, pp.291-298, June 1977
- [38] H.O. Granberg, *Broadband Transformers and Power Combining Techniques for RF*, Motorola Application Note AN749, Motorola.

- [39] H. Granberg, "Applying Power MOSFETs in Class D/E RF Power Amplifier Design", Motorola Application Note AR141, Motorola. Reprinted from RF DESIGN, June, 1985.
- [40] H. Granberg, "Good RF Construction Practices and Techniques", Motorola Application Note AR164, Motorola. Reprinted from RF DESIGN, September, 1980.
- [41] N. Dye and H. Granberg, "Using RF Transistors: Power Construction Techniques", Electronics World + Wireless World, March 1994.
- [42] *HP Application Note 1045, High-Speed Fiber-Optic Link*, Hewlett Packard, 1991.
- [43] M.K. Kazimierczuk, "Analysis of a Class-E Zero-Voltage-Switching Rectifier", *IEEE Trans. on Circuits and Systems*, vol. 37, no. 6, pp.747-755, June 1990
- [44] R.L. Steigerwald, "High-Frequency Resonant Transistor DC-DC Converters", *IEEE Trans. on Industrial Electronics*, vol. IE-31, no. 2, pp.181-191, May 1984
- [45] R.L. Steigerwald, "A Comparison of Half-Bridge Resonant Converter Topologies", *IEEE Trans. on Power Electronics*, vol. 3, no. 2, pp.174 -182, April 1988
- [46] F. H. Raab, "Low Cost High-Efficiency HF Power Amplifiers," *Proc. Nordic Shortwave Conf.*, Fårö, Sweden, August 1998.
- [47] F. H. Raab and D.J. Rupp, "Quasi-complementary Class-D HF Power Amplifier," *RF Design*, vol. 15, no. 9, pp. 103-110, Sept. 1992.
- [48] F. H. Raab and D.J. Rupp, "HF Power Amplifier operates in both Class-B and Class-D", *Proc. RF Expo West '93*, San Jose, CA, pp. 114 -124, March 1993. [TP92-7]
- [49] G.J. Krausse, "Advanced Power MOSFET generates 1kW RF power in the HF band," *Proc. RF Expo West '93*, San Jose, CA, pp. 81-87, March 1993. [P-249]
- [50] M.K. Kazimierczuk, W. Szaraniec, and S. Wang, "Analysis and Design of a parallel resonant converter at high Q_L ", *IEEE Trans. on Aerospace and Electronic Systems*, vol. 28, pp. 35-49, January 1992.
- [51] M.K. Kazimierczuk and S. Wang, "Frequency-domain Analysis of a series resonant converter for continuous conduction mode," *IEEE Trans. on Power Electronics*, vol. 7, pp. 270-279, April 1992.
- [52] M.K. Kazimierczuk and W. Szaraniec, "Class-D zero-voltage-switching inverter with only one shunt capacitor," *em IEEE Proc. Part B, Electric Power Applications*, vol. 139, pp. 449-456, September.
- [53] M.K. Kazimierczuk and D. Czarkowski, *Resonant Power Converters*, John Wiley & Sons, 1981.
- [54] D. Czarkowski and M.K. Kazimierczuk, "ZVS Class-D series resonant inverter - Discrete-time state-space simulation and experimental results," *IEEE Trans. on Circuits and Systems*, vol. 11, pp. 1141-1147, June 1990.
- [55] T.B. Mader, "Quasi-optical Class-E power amplifiers," *Ph.D. Dissertation*, University of Colorado, Boulder, 1995.
- [56] N.O. Sokal, "Classes A through S - How they operate, and when to use Each," Available from Design Automation, Inc. 4 Tyler Road, Lexington, MA.
- [57] *HB-Plus Simulation Program*, available from Design Automation, Inc. 4 Tyler Road, Lexington, MA.